Experimental studies of the therapeutic and toxic effects of FOLFIRI chemotherapy in colon cancer

by

Gauhar Ali

A thesis submitted in partial fulfillment of the requirements for the degree of

Master of Science

in

Cancer Sciences

Department of Oncology
University of Alberta

ABSTRACT

Introduction:

Chemotherapy is an essential component of cancer treatment and can be effective in controlling tumor growth and increasing the likelihood of remission accompanied with increased survival. However, chemotherapy is associated with substantial acute and long-lasting toxicity which have detrimental effects on an individual's quality of life. The therapeutic and toxic effects of chemotherapy regimens is constantly under investigation so as to maximize anti-tumor activity whilst minimizing treatment-associated toxicity.

Several cancer therapies induce muscle fibre atrophy; this treatment-associated wasting is not well understood and has been investigated for single agents in experimental studies in healthy animals. Therapy-induced muscle atrophy has not been investigated within the complex interplay among tumor, chemotherapy regimen and treatment response. Possible interactions between cancer and treatment in development of muscle wasting remain uncharacterized. The complement system is an inflammatory component of immune responses which may contribute to treatment-associated muscle wasting.

Methods:

A preclinical model with Fischer 344 rats bearing the Ward colon adenocarcinoma were treated with FOLFIRI (irinotecan/5-fluorouracil) at a dose and schedule which recapitulates treatment response and toxicity that align with human patient experience. HEALTHY controls were compared with TUMOR rats and TUMOR+FOLFIRI rats given 2 weekly cycles of FOLFIRI (n=8/group). Gastrocnemius muscle fibre cross sectional area (CSA) was assessed as an index of atrophy. mRNA sequencing of gastrocnemius was performed. Differential gene

expression (DE) was assessed (fold-change≥1.5; p-value<0.05) and Ingenuity Pathway Analysis (IPA) used for functional annotation of DE mRNAs.

In a second study, rats were randomized to receive an orally active, small molecular weight inhibitor of the complement system at the start of FOLFIRI treatment; treatment-associated toxicity was assessed via changes in body weight and food intake and tumor response was assessed through tumor measurements.

Results:

Compared with HEALTHY, TUMOR growth (0.57±0.1% of body weight) resulted in a -22.2% ($p<0.05$) reduction in *gastrocnemius* mean fiber CSA. FOLFIRI shrank the tumor (-89%) and induced further -22% reduction in muscle fibre CSA. Muscles of TUMOR vs HEALTHY showed 1283 DE transcripts and 43 DE canonical pathways($p<0.05$). TUMOR+FOLFIRI expanded DE to 2095 transcripts and 72 canonical pathways ($p<0.05$). The top 4 pathways associated with TUMOR were ($p<0.01$) *Adipogenesis*, *EIF2 Signaling*, *Transcriptional Regulatory Network in Embryonic Stem Cells*, and *Actin Cytoskeleton Signaling;* in TUMOR+FOLFIRI they were ($p<0.001$) *Protein Ubiquitination*, *EIF2 Signaling*, *Hepatic Fibrosis / Stellate Cell Activation* and *ATM Signaling*.

Complement inhibitor appeared safe, showing no effect on rat body weight or food intake; colon tumor shrunk rapidly in the presence of this agent and histological examination showed that tumor was eliminated with only residual secondary lymphoid reaction present at tumor site.

Conclusions:

Tumor and FOLFIRI resulted in progressive atrophy and changes in skeletal muscle transcriptome. FOLFIRI specifically exacerbates a catabolic transcriptional program, in spite of robust tumor response. Complement inhibitor potentiated tumor response to FOLFIRI and this requires further investigation.

PREFACE

This master's thesis is original work by Gauhar Ali. No part of this thesis has been previously published. Animal work presented in Chapter's 2 and 3 were approved by the University of Alberta Institutional Animal Care Committee and conducted in the Protocol RES006429: "*Dietary EPA and DHA to Enhance Tumor Response and Protect against Chemotherapy Related Myosteatosis in an experimental model of colorectal cancer*", in accordance with the guidelines of the Canadian Council on Animal Care.

Two experimental series are described in Chapters 2 and 3. Chapter 2 is derived from a long-standing collaboration between Baracos, Mazurak and Damaraju Laboratories, such that we conduct experimental work with common personnel and technical support. I had access to banked samples and data sets which I analyzed to understand the sequential effects of a colorectal adenocarcinoma and FOLFIRI treatment on muscle atrophy. This chapter was written in a manuscript format and will be submitted for publication to Clinical Cancer Research. I contributed with conceptualization, data analysis, interpretation, and manuscript writing. Vickie E. Baracos contributed with conceptualization and manuscript editing. Vera C. Mazurak, Sambasivarao Damaraju and Bhumi Bhatt contributed with conceptualization, global gene database generation, analysis methodology and interpretation, and manuscript editing.

Chapter 3 was an independent experimental series which I designed and executed through coordination with AURIN Biotech Inc. via MITACS Accelerate, to test a novel orally active inhibitor of the complement system. I contributed with conceptualization of the study design, rodent experiments, animal care, sample collection, data analysis, interpretation, and manuscript writing. Vickie E. Baracos and Vera C. Mazurak contributed with conceptualization and manuscript editing.

DEDICATION

To

My parents, Gulzar and Riaz Ali
I would not have been able to complete this journey without you. Thank you for your unconditional support and love. You have always encouraged me to pursue my dreams. Thank you for the sacrifices you have made for our family.
I love you immensely.

My brother, Raafi Ali
You are an inspiration to me and I cannot thank you enough for your ongoing support, guidance and encouragement – I love you very much.

THE ABILITY TO MAKE JUDGEMENTS THAT ARE GROUNDED IN SOLID INFORMATION, AND EMPLOY CAREFUL ANALYSIS, SHOULD BE ONE OF THE MOST IMPORTANT GOALS FOR ANY EDUCATIONAL ENDEAVOR.

~ AGA KHAN IV

ACKNOWLEDGMENTS

I would like to acknowledge all the financial support I have received throughout my graduate studies. I am fortunate to have received funding from AURIN Biotech Inc. and MITACS Accelerate and to have received the Alberta Graduate Excellence Scholarship from the University of Alberta as well as the Sarah and Nancy South Memorial Graduate Studentship in Oncology from the Cancer Research Institute of Northern Alberta (CRINA). I am grateful to have had continuous financial support which made it possible to pursue my academic interests.

My supervisor, Dr. Vickie Baracos – thank you for taking a chance on an "enthusiastic but inexperienced" young man. Your passion for science and research was truly infectious and you have been an essential part of my growth over the past several years. Through the example you set, you have taught me the importance of a steadfast work ethic, humility towards all and striving to live a balanced life. Thank you for your mentorship, unconditional support at every junction box, untiring effort, patience, and insightful guidance. You have shared some of the most valuable lessons with me which I will hold on to for the rest of my life.

Dr. Vera Mazurak – thank you for your mentorship, encouragement, and guidance over the last several years. You have played a pivotal role in my development and the collaborative opportunities we have had has made this journey unique and unforgettable. Thank you for fostering an environment of support and encouraging me to always strive for excellence.

I would like to thank Dr. Sambasivarao Damaraju. I am tremendously grateful for your guidance and mentorship over the years. Thank you for always sharing your expertise and ongoing support in advancing my project.

Dr. Michael Sawyer – thank you for sharing your extensive knowledge and expertise throughout this project. Collaborating with you has provided me valuable insight about clinical practice and for this I am very grateful.

Abha Dunichand-Hoedl and Fatima Muzaffar you have been critical people throughout this journey. I will be forever thankful for your encouragement, support, love, kindness, and friendship. Thank you for everything.

A special thank you to Bhumi, Peter, Maryam, Magaly, Sarah, Dhruvesh, Pamela, Sue, Stanley, Jenna, Tianna, Hailey, Dr. Leyla Baghersad-Renani, Dr. MD Monirujjaman, Dr. Ana Anoveros-Barrera, Dr. Amrit Bhullar, Dr. Marnie Newell, Dr. Stephane Servais, Dr. Cathy Kubrak - your friendship, and support has been tremendous, and I will hold on to the memories we made.

Thank you to the people I love most in the world. To my parents, Gulzar and Riaz Ali, thank you for your sacrifices and everything you do for our family. To my brother, Raafi Ali, thank you for always being in my corner and your unconditional support. My accomplishments and successes are a reflection of all of you.

TABLE OF CONTENTS

CHAPTER 1 INTRODUCTION AND RESEARCH PLAN

1.1 Introduction 1

1.2 Research Plan 5

1.3 Literature Cited 7

CHAPTER 2 COLON CANCER TREATMENT WITH FOLFIRI EXACERBATES MUSCLE FIBRE ATROPHY AND INDUCES A CATABOLIC TRANSCRIPTIONAL PROGRAM IN SKELETAL MUSCLE

2.1 Introduction 14

2.2 Materials and Methods 15

2.2.1 Animal Model and Study Design 15

2.2.2 Skeletal Muscle Tissue and Fibre Cross Sectional Area (CSA) 17

2.2.3 Total RNA Extraction 17

2.2.4 RNA Sequencing and Differential Expression (DE) Analysis 18

2.2.5 Ingenuity Pathway Analysis - Canonical Pathways 19

2.3 Results 19

2.3.1 Treatment with FOLFIRI controls tumor growth but exacerbates muscle atrophy and induces a second wave of transcriptional change in gastrocnemius muscle 19

2.3.2 Functional annotation of tumor and chemotherapy induced mRNA expression in gastrocnemius muscle 20

2.3.2.1 Ubiquitin-dependent proteolysis 21

2.3.2.2 Cell-death associated pathways: Death Receptor Signaling, Apoptosis

Signaling and Necroptosis 22

2.3.2.3 Unfolded protein response, amino acid catabolism and skeletal muscle-specific atrophy gene regulators are prominent after tumor growth and FOLFIRI treatment 23

2.3.2.4 Extracellular matrix (ECM)-related transcripts are modified by tumor and exacerbated by FOLFIRI treatment 24

2.3.2.5 Transcriptional regulator profile aligns with differential expression and canonical pathways 25

2.4 Discussion 27

FIGURES.....32

TABLES.....35

LITERATURE CITED 49

CHAPTER 3 TUMOR RESPONSE TO FOLFIRI CHEMOTHERAPY IS MODIFIED BY TARGETING THE COMPLEMENT SYSTEM IN RATS BEARING THE WARD COLON TUMOR

3.1 Introduction.....57

3.2 Materials and Methods.....59

3.2.1 Animal Model and Study Design.....59

3.2.2 Tumor Response 61

3.2.3 Safety/Toxicity Assessment: Body Weight and Food Intake.....61

3.2.4 Statistical Analysis.....62

3.3 Results.....62

3.3.1 AUR1402 treatment is safe and does not modify gastrointestinal toxicity induced by

FOLFIRI chemotherapy.....62

3.3.2 Treatment with AUR1402 confers an augmented tumor response to FOLFIRI chemotherapy.....63

3.3.3 Histological assessment confirms elimination of tumor cells following AUR1402 treatment 64

3.4 Discussion 66

FIGURES.....71

LITERATURE CITED 78

CHAPTER 4 GENERAL DISCUSSION AND CONCLUSIONS

4.1 General Summary and Review of Objectives and Hypotheses.....83

4.2 Considerations for Future Studies.....86

4.3 Conclusion 88

LITERATURE CITED 90

Bibliography 93

LIST OF TABLES

Table 2-1. Tumor-bearing versus healthy rats – Ingenuity Pathway Analysis (IPA)® Canonical Pathways

Table 2-2. Tumor-bearing – FOLFIRI versus healthy rats – Ingenuity Pathway Analysis (IPA)® Canonical Pathways

Table 2-3. Transcripts involved in the EIF2 Signaling Pathway – Translational Regulation

Table 2-4. Transcripts involved in the Protein Ubiquitination Pathway

Table 2-5. Transcripts involved in cell death-associated signaling including Death Receptor Signaling, Necroptosis Signaling Pathway, Apoptosis Signaling and Autophagy

Table 2-6. Transcripts involved in the Unfolded Protein Response pathway and modification of myofibril-derived amino acids including Valine Degradation I and Branched-chain α-keto acid Dehydrogenase Complex (BCKDHC) pathways

Table 2-7. Transcripts involved in modification of the extracellular matrix including Hepatic Fibrosis/ Hepatic Stellate Cell Activation, GP6 Signaling Pathway, Apelin Liver Signaling Pathway and Hepatic Fibrosis Signaling Pathway

Table 2-8. Transcriptional regulators affected by tumor and FOLFIRI

LIST OF FIGURES

Figure 2-1. Phenotype of animal model of colon cancer and FOLFIRI treatment

Figure 2-2. Differential Gene Expression (DE) of skeletal muscle mRNA from tumor-bearing and FOLFIRI treated animals relative to healthy controls

Figure 2-3. Ingenuity pathway analysis of canonical pathways affected by tumor and chemotherapy treatment

Figure 3-1. The Three Activation Pathways of Complement: the Classical, Mannose-Binding Lectin, and Alternative Pathways

Figure 3-2. Study design to test AUR1402 in an animal model of colorectal cancer and chemotherapy treatment

Figure 3-3. Effect of AUR1402 treatment on gastrointestinal toxicity induced by FOLFIRI chemotherapy

Figure 3-4. Effect of AUR1402 on tumor response to FOLFIRI chemotherapy

Figure 3-5. Tumor histology of FOLFIRI treated rats with or without AUR1402

Figure 3-6. Enlarged image of Figure 3-5C to visualize morphological features of Control rats

Figure 3-7. Enlarged image of Figure 3-5D to visualize morphological features of AUR1402 treated rats

LIST OF SYMBOLS AND ABBREVIATIONS

5-FU	5-fluorouracil
ALDH6A1	aldehyde dehydrogenase 6 family, member A1
ANOVA	analysis of variance
ATA	aurin tricarboxylic acid
ATG	Autophagy related
BAK1	BCL1-antagonist/killer 1
BCKDHC	branched-chain α-keto acid dehydrogenase complex
BCL2	B-cell leukemia/lymphoma 2
BCLAF1	BCL2 associated transcription factor 1
C1	complement 1
C3	complement 3
C5	complement 5
CASP1	caspase-1
COL	collagen
CPT-11	irinotecan (7-ethyl-10-[4-(1-piperidino)-1-piperidino]carbonyloxy-camptothecin
CSA	cross sectional area

CT	computed tomography
CTCAE	Common Terminology Criteria for Adverse Events
CUL1	cullin 1
DBT	dihydrolipoamide branched chain transacylase E2
DDIT3	DNA-damage inducible transcript 3
DE	differential gene expression
DNA	deoxyribonucleic acid
ECM	extracellular matrix
EIF	eukaryotic translation initiation factor
EMT	epithelial-to-mesenchymal transition
FOLFIRI	5-fluorouracil (5-FU) + irinotecan (CPT-11)
FBN	Fibrillin
GI	gastrointestinal
H&E	haematoxylin and eosin
Hsp	heat shock protein
IFN	interferon
IL	interleukin

i.p.	intraperitoneal(ly)
IPA	Ingenuity Pathway Analysis®
ITG	integrin
LAM	laminin
MAC	membrane attack complex
MAP3K7	mitogen-activated protein kinase kinase kinase 7
MDSC	myeloid-derived suppressor cell
MYOD1	myogenic differentiation 1
NF-κB	nuclear factor-κB
NKAP	NFKβ activating protein
PAX7	paired box 7
PDAC	pancreatic ductal adenocarcinoma
PD-L1	programmed death-ligand 1
PSMA4	proteasome 20S subunit alpha 4
PSMC6	proteasome 26S subunit, ATPase 6
RNA	ribonucleic acid
s.c.	subcutaneous(ly)

SIRS	systemic inflammatory response syndrome
SN-38	7-ethyl-10-hydroxycamptothecin
TAM	tumor-associated macrophage
TBM	tingible body macrophage
TGF-β	transforming growth factor-β
TH	T helper
TME	tumor microenvironment
TNF	tumor necrosis factor
TS	thymidylate synthase
UBE3A	ubiquitin protein ligase E3A
UPR	unfolded protein response
USP	ubiquitin-specific peptidase
VEGF	vascular endothelial growth factor

CHAPTER 1: INTRODUCTION AND RESEARCH PLAN

1.1 Introduction

Discovery of anti-cancer agents including chemotherapeutic compounds has been a predominant focus of research over the last several decades. This has led to the development of treatment options characterized by effective control of tumor growth and decreasing tumor volume which has in turn led to prolonged life expectancy of patients with cancer. However, toxicity is inherent to chemotherapy and the use of chemotherapy agents is in large part dependent on the therapeutic index, defined as the ratio between doses that are efficacious in conferring death of tumor tissue and that which result in toxicity to otherwise healthy tissue. All proliferating cell types, such as those comprising the gastrointestinal (GI) mucosa, for example, are potential targets for cancer chemotherapy; this makes chemotherapy a science of selective toxicity.

It is estimated that colorectal cancer will account for 8.6% of all cancer deaths in 2022, based on cancer trends in the United States (Siegel et al., 2022). The current standard of care for metastatic colorectal cancer is treatment with a fluoropyrimidine such as 5-fluorouracil (5-FU), in various combinations and schedules with irinotecan (CPT-11) (FOLFIRI) or oxaliplatin (FOLFOX) (Benson et al., 2017; Van Cutsem et al., 2016). 5-FU facilitates misincorporation of fluoronucleotides into RNA and DNA and inhibits thymidylate synthase (TS) (Longley et al., 2003). Irinotecan (7-ethyl-10-[4-(1-piperidino)-1-piperidino] carbonyloxy-camptothecin, CPT-11, Camptosar®) is a camptothecin derivative which is converted to its active metabolite, 7-ethyl-lo-hydroxy-camptothecin (SN-38), that functions as a topoisomerase I inhibitor and inhibits DNA re-ligation (Armand et al., 1995; Rothenberg, 2001). The FOLFIRI chemotherapy regimen is associated with extensive gastrointestinal toxicity which includes late-onset diarrhea (a hallmark

toxicity associated with CPT-11), the severity of which can result in life threatening dehydration; this is one of the main underlying causes of morbidity in patients treated with FOLFIRI (JR Hecht, 1998).

While gastrointestinal toxicity is prominent in CPT-11-containing regimens, side effects of therapy are by no means restricted to the gastrointestinal system. Muscle atrophy is independently prognostic for survival in cancer patients (Martin et al., 2013) and low muscle mass is well established as conferring poorer response to treatment, and shortened survival in cancer patients (Aversa et al., 2017; Bozzetti & Bozzetti, 2017; Rier et al., 2016; Shachar et al., 2016; Vega et al., 2016). Muscle atrophy worsens during chemotherapy treatment (Jang et al., 2020). In colorectal cancer specifically, several studies have related low muscle mass to risk of surgical complications (Huang et al., 2015; Nakanishi et al., 2018), prolonged hospital stay (Boer et al., 2016; Martin et al., 2018) and mortality (Black et al., 2017; Cespedes Feliciano et al., 2017). FOLFIRI-treated patients experience significant loss of body weight as well as muscle mass (Jung et al., 2015) which, over an acute treatment period (over 50-200 days), equates to that incurred from 25 or 30 years of aging in an otherwise healthy individual (Blauwhoff-Buskermolen et al., 2016). As such, the extent to which FOLFIRI-associated gastrointestinal toxicity may extend to peripheral tissues such as the skeletal muscle is of interest. While observational studies have identified a relationship between low muscle mass and clinical outcomes and survival, the biology of these features and how they develop are not well understood.

Elucidating underlying mechanisms driving muscle mass loss and developing a greater understanding of the transcriptional program driving muscle fiber atrophy in malignant disease is

essential. This would require patient skeletal muscle biopsies, however, due to the invasiveness of the procedure and ethical considerations, multiple skeletal muscle biopsies over the course of treatment are not feasible in vulnerable human populations (Anoveros-barrera et al., 2019). As such, clinically translatable experimental models are required to define effects of a tumor, chemotherapy, and recovery on metabolic events in skeletal muscle. In various animal models, study designs include tumor growth to an extremely high burden (e.g. 10% of body weight) leading to extreme muscle (-25%) and fat (-90%) depletion (Barreto et al., 2016; Sun et al., 2016; Tseng et al., 2015). Animal models that have been used to date to investigate chemotherapy-associated muscle wasting include study designs where individual agents (e.g., camptothecins, anthracyclines, fluoropyrimidines and platinum-based compounds) are administered to healthy animals; these studies describe the extent of muscle atrophy and catabolic and inflammatory signatures that are induced by antineoplastic agents on muscle (Barreto et al., 2016; Seo et al., 2021; Sorensen et al., 2017). However, these models provide no insight into how these effects occur in the presence of a tumor, nor do they characterize the response of muscles to a multi-drug regimen, such as FOLFIRI.

Tumor and chemotherapy occur simultaneously in the clinical setting and effects of the tumor and of chemotherapy could be unique and quantitatively important in development and progression of muscle wasting. Although studying the effects of a tumor and chemotherapy separately may be useful, it does not account for the possibility that they synergize with each other. The successive treatment of tumor is part of the clinical reality; however, the degree of tumor related progression as well as dose and total amount of chemotherapy that are permitted, are important considerations. There is no instance in the literature where it can be determined if the

clinical reality of treatment with sequential cycles of chemotherapy induces further change than that which is induced by tumor growth.

If endeavoring to define sequential effects of a tumor and chemotherapy on transcriptional events in skeletal muscle, a model which aligns with the clinical experience of patients with cancer is required; this must be scaled to the clinical scenario and consider the type of cancer, corresponding chemotherapy, extent of tumor growth as well as a dose and schedule of the chemotherapy treatment plan which confers the treatment response and toxicity generally experienced by patients on that treatment plan. In our preclinical model of the Fischer 344 rat bearing the Ward colorectal carcinoma, animals exhibit muscle atrophy and myosteatosis, both of which are exacerbated following chemotherapy, as is observed in patients (Almasud et al., 2017; Murphy et al., 2011a, 2011b). The chemotherapy treatment regimen used in our model of a sequential dosage of CPT-11 and 5-FU is comparable to the chemotherapy administered in clinic and has been evaluated for its anti-tumor efficacy and therapeutic selectivity (Cao & Rustum, 2000). It has been determined that the therapeutic index for this regimen is significantly increased when CPT-11 is administered 24 hours prior to 5-FU and the toxicity observed, including the kinetics of acute and delayed diarrhea, are consistent with those observed in patients treated with CPT-11 (Almasud et al., 2017; Xue et al., 2007).

Patients who experience cancer-associated muscle wasting develop distinctive tumor-related metabolic changes, including inflammatory and immune responses, which may, in part, contribute to skeletal muscle and adipose tissue loss (Baracos et al., 2018). Both inflammatory cells and inflammatory molecules are thought to participate in signaling of wasting at the muscle

(and adipocyte) cell level. A highly complex component of the immune system, which over the past decade has become a focus of anti-cancer therapy, is the complement system (Macor et al., 2018). The complement system was most extensively described with its role in inflammatory immune responses to viral and bacterial infections (Blajchman & Ozge-Anwar, 1986; Walport, 2001a, 2001b). However, recent evidence suggests that complement responses in the tumor microenvironment may contribute to the repertoire of strategies employed by tumor cells to evade host immune responses (Afshar-Kharghan, 2017; Kolev et al., 2022). Complement inhibitors are a class of anti-inflammatory therapeutic agents which have been under investigation, particularly in pathologies that include aberrant inflammatory processes (McGeer et al., 2017; Ricklin & Lambris, 2008; Ross et al., 1999). This class of therapies is of potential interest as modifiers of tumor growth, tumor response to chemotherapy, as well as tissue level toxicities in organs and tissues of the tumor-bearing host.

1.2 Research Plan

This thesis work is composed of 2 interrelated, individual sub-studies which have their own discrete emphases on addressing specific objectives and hypotheses:

Chapter 2 Title: Colon cancer treatment with FOLFIRI exacerbates muscle fiber atrophy and induces a catabolic transcriptional program in skeletal muscle

Hypothesis: tumor and chemotherapy each elicit unique and quantitatively important effects in the development and progression of muscle wasting.

Objective(s): investigate the sequential effect of colorectal adenocarcinoma and two cycles of FOLFIRI chemotherapy treatment on atrophy and evolution of gene expression in

skeletal muscle in a rat experimental model.

Chapter 3 Title: Tumor response to FOLFIRI chemotherapy is modified by targeting the complement system in rats bearing Ward colon tumor

Hypothesis: when combined with a FOLFIRI chemotherapy regimen, AUR1402, a complement inhibitor enhances anti-tumor efficacy of FOLFIRI.

Secondary Hypothesis: AUR1402 reduces FOLFIRI-associated gastrointestinal toxicity.

Objective(s): explore whether certain immunological reactions, namely inhibitors of the complement system, potentially affect treatment response to FOLFIRI chemotherapy in a favorable manner with enhanced anti-cancer efficacy and/or reduced FOLFIRI-associated gastrointestinal toxicity in the same experimental model that is used in Chapter 2.

Chapter 4 provides an overall discussion and directions for future research.

1.3 Literature Cited

Afshar-Kharghan, V. (2017). The role of the complement system in cancer. *Journal of Clinical Investigation*, *127*(3), 780–789. https://doi.org/10.1172/JCI90962

Almasud, A. A., Giles, K. H., Miklavcic, J. J., Martins, K. J. B., Baracos, V. E., Putman, C. T., Guan, L. L., & Mazurak, V. C. (2017). Fish oil mitigates myosteatosis and improves chemotherapy efficacy in a preclinical model of colon cancer. *PLoS ONE*, *12*(8), 1–17. https://doi.org/10.1371/journal.pone.0183576

Anoveros-barrera, A., Bhullar, A. S., Stretch, C., Esfandiari, N., Dunichand-hoedl, A. R., Karen, J. B., Bigam, D., Khadaroo, R. G., Mcmullen, T., Bathe, O. F., Damaraju, S., Richard, J., Putman, C. T., Baracos, V. E., & Mazurak, V. C. (2019). *Clinical and biological characterization of skeletal muscle tissue biopsies of surgical cancer patients*. *December 2018*, 1356–1377. https://doi.org/10.1002/jcsm.12466

Armand, J. P., Ducreux, M., Mahjoubi, M., Abigerges, D., Bugat, R., Chabot, G., Herait, P., de Forni, M., & Rougier, P. (1995). CPT-11 (Irinotecan) in the treatment of colorectal cancer. *European Journal of Cancer*, *31*(7–8), 1283–1287. https://doi.org/10.1016/0959-8049(95)00212-2

Aversa, Z., Costelli, P., & Muscaritoli, M. (2017). Cancer-induced muscle wasting: Latest findings in prevention and treatment. *Therapeutic Advances in Medical Oncology*, *9*(5), 369–382. https://doi.org/10.1177/1758834017698643

Baracos, V. E., Martin, L., Korc, M., Guttridge, D. C., & Fearon, K. C. H. (2018). Cancer-associated cachexia. *Nature Reviews Disease Primers*, *4*(1), 1–18. https://doi.org/10.1038/nrdp.2017.105

Barreto, R., Mandili, G., Witzmann, F. A., Novelli, F., Zimmers, T. A., & Bonetto, A. (2016). Cancer and chemotherapy contribute to muscle loss by activating common signaling pathways. *Frontiers in Physiology*, *7*(OCT), 1–13. https://doi.org/10.3389/fphys.2016.00472

Benson, A. B., Venook, A. P., Bekaii-Saab, T., Chan, E., Chen, Y.-J., Cooper, H. S., Engstrom, P. F., Enzinger, P. C., Fenton, M. J., Fuchs, C. S., Grem, J. L., Hunt, S., Kamel, A., Leong, L. A., Lin, E., Messersmith, W., Mulcahy, M. F., Murphy, J. D., Nurkin, S., … Freedman-Cass, D. A. (2017). Colon Cancer, Version 1.2017. *Journal of the National Comprehensive Cancer Network*, *15*(3), 1028–1059. https://doi.org/10.6004/jnccn.2014.0099

Black, D., Mackay, C., Ramsay, G., Hamoodi, Z., Nanthakumaran, S., Park, K. G. M., Loudon, M. A., & Richards, C. H. (2017). Prognostic Value of Computed Tomography: Measured Parameters of Body Composition in Primary Operable Gastrointestinal Cancers. *Annals of Surgical Oncology*, *24*(8), 2241–2251. https://doi.org/10.1245/s10434-017-5829-z

Blajchman, M. A., & Ozge-Anwar, A. H. (1986). The role of the complement system in hemostasis. *Progress in Hematology*, *14*(3), 149–182.

Blauwhoff-Buskermolen, S., Versteeg, K. S., De Van Der Schueren, M. A. E., Den Braver, N. R., Berkhof, J., Langius, J. A. E., & Verheul, H. M. W. (2016). Loss of muscle mass during chemotherapy is predictive for poor survival of patients with metastatic colorectal cancer. *Journal of Clinical Oncology*, *34*(12), 1339–1344. https://doi.org/10.1200/JCO.2015.63.6043

Boer, B. C., de Graaff, F., Brusse-Keizer, M., Bouman, D. E., Slump, C. H., Slee-Valentijn, M., & Klaase, J. M. (2016). Skeletal muscle mass and quality as risk factors for postoperative

outcome after open colon resection for cancer. *International Journal of Colorectal Disease*, *31*(6), 1117–1124. https://doi.org/10.1007/s00384-016-2538-1

Bozzetti, F., & Bozzetti, F. (2017). *Forcing the vicious circle: Sarcopenia increases toxicity, decreases response to chemotherapy and worsens with chemotherapy*. https://doi.org/10.1093/annonc/mdx271

Cao, S., & Rustum, Y. M. (2000). Synergistic antitumor activity of irinotecan in combination with 5-fluorouracil rats bearing advanced colorectal cancer: Role of drug sequence and dose. *Cancer Research*, *60*(14), 3717–3721.

Cespedes Feliciano, E. M., Lee, V. S., Prado, C. M., Meyerhardt, J. A., Alexeeff, S., Kroenke, C. H., Xiao, J., Castillo, A. L., & Caan, B. J. (2017). Muscle mass at the time of diagnosis of nonmetastatic colon cancer and early discontinuation of chemotherapy, delays, and dose reductions on adjuvant FOLFOX: The C-SCANS study. *Cancer*, *123*(24), 4868–4877. https://doi.org/10.1002/cncr.30950

Huang, D.-D., Wang, S.-L., Zhuang, C.-L., Zheng, B.-S., Lu, J.-X., Chen, F.-F., Zhou, C.-J., Shen, X., & Yu, Z. (2015). Sarcopenia, as defined by low muscle mass, strength and physical performance, predicts complications after surgery for colorectal cancer. *Colorectal Disease*, *17*(11), O256–O264. https://doi.org/10.1111/codi.13067

Jang, M. K., Park, C., Hong, S., Li, H., Rhee, E., & Doorenbos, A. Z. (2020). Skeletal Muscle Mass Change During Chemotherapy: A Systematic Review and Meta-analysis. *Anticancer Research*, *40*(5), 2409–2418. https://doi.org/10.21873/anticanres.14210

JR Hecht. (1998). Gastrointestinal Toxicity of Irinotecan. *Oncology*, *12*(8), 72–78.

Jung, H.-W., Kim, J. W., Kim, J.-Y., Kim, S.-W., Yang, H. K., Lee, J. W., Lee, K.-W., Kim, D.-W., Kang, S.-B., Kim, K., Kim, C.-H., & Kim, J. H. (2015). Effect of muscle mass on

toxicity and survival in patients with colon cancer undergoing adjuvant chemotherapy. *Supportive Care in Cancer*, *23*(3), 687–694. https://doi.org/10.1007/s00520-014-2418-6

Kolev, M., Das, M., Gerber, M., Baver, S., Deschatelets, P., & Markiewski, M. M. (2022). Inside-Out of Complement in Cancer. *Frontiers in Immunology*, *13*, 931273. https://doi.org/10.3389/fimmu.2022.931273

Longley, D. B., Harkin, D. P., & Johnston, P. G. (2003). 5-Fluorouracil: Mechanisms of action and clinical strategies. *Nature Reviews Cancer*, *3*(5), 330–338. https://doi.org/10.1038/nrc1074

Macor, P., Capolla, S., & Tedesco, F. (2018). Complement as a Biological Tool to Control Tumor Growth. *Frontiers in Immunology*, *9*, 2203. https://doi.org/10.3389/fimmu.2018.02203

Martin, L., Birdsell, L., MacDonald, N., Reiman, T., Clandinin, M. T., McCargar, L. J., Murphy, R., Ghosh, S., Sawyer, M. B., & Baracos, V. E. (2013). Cancer cachexia in the age of obesity: Skeletal muscle depletion is a powerful prognostic factor, independent of body mass index. *Journal of Clinical Oncology*, *31*(12), 1539–1547. https://doi.org/10.1200/JCO.2012.45.2722

Martin, L., Hopkins, J., Malietzis, G., Jenkins, J. T., Sawyer, M. B., Brisebois, R., MacLean, A., Nelson, G., Gramlich, L., & Baracos, V. E. (2018). Assessment of Computed Tomography (CT)-Defined Muscle and Adipose Tissue Features in Relation to Short-Term Outcomes After Elective Surgery for Colorectal Cancer: A Multicenter Approach. *Annals of Surgical Oncology*, *25*(9), 2669–2680. https://doi.org/10.1245/s10434-018-6652-x

McGeer, P. L., Lee, M., & McGeer, E. G. (2017). A review of human diseases caused or exacerbated by aberrant complement activation. *Neurobiology of Aging*, *52*, 12–22. https://doi.org/10.1016/j.neurobiolaging.2016.12.017

Murphy, R. A., Mourtzakis, M., Chu, Q. S. C., Baracos, V. E., Reiman, T., & Mazurak, V. C. (2011a). Nutritional intervention with fish oil provides a benefit over standard of care for weight and skeletal muscle mass in patients with nonsmall cell lung cancer receiving chemotherapy. *Cancer*, *117*(8), 1775–1782. https://doi.org/10.1002/cncr.25709

Murphy, R. A., Mourtzakis, M., Chu, Q. S. C., Baracos, V. E., Reiman, T., & Mazurak, V. C. (2011b). Supplementation with fish oil increases first-line chemotherapy efficacy in patients with advanced nonsmall cell lung cancer. *Cancer*, *117*(16), 3774–3780. https://doi.org/10.1002/cncr.25933

Nakanishi, R., Oki, E., Sasaki, S., Hirose, K., Jogo, T., Edahiro, K., Korehisa, S., Taniguchi, D., Kudo, K., Kurashige, J., Sugiyama, M., Nakashima, Y., Ohgaki, K., Saeki, H., & Maehara, Y. (2018). Sarcopenia is an independent predictor of complications after colorectal cancer surgery. *Surgery Today*, *48*(2), 151–157. https://doi.org/10.1007/s00595-017-1564-0

Ricklin, D., & Lambris, J. D. (2008). Compstatin: A complement inhibitor on its way to clinical application. *Advances in Experimental Medicine and Biology*, *632*(Davis 2006), 273–292. https://doi.org/10.1007/978-0-387-78952-1_20

Rier, H. N., Jager, A., Sleijfer, S., Maier, A. B., & Levin, M. (2016). The Prevalence and Prognostic Value of Low Muscle Mass in Cancer Patients: A Review of the Literature. *The Oncologist*, *21*(11), 1396–1409. https://doi.org/10.1634/theoncologist.2016-0066

Ross, G. D., Veˇtvicˇka, V., Yan, J., Xia, Y., & Veˇtvicˇkova, J. (1999). *Therapeutic intervention with complement and b-glucan in cancer*. 14.

Rothenberg, M. L. (2001). Irinotecan (CPT-11): Recent Developments and Future Directions–Colorectal Cancer and Beyond. *The Oncologist*, *6*(1), 66–80. https://doi.org/10.1634/theoncologist.6-1-66

Seo, D. Y., Bae, J. H., Zhang, D., Song, W., Kwak, H., Heo, J., & Jung, S. (2021). *Effects of cisplatin on mitochondrial function and autophagy-related proteins in skeletal muscle of rats*. *54*(October), 575–580.

Shachar, S. S., Williams, G. R., Muss, H. B., & Nishijima, T. F. (2016). Prognostic value of sarcopenia in adults with solid tumours: A meta-analysis and systematic review. *European Journal of Cancer*, *57*, 58–67. https://doi.org/10.1016/j.ejca.2015.12.030

Siegel, R. L., Miller, K. D., Fuchs, H. E., & Jemal, A. (2022). Cancer statistics, 2022. *CA: A Cancer Journal for Clinicians*, *72*(1), 7–33. https://doi.org/10.3322/caac.21708

Sorensen, J. C., Petersen, A. C., Timpani, C. A., Campelj, D. G., Cook, J., Trewin, A. J., Stojanovska, V., Stewart, M., Hayes, A., & Rybalka, E. (2017). BGP-15 protects against oxaliplatin-induced skeletal myopathy and mitochondrial reactive oxygen species production in mice. *Frontiers in Pharmacology*, *8*(APR), 1–19. https://doi.org/10.3389/fphar.2017.00137

Sun, R., Zhang, S., Lu, X., Hu, W., Lou, N., Zhao, Y., Zhou, J., Zhang, X., & Yang, H. (2016). Comparative molecular analysis of early and late cancer cachexia-induced muscle wasting in mouse models. *Oncology Reports*, *36*(6), 3291–3302. https://doi.org/10.3892/or.2016.5165

Tseng, Y. C., Kulp, S. K., Lai, I. L., Hsu, E. C., He, W. A., Frankhouser, D. E., Yan, P. S., Mo, X., Bloomston, M., Lesinski, G. B., Marcucci, G., Guttridge, D. C., Bekaii-Saab, T., & Chen, C. S. (2015). Preclinical Investigation of the Novel Histone Deacetylase Inhibitor AR-42 in the Treatment of Cancer-Induced Cachexia. *Journal of the National Cancer Institute*, *107*(12), djv274. https://doi.org/10.1093/jnci/djv274

Van Cutsem, E., Cervantes, A., Adam, R., Sobrero, A., Van Krieken, J. H., Aderka, D., Aranda Aguilar, E., Bardelli, A., Benson, A., Bodoky, G., Ciardiello, F., D'Hoore, A., Diaz-Rubio, E., Douillard, J.-Y., Ducreux, M., Falcone, A., Grothey, A., Gruenberger, T., Haustermans, K., … Arnold, D. (2016). ESMO consensus guidelines for the management of patients with metastatic colorectal cancer. *Annals of Oncology*, *27*(8), 1386–1422. https://doi.org/10.1093/annonc/mdw235

Vega, M. C. M. D., Laviano, A., & Pimentel, G. D. (2016). Sarcopenia and chemotherapy-mediated toxicity. *Einstein (Sao Paulo, Brazil)*, *14*(4), 580–584. https://doi.org/10.1590/S1679-45082016MD3740

Walport, M. J. (2001a). Complement. First of two parts. *New England Journal of Medicine*, *344*(14), 1058–1066. https://doi.org/10.1056/NEJM200104053441406

Walport, M. J. (2001b). Complement. Second of two parts. *New England Journal of Medicine*, *344*(15), 1140–1144. https://doi.org/10.1056/NEJM200104123441506

Xue, H., Sawyer, M. B., Field, C. J., Dieleman, L. A., & Baracos, V. E. (2007). Nutritional modulation of antitumor efficacy and diarrhea toxicity related to irinotecan chemotherapy in rats bearing the ward colon tumor. *Clinical Cancer Research*, *13*(23), 7146–7154. https://doi.org/10.1158/1078-0432.CCR-07-0823

CHAPTER 2: COLON CANCER TREATMENT WITH FOLFIRI EXACERBATES MUSCLE FIBRE ATROPHY AND INDUCES A CATABOLIC TRANSCRIPTIONAL PROGRAM IN SKELETAL MUSCLE

2.1 Introduction

For almost two decades, it has been known that skeletal muscle atrophy resulting from a wide range of physiological and pathological conditions is controlled by a common transcriptional program of atrophy gene expression (*atrogins*) (Lecker et al., 2004). With the advent of increasingly comprehensive transcriptome profiling technologies, understanding of key players including master regulators and transcriptional factors that are fundamental in orchestrating this program has been substantially enhanced (Peris-Moreno et al., 2020, 2021; Taillandier & Polge, 2019). Malignant disease can invoke this atrophy gene transcriptional program in skeletal muscle (Baracos et al., 2018); however, this may be invoked by several factors in addition to the tumor. There is evidence for direct cytotoxicity of cancer therapies on muscle cells (Ahn et al., 2021; Campelj et al., 2020; Damaraju et al., 2018; VanderVeen et al., 2022). Multiple specific agents (5-FU, lenvatinib, CPT11, cisplatin, doxorubicin, imatinib, sorafenib, sunitinib, regorafenib, cabozantinib, rapamycin) activate intracellular signals and initiate a transcriptional program leading to autophagy and degradation of myofibrillar proteins. FOLFOX regimen-related myopathy has been studied in mice (Halle et al., 2022), however effects of multidrug regimens on human muscle are uncharacterized. Thus, we hypothesize that tumor and chemotherapy each elicit unique and quantitatively important effects in the development and progression of muscle wasting. It is not known how these inputs might cause evolution of gene expression in muscle over time,

owing to the sequential nature of the genesis and growth of tumor, diagnosis, and subsequent initiation of cycles of chemotherapy.

Low muscle mass associates with poorer responses to treatment and is independently prognostic for survival in patients with cancer (Daly et al., 2018; Järvinen et al., 2018; L. Martin et al., 2013). Developing a greater understanding of the transcriptional program driving muscle fibre atrophy in malignant disease is essential and requires analysis of patient skeletal muscle biopsies. However, due to the invasiveness of the procedure and ethical considerations, multiple biopsies over time are not feasible in vulnerable human populations (Anoveros-barrera et al., 2019). As such, a model which aligns with the clinical experience of patients with cancer, is required to define the respective effects of a tumor and chemotherapy, on transcriptional events in skeletal muscle. Here, we adopt a focus on colon cancer which is typically treated in advanced stage with regimens including 2 cytotoxic agents: 5-fluourouracil (5-FU) and irinotecan (CPT-11). In clinical studies, patients with colon cancers treated with these agents show rapid loss of skeletal muscle mass (Blauwhoff-Buskermolen et al., 2016; Jung et al., 2015).

2.2 Materials and Methods

2.2.1 Animal Model and Study Design

The preclinical animal model for tumor and chemotherapy-associated muscle loss used in this study, was developed by Cao and Rustum (Cao & Rustum, 2000). These authors developed a regimen of 5-FU and CPT-11 in the Fischer 344 rat bearing the Ward colorectal carcinoma, optimized in dose and schedule to confer a therapeutic index aligned with clinical experience in terms of tumor control and degree of treatment toxicity (Cao & Rustum, 2000). Briefly, the Ward

colorectal carcinoma (0.05g) was subcutaneously implanted on the flank of female Fischer 344 rats aged 11-12 weeks. The tumor was subcutaneously introduced to enable assessment of the rate of tumor growth and response to treatment. Cycles of treatment consisted of CPT-11 [50 mg/kg body weight, intraperitoneal], followed 24 h later 5-FU [50 mg/kg body weight, intraperitoneal]. This treatment is hereafter referred to as FOLFIRI. Atropine (1mg/kg body weight, subcutaneous) was administered prior to each CPT-11 injection to alleviate early onset cholinergic symptoms. Consistent with our prior studies with this model (Almasud et al., 2017; Xue et al., 2009) rats were provided a nutritionally complete diet based on the American Institute of Nutrition-76 wherein 40% of total energy is obtained from fat (polysaturated:saturated ratio of 0.35), 40% from carbohydrates and 20% from protein, which represents the estimated typical North American dietary pattern in patients with cancer (Xue et al., 2009).

Study Design. A schematic of the study is shown (Figure 2-1A). Healthy, tumor bearing, and tumor-bearing treated with FOLFIRI (n=8/group) were compared. Two weeks following tumor implantation (Day 0), rats were euthanized (TUMOR) or had 2 cycles of chemotherapy (TUMOR+FOLFIRI). The day of tumor implantation was specified as Day 0. Cycle-1 included CPT-11 [50 mg/kg body weight, intraperitoneal] administered on Day 14 and 5-FU [50 mg/kg body weight, intraperitoneal] administered on Day 15. Cycle-2 consisted of the same regimen occurring one week after cycle-1 [Days 21 and 22].

Skeletal muscle was assessed for atrophy in TUMOR and TUMOR+FOLFIRI, relative to HEALTHY rats. All skeletal muscle measures were conducted in the *gastrocnemius*. Transverse serial sections of muscle were visualized via Hematoxylin stain. The reference group (HEALTHY; n=8) did not undergo tumor implantation or receive FOLFIRI and were handled in the same

manner as the experimental groups. Carbon dioxide (CO_2) asphyxiation was used for euthanization of rats.

2.2.2 Skeletal Muscle Tissue & Fibre Cross Sectional Area (CSA)

Gastrocnemius muscle was dissected and handled as previously described (Almasud et al., 2017). To preserve morphological integrity, muscle was frozen in isopentane (2-methylbutane) cooled at −160°C in liquid nitrogen and stored at -80°C. Transverse serial sections (10 µm thickness) were obtained via cryosection (cryostat Leica model CM300) at −22°C and mounted onto Apex™ superior adhesive slides (Leica Biosystems). Hematoxylin stain was performed to visually delineate muscle fibres for CSA assessment (n=5 per group). Muscle sections were visualized with a ZEISS AXIO Compound Light Microscope (AX10 Scope A.1, Carl Zeiss Group, Toronto, ON, Canada) at 200× magnification. Images were collated with the color images taken with an Optronics MacroFire Digital Camera (Optronics, Goleta, CA, USA) using a Leica TCS-SP2 spectral confocal and multiphoton system (Leica Camera, Solms, Germany). Muscle fibre CSA from 200 fibres were evaluated and images were analyzed using Image J software.

2.2.3 Total RNA Extraction

Total RNA was extracted as previously described (Almasud et al., 2017), from *gastrocnemius* muscle (n=5 per group) using the MagMax-96 total RNA isolation Kit (Ambion, Austin, TX, USA) following the manufacturer's protocol. For assessing RNA quantity and quality,

a NanoDrop spectrophotometer (Thermo Scientific, Wilmington, DE) and Agilent 2100 Bioanalyzer (Agilent Technologies, Santa Clara, CA, USA) were used, respectively.

2.2.4 RNA Sequencing & Differential Expression (DE) Analysis

Services from PlantBiosis Ltd were used from library preparation to the generation of (.bam) files. RNA-seq libraries were prepared using TruSeq Stranded Total RNA with Ribo-Zero™ Human/Mouse/Rat, TruSeq Stranded Total RNA according to manufacturer's instructions. Total RNA (1µg per sample and a RIN value of >8.0) was used as an input material, depleted of rRNA and the remaining RNA was purified, fragmented and used for cDNA synthesis. Samples were sequenced on Illumina NextSeq 500 using high throughput 2x150 nt runs (bi-directional paired-end reads) with the density of 35 samples per flow cell to generate 10-13 million reads per sample. Base-calling and de-multiplexing was performed using 87 Illumina CASAVA 1.9 with default settings. Adapter trimming was done using Trim Galore v.0.4.1. Quality control of the sequenced reads was performed using FastQC v.0.11.4. Trimmed sequences were aligned to the rat reference genome using Tophat 2.0.10 with Bowtie2. Rat Genome (Rnor 6, Ensembl) was downloaded from the iGENOME website and served as a rat reference genome. Aligned sequences were saved as .sam files which were then converted to .bam files and were used for further data processing. Data analysis of the (.bam) files was performed using Partek Flow software. mRNAs were annotated using Ensembl Rattus norvegicus Rnor-6.0.92. Differential Expression analysis was performed using DEseq2 (Fold-change cut-off ≥1.5 and P-value<0.05.

2.2.5 Ingenuity Pathway Analysis – Canonical Pathways

Pathway analysis and functional annotation was conducted using Ingenuity Pathway Analysis®(IPA) ("Ingenuity Pathway Analysis," n.d.) (QIAGEN Inc). P-value in IPA is calculated using Fisher's exact test and determines the probability that the association between genes identified within a given pathway is explained by chance alone. -log(p-value) threshold of 1.3 (equivalent to a nominal p-value of 0.05) was used to define statistically significant pathways.

2.3 Results

2.3.1 Treatment with FOLFIRI controls tumor growth but exacerbates muscle atrophy and induces a second wave of transcriptional change in gastrocnemius muscle.

Both tumor and FOLFIRI elicited muscle fibre atrophy and their combined effect was substantial. After 14 days, the Ward colon tumor reached 0.89±0.17cm^3 (0.57±0.11% of body weight) and elicited a -22.2% ($p<0.05$) reduction in *gastrocnemius* fibre CSA, from 2607 μm^2 [95%CI=2387-2827, $p<0.05$] to 2030 μm^2 [95%CI=1543-2516, $p<0.05$] (Figure 2-1). Administration of 2 cycles of FOLFIRI treatment to tumor-bearing animals shrank the tumor by 89% ($p<0.01$) and elicited an additional 22% reduction in muscle fibre CSA (to 1579 μm^2 [95%CI=1135-2022, $p<0.05$] ($p<0.05$) (Figure 2-1B & C). These effects were specific to muscle; FOLFIRI-treated rats lost no more than 5% of baseline body weight during tumor growth and treatment cycles (Figure 2-1D). Weight loss occurred in the first 3 days after each cycle, followed by partial weight regain.

RNA sequencing analysis revealed 1283 differentially expressed (DE) transcripts ($p<0.05$) in tumor-bearing rats compared to healthy controls. These findings are summarized in Figure 2-2 wherein the top 30 (by p-value) most significant transcripts are presented (Figure 2-2C). While FOLFIRI shrank the tumor to a large extent, RNA sequencing analysis of muscles of treated animals showed a further large increase in the number of DE transcripts (n=2095, relative to healthy controls), a 63% increase relative to the number of DE transcripts elicited by tumor alone (Figure 2-2A); 1186 DE transcripts of these were unique to FOLFIRI treated rats.

2.3.2 Functional annotation of tumor and chemotherapy induced mRNA expression in gastrocnemius muscle

IPA functional annotation of the DE transcripts (summarized in Figure 2-3) revealed 40 DE canonical pathways ($p<0.05$) by TUMOR vs HEALTHY (Table 2-1). Functional annotation identified a total of n=69 DE canonical pathways following FOLFIRI treatment (Figure 2-3A & B, Table 2-2). The top 10 DE canonical pathways (by p-value) affected by TUMOR and TUMOR+FOLFIRI are presented in Figure 2-3C.

There was extensive DE elicited by the tumor alone. The tumor suppressive FOLFIRI regimen induced further DE in muscle, and this was in some cases occurring in pathways already altered by the tumor, while other pathways were uniquely altered by FOLFIRI. For example, the top DE canonical pathway associated with TUMOR was *adipogenesis*, while after FOLFIRI it was *protein ubiquitination*. However, *EIF2 Signaling* was identified as the second-most affected canonical pathway by tumor alone as well as TUMOR+FOLFIRI, compared to healthy control (Figure 2-3C). 13 transcripts corresponding to subunits of Eukaryotic Translation Initiation Factors

(EIF2, EIF3, EIF5) as well as 60 and 40S ribosomal subunits were upregulated by tumor with a sustained increased expression pattern with FOLFIRI treatment (Table 2-3). FOLFIRI induced upregulation of an additional 11 transcripts including those associated with subunits of EIF3 and EIF4, 60 and 40S ribosomal subunits as well as vascular endothelial growth factor A (VEGFA).

Based on IPA functional annotation, further details are provided in this section regarding the DE possibly or likely related to muscle atrophy.

2.3.2.1 Ubiquitin-dependent proteolysis

A common pathway by which intracellular proteins in skeletal muscle are degraded and which is activated during cancer-associated muscle catabolism, is the ubiquitin proteasome proteolytic system (Blackwell et al., 2018; Lecker et al., 2004). IPA analysis of TUMOR+FOLFIRI vs HEALTHY revealed the top pathway as *Protein Ubiquitination* (Figure 2-3C; Table 2-2). Of note, n=40 (70%) of transcripts encoding molecules in the *protein ubiquitination pathway* were differentially expressed following FOLFIRI treatment (Table 2-4). Transcript-level expression of multiple heat shock proteins including 9 members of the HSP40 family as well as other HSPs, ubiquitin conjugating enzymes as well as ubiquitin-specific peptidases (USPs) were upregulated following FOLFIRI treatment. Polyubiquitinated substrates are targeted to the 26S proteasome and rapidly degraded (Attaix et al., 1998). Expression of transcripts associated with proteasome subunits (proteasome 20S subunit alpha 4 (PSMA4)) and proteasome 26S subunit, ATPase 6 (PSMC6), were induced by FOLFIRI. Additionally, expression of E3 ubiquitin-protein ligase complex components including cullin 1 (CUL1) and ubiquitin protein ligase E3A (UBE3A), a key regulator of the ubiquitin-dependent catabolic program in skeletal muscle, was upregulated following FOLFIRI treatment. Compared with the pervasive

effect of FOLFIRI on the *protein ubiquitination pathway*, a relatively muted response was elicited by tumor alone. The canonical pathway did not meet criteria for statistical significance in TUMOR vs HEALTHY comparison. However, there were n=11 DE transcripts elicited by tumor, including Ubiquitin D, two proteasome subunits (PSMA4, PCMC6), CUL1, and several ubiquitin-specific peptidases. These were all up-regulated by tumor and their fold-increase were sustained or increased after FOLFIRI treatment.

2.3.2.2 Cell-death associated pathways: Death Receptor Signaling, Apoptosis Signaling and Necroptosis

IPA canonical pathway analysis revealed a predominant signal of pathways common to cellular death included *Death Receptor Signaling, Apoptosis Signaling* and *Necroptosis Signaling Pathway*, all ($p<0.01$) of which were induced by FOLFIRI treatment (Table 2-2); these canonical pathways did not meet criteria for statistical significance in the TUMOR vs HEALTHY comparison. Key regulators of apoptotic responses were increased following FOLFIRI treatment (Table 2-5). These included BCL2 apoptosis regulator, and BCL2 Associated Transcription Factor 1 (BCLAF1), a transcriptional repressor that interacts with several members of the BCL2 family of proteins to induce apoptosis (Yu et al., 2022). Concordantly, BCL1-antagonist/killer 1 (BAK1) was downregulated 1.5-fold following FOLFIRI treatment. In addition, transcripts encoding cysteine-aspartic acid protease (caspase) involved in the execution-phase of cell apoptosis, (CASP1) (Belizário et al., 2001; Riedl & Shi, 2004) was increased after FOLFIRI treatment. Similar to the *protein ubiquitination pathway*, there were nonetheless some DE transcripts in TUMOR versus healthy, including BCL2, BCLAF1 and CASP1. Transcripts encoding regulatory molecules of autophagy responses were upregulated by tumor and sustained after FOLFIRI

treatment. These included autophagy-related 3 (ATG3), a ubiquitin-like-conjugating enzyme involved in cell-death related autophagy (Parzych & Klionsky, 2014) 1.7-fold increase by tumor; this effect was sustained with a 2.0-fold DE after FOLFIRI treatment. Autophagy related 10 (ATG10) is an E2-like enzyme which catalyzes the conjugation of ATG12 to ATG5, which is essential for autophagosome formation; the expression of both ATG10 and ATG12 were each upregulated 1.6-fold by FOLFIRI and not tumor alone.

2.3.2.3 Unfolded protein response, amino acid catabolism and skeletal muscle-specific atrophy gene regulators are prominent after tumor growth and FOLFIRI treatment

The *Unfolded Protein Response* pathway was induced by FOLFIRI treatment, and this may be consistent with the effects noted for Ubiquitin proteasome and autophagy responses (Gallot & Bohnert, 2021). Branched chain amino acid metabolism is a well characterized sequala of muscle protein degradation and a part of the atrophy gene response (Eley et al., 2007). *Valine Degradation I* as well as *Branched-chain α-keto acid Dehydrogenase Complex (BCKDHC)* were also induced in muscles after FOLFIRI treatment (Table 2-2). Aldehyde dehydrogenase 6 family, member A1 (ALDH6A1) is implicated in catabolism of branched chain amino acids, including valine and was increased following tumor growth and FOLFIRI treatment (Table 2-6). In addition, subunits of BCKDHC, involved in metabolism of branched chain amino acids (valine, leucine, isoleucine) (Argilés & López-Soriano, 1991) including dihydrolipoamide branched chain transacylase E2 (DBT), were upregulated following FOLFIRI treatment.

DNA-damage inducible transcript 3 (DDIT3) is a multifunctional transcription factor which mediates ER-mediated cell death by promoting expression of genes involved in cellular

amino acid metabolic processes, mRNA translation and the unfolded protein response (UPR) in response to ER stress (Bohnert et al., 2016). Expression of DDIT3 in muscle was upregulated by tumor and by FOLFIRI treatment (Table 2-6). DDIT3 positively regulates the transcription of peptide inflammatory mediators of muscle wasting including interleukin-6 (IL-6), a key regulator of skeletal muscle as well as interleukin-8 (IL-8), which is associated with muscle wasting in gastroesophageal cancers (J. L. Chen et al., 2016; Krzystek-korpacka et al., 2007).

In addition to IL-6, proinflammatory cytokines including tumor necrosis factor alpha (TNFα) are primary catabolic mediators of muscle wasting and can induce transcription factors including nuclear factor-κB (NF-κB) to promote expression of E3 ubiquitin ligases and autophagy as well as pro-cachectic genes (Ma et al., 2017). NFKβ activating protein (NKAP) was increased 1.8-fold by FOLFIRI (Table 2-6). Members of the transforming growth factor-β (TGFβ) superfamily including activins and TGFβ are potent signaling molecule implicated in the development and progression of cancer-associated skeletal muscle atrophy (J. L. Chen et al., 2016). TGF-beta activated kinase 1 (MAP3K7) binding protein 3 (TAB3) can induce NFKβ activation (Mihaly & Morioka, 2014); TAB3 expression was increased to 2.3-fold by FOLFIRI treatment. The expression of both NKAP and TAB3 was also increased by tumor. In addition, FOLFIRI induced a 1.6-fold increase in expression of transforming growth factor beta receptor 1 (TGFBR1). The receptor of Activin A (ACVR1) was upregulated more than 7-fold following FOLFIRI treatment (Table 2-6).

2.3.2.4 Extracellular matrix (ECM)-related transcripts are modified by tumor and exacerbated by FOLFIRI treatment

Extracellular matrix pathways are a well-recognized element of the atrophy gene transcriptional response in skeletal muscle (A. Martin & Freyssenet, 2021). Fibrosis-related pathways including *Hepatic Fibrosis Signaling Pathway* and *Hepatic Fibrosis / Hepatic Stellate Cell Activation* as well as collagen-related including *GP6 Signaling Pathway* were DE after tumor as well as FOLFIRI treatment (Tables 2-1 & 2-2). Tumor growth resulted in downregulation of transcripts encoding fibrillar collagens including COL3A1, COL5A1, and COL5A3); this expression pattern was sustained following FOLFIRI treatment (Table 2-7). FOLFIRI treatment resulted in downregulation of additional structural fibrillar collagens such as (COL7A1, microfibrils (COL6A1, COL6A2) and extracellular matrix (ECM) proteins (COL18A1). Furthermore, major structural components of basement membranes were downregulated with tumor growth (COL4A1, COL4A3, COL4A4, COL4A5) and laminins (LAMB1, LAMC1); a sustained reduction was found after FOLFIRI treatment COL4A1, COL4A2, COL4A3, COL4A4, COL4A5) and laminin (LAMA2, LAMA4, LAMA5, LAMB1, LAMC1). FOLFIRI treatment also resulted in downregulation of transcripts encoding additional extracellular matrix components including the glycoprotein fibrillin 1 (FBN1) and components of connective tissue microfibrils (FBN2). Transcripts encoding alpha (ITGA) and beta (ITGB) subunits of integrin, an integral membrane protein involved in attachment of muscle tissue to ECM, display a similar pattern with downregulation by tumor (ITGAM, ITGB2, ITGB3), and by FOLFIRI treatment (ITGA8, ITGA11).

2.3.2.5 Transcriptional regulator profile aligns with differential expression and canonical pathways

We employed a function in IPA which permits assessment of a transcription factor profile that aligns with the DE and canonical pathway analysis (Table 2-8). Consistent with other transcriptional changes noted in the above sections, there were no common transcriptional regulatory elements identified in tumor-bearing and FOLFIRI-treated rats. There is a genesis of transcription that is quite specific to tumor and a distinct transcriptional genesis that is specific to FOLFIRI. Myogenic differentiation 1 (MYOD1) and paired box 7 (PAX7) are both muscle specific transcription factors that regulate myogenesis and myofibrillar repair (He et al., 2013; Yang et al., 2020). Consistent with findings at the transcription level, MYOD1 is uniquely downregulated by tumor whereas PAX7 is downregulated by tumor and sequential FOLFIRI treatment.

2.4 Discussion

Our results support and confirm the suspicion that there are skeletal-muscle specific side effects of antineoplastic therapy. Both the effect of the tumor and of the chemotherapy are unique and quantitatively important in the development and progression of muscle wasting. While most research on muscle wasting in cancer has focused on the direct and indirect effects of tumor, both clinical and experimental evidence suggest that treatment-related wasting is of substantial magnitude. It has been established that a complex tumor secretome contributes to cancer-associated muscle wasting, however, the skeletal muscle is also susceptible to direct damage by chemotherapy exposure (Schiessel & Baracos, 2018).

Presence of a tumor in addition to treatment with sequential cycles of chemotherapy results in a succession of changes in skeletal muscle, which are each unique and bring into the understanding that at each point along this trajectory, the muscle is responding dynamically; this means that a multitude of responses are turned on or off and this is not a steady state where a standardized set of biological functions are invoked. It is notable that effective tumor control in no way mitigated muscle atrophy; rather it substantially worsened it. Perhaps not surprisingly, given the cytotoxic nature of the molecules used in cancer therapy, a transcriptional signature of great complexity was induced in muscle by the combination of 5-FU and CPT-11.

We endeavored to better understand this signature using IPA and identified cellular pathways associated with tumor- and FOLFIRI-induced muscle wasting. Alterations indicate activation of the ubiquitin proteasome pathway by FOLFIRI treatment; this included increased expression of transcriptional regulators of E3 ubiquitin ligases, autophagy genes, multiple heat shock proteins (HSPs), ubiquitin conjugating enzymes, ubiquitin-specific peptidases (USPs) and

26S proteasome subunits. This is concordant with previous literature that have described the ubiquitin proteasome proteolytic system as one of the predominant underlying mechanisms involved in skeletal muscle degradation. To some extent these pathways appeared to have been launched, or primed, by the presence of the tumor, as the tumor bearing state consistently appeared to show early induction of pathway elements.

Consistent with effects noted for ubiquitin proteasome and autophagy signatures, FOLFIRI-associated pathways also included the unfolded protein response (UPR) and amino acid degradation and metabolism; these are well characterized sequelae of muscle protein degradation and as essential components of the atrophy gene response (Eley et al., 2007; Gallot & Bohnert, 2021). In addition to perturbations to cellular conditions which can lead to ER stress, the UPR may also be activated by chemicals including antineoplastic therapies such as cisplatin (R. Chen et al., 2011). The UPR is a mechanism to restore cellular homoeostasis, and its failure will lead to initiation of apoptosis. Interestingly, we find a prominent gene signature associated with FOLFIRI-treatment suggestive of cellular death via apoptosis and necroptosis.

Atrophy gene transcriptional response in skeletal muscle involves changes to various elements of cellular and tissue structure including the extracellular matrix and basement membranes. We identified negative regulation of several structural components by tumor and FOLFIRI, namely: integrins, fibrillar collagens, glycoproteins such as laminin, connective tissue proteins including microfibrils and integral membrane proteins. Taken together, these findings suggest adverse effects to cellular morphology and structure associated with activation of transcriptional programs contributing to muscle protein degradation and atrophy gene response which may be a consequence of FOLFIRI-associated toxicity.

Common toxicities associated with chemotherapy include myelosuppression, mucositis, nausea, vomiting, diarrhea, reduced food intake, alopecia, fatigue, sterility, infertility, and infusion reactions. Furthermore, there is an increased risk of infections due to immunosuppression. Muscle-specific side effects are, by contrast, much less considered. In the Common Terminology Criteria for Adverse Events (CTCAE), skeletal muscle is covered, however in a very limited fashion; specifically, myositis, "generalized muscle weakness", or weakness in specific in areas (e.g. limb, trunk, face, pelvic floor), myalgia, cramps, rhabdomyolysis and trismus. The notion of drug-specific adverse reactions taking place in muscle has not been within the lens of medical oncology, or toxicology. While toxicogenomics is a well-developed field (Fabian et al., 2011; Merrick & Bruno, 2004), it is one which is almost silent with respect to effects of cytotoxic antineoplastic therapies on skeletal muscle. It is interesting to consider our findings in light of the consensus view of toxicant-induced gene expression (Jennings et al., 2013); Jennings and coworkers discuss the potential of technologies such as transcriptomics to perform tissue-specific assessment to predict and better understand mechanistic and cellular responses to toxicity associated with pharmacological interventions. This may be the key to not only elucidate cellular pathways which have been perturbed, but more importantly, identify bio-signatures attributable to antineoplastic agents and muscle-specific toxicity.

Lack of attention to muscle – specific toxicity of cancer therapies would seem to be a deficiency, given that the magnitude of muscle losses reported in studies of patients is considerable. In a 2020 meta-analysis of 15 investigations, Jang et al. (2020) found a mean loss in skeletal muscle index during chemotherapy in males of -4.52 cm^2/m^2, 95%CI=3.34-5.71 and in females -2.86 cm^2/m^2, 95%CI=0.81-4.92. These losses were acute (over 50-200 days) encompassing a specific treatment plan. To put this in context, in a study of CT-defined muscle

mass in 1073 healthy kidney donors (Van Vugt et al. 2019) L3-MI of men between 20 and 60 years of age was lower by -1.53 cm^2/m^2 per decade of aging and for women this difference across the same age categories was -0.65 cm^2/m^2. Thus, muscle losses over 100 d of cancer therapy are of similar magnitude to at least 2 decades of age-related muscle loss.

The successive treatment of tumor is part of the clinical reality; however, the degree of tumor related progression as well as dose and total amount of chemotherapy that are permitted, are important considerations. Scale is also an important component of studying muscle wasting in animal models. To understand the response of muscle to tumor and chemotherapy, it is important to determine at what stage of tumor growth and at what dose and duration of chemotherapy this will be assessed. Scaling seems to not have been considered, generally, in animal models studying tumor- and chemotherapy-associated muscle wasting. In various animal models, study designs include tumor growth to extremely high burden (e.g. 10% body weight) leading to extreme muscle (-25%) and fat depletion (-90%) (Barreto, Mandili, et al., 2016; Sun et al., 2016; Tseng et al., 2015); these results are difficult to scale to the clinical reality.

Our inquiry was modeled on a specific regimen aligned with a specific tumor histologic type. The majority of earlier studies (Barreto, Mandili, et al., 2016; Barreto, Waning, et al., 2016) focused on single agent treatments in healthy animals. The effects of the tumor and chemotherapy occur simultaneously in the clinical setting. Although studying effects of a tumor and chemotherapy separately may be useful, it does not account for the possibility that they ineract with each other. A study conducted by Pin and coworkers (2019) is one of the few models which has included animals with healthy controls, tumor, just chemotherapy and both tumor and chemotherapy (5-FU and CPT-11) (Pin et al., 2019). The primary outcome of this study was

metabolomics based, not differential gene expression and this precludes direct comparison between the 2 studies. However, Pin et al. (2019) did observe specific effects associated with CPT-11 + 5-FU therapy, both in health and in C26 colon adenocarcinoma-bearing mice.

We attempted to model the treatment setting of locally advanced colon cancer, respecting tumor mass, regimen and schedule, treatment response and toxicity, as well as other factors, including diet. While it is not possible to align the exact magnitude of response to tumor and chemotherapy in our rats, with the clinical evolution of skeletal muscle wasting, our studies do reveal the additivity of tumor and treatment effects. Many important facets remain to be uncovered and further combinations, cancer types and therapy require testing. The potential prevention or reversibility of the changes that we documented in muscle are untested.

FIGURES

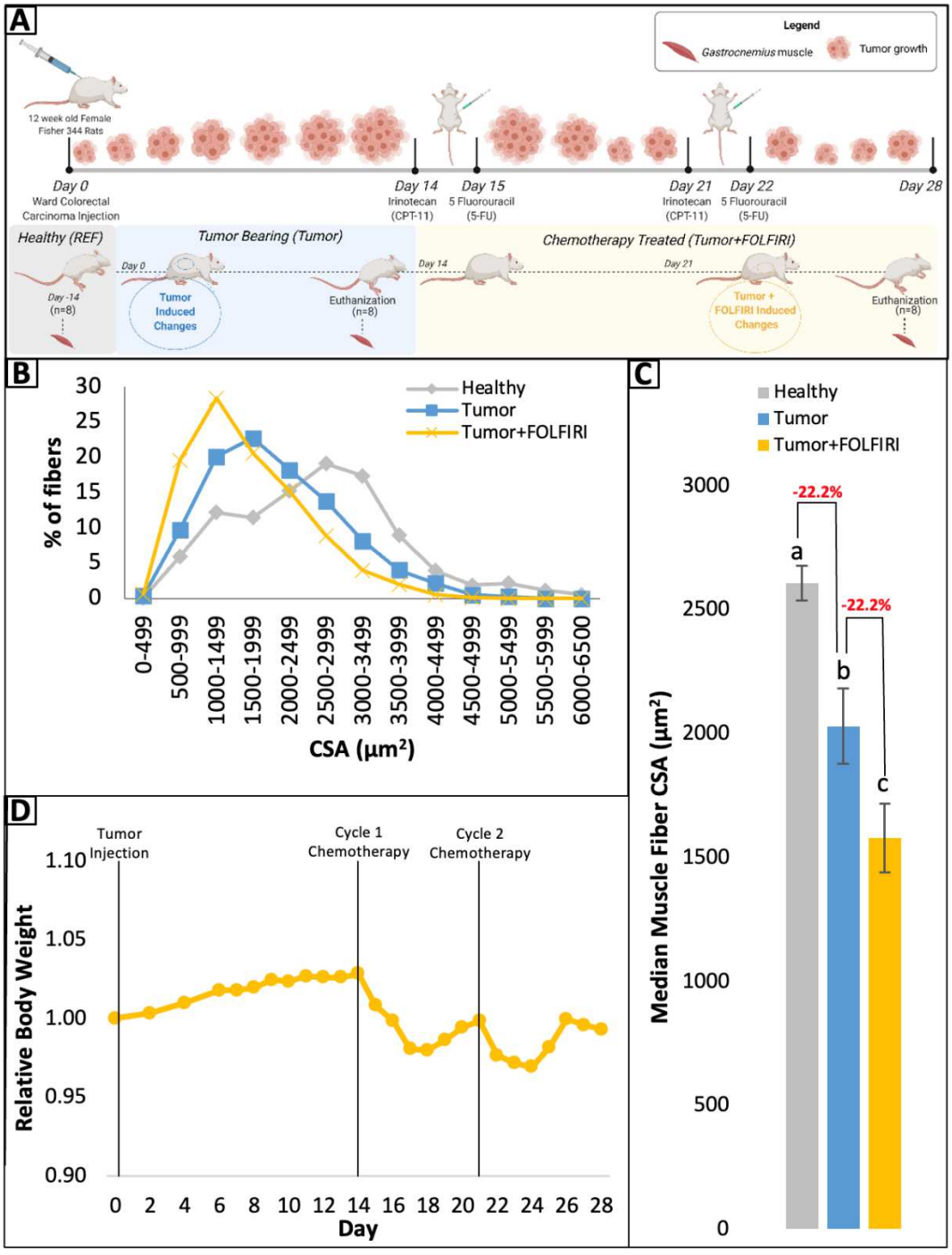

Figure 2-1. Phenotype of animal model of colon cancer and FOLFIRI treatment. A) Time course of study design. **B)** *Gastrocnemius* muscle fibre cross sectional area (CSA) distribution of healthy, tumor-bearing and FOLFIRI-treated animals. C) Average muscle fibre CSA; a,b denotes

difference at p<0.05 using Kruskal-Wallis ANOVA. Values presented as median±SE. D) Change in body weight of animals following tumor injection and sequential FOLFIRI treatments, relative to baseline. Figure 1A created using BioRender.

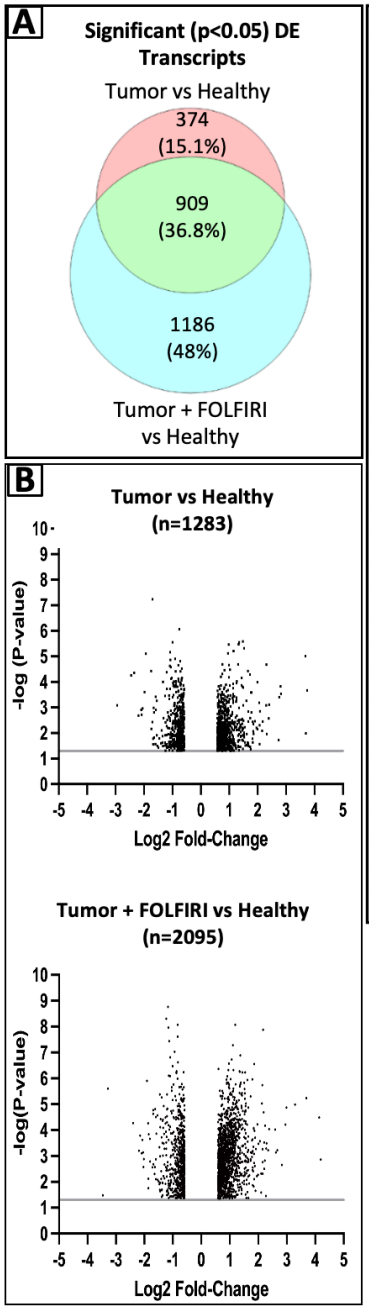

C

Tumor vs Healthy		
Gene Name	P-value	Log2 Fold-Change
LOC100912564	7.90E-06	-1.93
Hist1h2bo	3.73E-05	-1.75
Socs3	5.76E-08	-1.70
Castor1	2.33E-05	-1.09
Col5a3	6.94E-06	-1.08
Det1	1.38E-05	-1.07
Ankrd9	2.62E-05	-1.06
Col4a5	2.83E-06	-1.00
Tmem205	1.25E-05	-0.91
Col4a1	3.92E-05	-0.89
Tmem120a	2.26E-05	-0.79
Lrrc41	8.76E-07	-0.76
Eif2d	1.54E-05	-0.73
Cacng1	3.86E-05	-0.72
Fbxo6	3.05E-05	-0.67
AABR07027267.1	9.87E-06	3.68
Exph5	2.10E-05	2.31
Prmt6	3.74E-05	1.66
AABR07043748.1	4.76E-06	1.52
Esm1	2.54E-06	1.48
Cxadr	2.79E-06	1.35
Vtcn1	3.30E-06	1.33
Ofd1	2.06E-05	1.31
Tnnt1	6.14E-06	1.15
Mettl21c	3.30E-05	1.03
Myh7b	2.19E-05	0.99
Mecom	3.48E-06	0.98
Cep250	7.56E-06	0.95
Plekha1	3.46E-05	0.83
Arhgap29	2.06E-05	0.77

Tumor + FOLFIRI vs Healthy		
Gene Name	P-value	Log2 Fold-Change
Dusp1	5.00E-09	-1.23
Col4a5	1.74E-09	-1.17
Col4a1	1.09E-08	-1.16
Adcyap1r1	8.02E-07	-1.14
Col4a3	3.62E-08	-1.13
Cdyl	8.20E-07	-1.10
Lamb1	1.56E-07	-1.09
Col4a2	3.39E-07	-1.01
Tmem120a	9.29E-08	-0.94
Col4a4	6.32E-07	-0.88
Lamc1	5.80E-07	-0.87
Eya3	5.35E-07	-0.87
Get3	2.46E-08	-0.83
Lrrc41	8.53E-09	-0.83
Gpaa1	2.38E-07	-0.82
Atp1a2	5.75E-07	-0.62
Pin4	1.30E-08	2.17
Pts	2.80E-07	1.86
Ccdc88a	5.95E-07	1.54
Ofd1	5.87E-07	1.44
Rpl5	1.27E-07	1.37
Zrsr1	5.58E-07	1.35
Cetn2	5.40E-07	1.34
Rpl21	8.53E-09	1.19
Rap2c	4.77E-07	1.13
Ccdc127	5.30E-08	1.11
Mecom	1.84E-07	1.07
Rpl21	2.71E-07	0.97
Tomm7	4.78E-07	0.95
Rpl7	4.40E-07	0.61

Figure 2-2. Differential Gene Expression (DE) of skeletal muscle mRNA from tumor-bearing and FOLFIRI treated animals relative to healthy controls. A) Venn diagram of number of overlapping transcripts. B) Volcano plots of significant DE transcripts (fold-change cut-off ≥1.5 and p-value<0.05). C) Top 30 (by-p-value) most significant transcripts affected by tumor and tumor plus FOLFIRI.

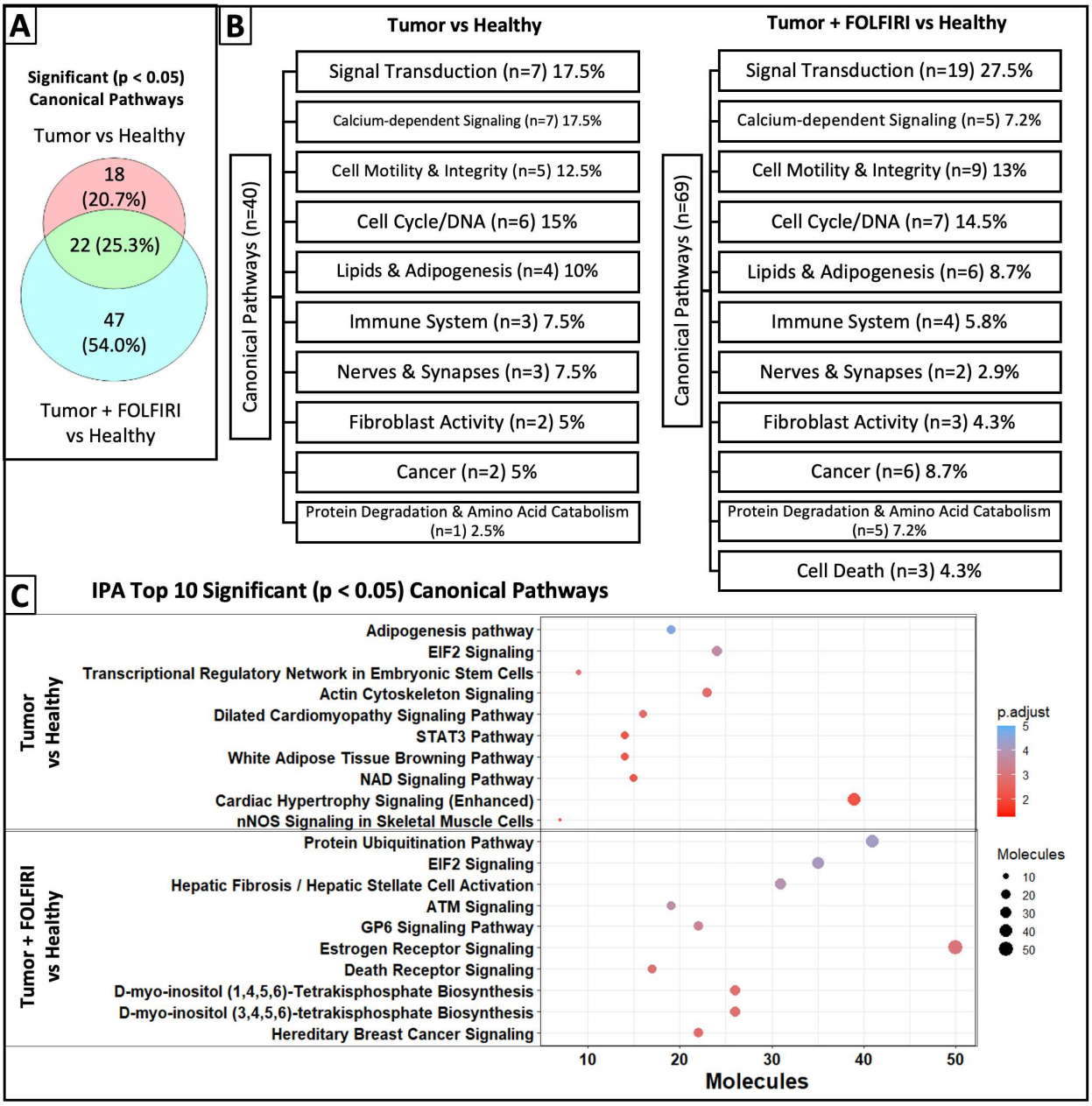

Figure 2-3. Ingenuity pathway analysis of canonical pathways affected by tumor and chemotherapy treatment. A) Venn diagram of number of unique and overlapping significant canonical pathways ($p < 0.05$). **B)** Canonical pathways categorized into common themes. **C)** Top 10 most significant pathways affected by tumor and tumor plus chemotherapy.

TABLES

Table 2-1. Tumor-bearing *versus* healthy rats – Ingenuity Pathway Analysis (IPA)® Canonical Pathways

Ingenuity Canonical Pathways	-log (p-value)	Molecules
Adipogenesis pathway	4.66	ARNTL,CEBPB,DDIT3,EZH2,FABP4,FBXW7,FGF1,FGFR2,FGFR3,HAT1,HDAC9,KLF3,KLF5,LEP,MNAT1,PLIN1,RBP1,SREBF1,TGFB1
EIF2 Signaling	3.74	ACTA1,BCL2,CDK11A,DDIT3,EIF1AX,EIF2AK2,EIF2S1,EIF2S2,EIF2S3,EIF3J,EIF5B,MYC,PIK3CB,RPL15,RPL21,RPL30,RPL4,RPL5,RPS10,RPS15,RPS24,RRAS,SREBF1,TRIB3
Transcriptional Regulatory Network in Embryonic Stem Cells	3.03	CDYL,H4C1,H4C14,H4C4,H4C6,H4C8,RIF1,SKIL,SMARCAD1
Actin Cytoskeleton Signaling	2.81	ACTA1,FGF1,FGF7,FGF9,IQGAP3,ITGAE,ITGAM,ITGB2,ITGB3,LIMK1,MYH10,MYH6,MYH7B,MYLK3,MYLPF,NCKAP1L,PIK3CB,Ppp1r12a,Ppp1r12b,RDX,ROCK1,RRAS,VAV2
Dilated Cardiomyopathy Signaling Pathway	2.79	ACTA1,ATP2A2,BCL2,CACNA1D,CACNA1S,CACNA2D3,CACNB4,CACNG1,DES,GNAS,MYH10, MYH6,MYH7B,SGCD,TNNC1,TNNT1
STAT3 Pathway	2.29	BCL2,CISH,EGFR,FGFR2,FGFR3,IL17RE,IL2RB,MAP3K10,MAP3K20,MYC,PIM1,RRAS,SOCS3,TGFB1
White Adipose Tissue Browning Pathway	2.27	ANGPT2,CACNA1D,CACNA1S,CACNA2D3,CACNB4,CACNG1,CEBPB,FGFR2,FGFR3,GNAS,LEP,PLIN1, PRKAB2,THRB
NAD Signaling Pathway	2.25	ACADM,ARNTL,CEBPB,DXO,H1f4,H2BC12,H2BC15,H2BC17,H2BC8,HSPD1,PIK3CB,PRKAB2,RYR3,SREBF1,TGFB1
Cardiac Hypertrophy Signaling (Enhanced)	2.2	ADRA1A,ADRA1D,ADRA2A,ATP2A2,CACNA1D,CACNA1S,CACNA2D3,CACNB4,CACNG1,ELK1,FGF1,FGF7,FGF9,FGFR2,FGFR3,GNAS,GNB1L,HDAC9,Il17d,IL17RE,IL2RB,ITGAE,ITGAM,ITGB2,ITGB3,LEP,MAP3K10,MAP3K20,MAPKAPK3,MYC,PIK3CB,ROCK1,RRAS,RYR3,TDP2,TGFB1,TNFSF13,WNT16,WNT4
nNOS Signaling in Skeletal Muscle Cells	2.14	CACNA1D,CACNA1S,CACNA2D3,CACNB4,CACNG1,RYR3,SNTB1
GP6 Signaling Pathway	2.12	APBB1IP,COL22A1,COL27A1,COL3A1,COL4A1,COL4A3,COL5A1,COL5A3,ITGB3,LAMB1,LAMC1,PIK3CB,VAV2
Calcium Signaling	2.12	ACTA1,ATP2A2,ATP2B1,CACNA1D,CACNA1S,CACNA2D3,CACNB4,CACNG1,CASQ2,GRIA4,HDAC9,MYH10,MYH6,MYH7B,RYR3,TNNC1, TNNT1,Tpm3,TRPC1

Bladder Cancer Signaling	2.03	DAPK1,EGFR,FGF1,FGF7,FGF9,FGFR3,HDAC9,MMP14,MMP19,MYC,RASSF1,RRAS
NER (Nucleotide Excision Repair, Enhanced Pathway)	2	CETN2,ERCC6,H4C1,H4C14,H4C4,H4C6,H4C8,MNAT1,POLD2,RFC1,TOP2A
Tumor Microenvironment Pathway	1.93	BCL2,COL3A1,CXCR4,FGF1,FGF7,FGF9,FOXO4,HLAA,ITGB3,LEP,MMP14,MMP19,MYC,PIK3CB,RRAS,TGFB1
Cellular Effects of Sildenafil (Viagra)	1.93	ACTA1,CACNA1D,CACNA1S,CACNA2D3,CACNB4,CACNG1,GNAS,KCNN1,MYH10,MYH6,MYH7B,MYLPF,Ppp1r12a,Ppp1r12b
Semaphorin Neuronal Repulsive Signaling Pathway	1.88	DPYSL3,ITGAE,ITGAM,ITGB2,ITGB3,LIMK1,MYLPF,PIK3CB,Ppp1r12a,Ppp1r12b,ROCK1,RRAS,SEMA3A,SMC3
ATM Signaling	1.77	CBX5,CDK1,FANCD2,H2AX,RAD50,SMC1A,SMC2,SMC3,TDP1,TLK2
Ferroptosis Signaling Pathway	1.77	ALOX5,ANGPTL4,CHAC1,FANCD2,H2AC18/H2AC19,H2AX,H2BC12,H2BC15,H2BC17,H2BC8,PRKAB2,RRAS
Hepatic Fibrosis Signaling Pathway	1.75	BCL2,CACNA1D,CACNA1S,CACNA2D3,CACNB4,CACNG1,CCDC88A,CEBPB,COL3A1,COL5A3,CSNK1G3,ELK1,EZH2,FOXO4,ITGAE,ITGAM,ITGB2,ITGB3,LEP,MYC,MYLK3,MYLPF,PIK3CB,Rhou,ROCK1,RRAS,TGFB1,TRPM7,WNT16,WNT4
Ephrin B Signaling	1.68	CXCR4,EFNB2,GNAS,GNB1L,ITSN2,LIMK1,ROCK1,VAV2
Amyotrophic Lateral Sclerosis Signaling	1.67	BCL2,CACNA1D,CACNA1S,CACNA2D3,CACNB4,CACNG1,CAPN7,CASP1,CYCS,GRIA4,PIK3CB
Regulation of Actin-based Motility by Rho	1.65	ACTA1,ITGAE,ITGAM,ITGB2,ITGB3,LIMK1,MYLPF,Ppp1r12a,Ppp1r12b,Rhou,ROCK1
Hepatic Fibrosis / Hepatic Stellate Cell Activation	1.63	BCL2,COL22A1,COL27A1,COL3A1,COL4A1,COL4A3,COL5A1,COL5A3,EGFR,FGF1,FGFR2,LEP,MYH10,MYH6,MYH7B,TGFB1
DNA Methylation and Transcriptional Repression Signaling	1.62	H4C1,H4C14,H4C4,H4C6,H4C8
Regulation of Cellular Mechanics by Calpain Protease	1.59	CAPN7,CCNE2,CDK1,EGFR,ITGAE,ITGAM,ITGB2,ITGB3,RRAS
Caveolar-mediated Endocytosis Signaling	1.59	ACTA1,CD55,EGFR,HLA-A,ITGAE,ITGAM,ITGB2,ITGB3
Complement System	1.53	C1QC,C7,CD55,ITGAM,ITGB2
Glycine Cleavage Complex	1.52	AMT,DLD
Signaling by Rho Family GTPases	1.49	ACTA1,ARFIP2,CDH2,DES,ELK1,GNAS,GNB1L,ITGAE,ITGAM,ITGB2,ITGB3,LIMK1,MAP3K10,MAP3K20,MYLPF,PIK3CB,RDX,Rhou,ROCK1,SEPTIN7
Coronavirus Pathogenesis Pathway	1.47	BCL2,CASP1,CCNE2,DDIT3,EEF1A2,ELK1,HDAC9,IRF3,NLRP3,NPM1,OAS1,RPS10,RPS15,RPS24,TGFB1,TRIM25
Role of Pattern Recognition Receptors in Recognition of Bacteria and Viruses	1.45	C1QC,CASP1,EIF2AK2,EIF2S1,Il17d,IRF3,LEP,NLRP3,OAS1,PIK3CB,TGFB1,TLR5,TNFSF13
Stearate Biosynthesis I (Animals)	1.41	ACOT7,PRXL2B,PTGR1,SLC27A6,TECR,THEM4
Cardiac Hypertrophy Signaling	1.4	ADRA1A,ADRA1D,ADRA2A,CACNA1D,CACNA1S,CACNA2D3,CACNB4,CACNG1,ELK1,GNAS,GNB1L,MAP3K10,MAPKAPK3,MYLPF,PIK3CB,Rhou,ROCK1,RRAS,TGFB1
Ceramide Degradation	1.39	ACER3,ASAH2
Cell Cycle: G1/S Checkpoint Regulation	1.37	CCNE2,CDKN2C,CUL1,HDAC9,MYC,RPL5,TGFB1

VEGF Signaling	1.34	ACTA1,BCL2,EIF1AX,EIF2S1,EIF2S2,EIF2S3,PIK3CB,ROCK1,RRAS
Senescence Pathway	1.33	CACNA1D,CACNA1S,CACNA2D3,CACNB4,CACNG1,CAPN7,CCNE2,CDC27,CDK1,CEBPB,DLD,EZH2,FOXO4,HIPK2,IRF3,ITSN2,MAPKAPK3,PIK3CB,RAD50,RRAS,TGFB1
Regulation of eIF4 and p70S6K Signaling	1.33	EIF1AX,EIF2S1,EIF2S2,EIF2S3,EIF3J,ITGAE,ITGAM,ITGB2,ITGB3,PIK3CB,RPS10,RPS15,RPS24,RRAS
Agrin Interactions at Neuromuscular Junction	1.32	ACTA1,EGFR,ERBB4,GABPA,LAMB1,LAMC1,RRAS

Table 2-2. Tumor-bearing – FOLFIRI *versus* healthy rats – Ingenuity Pathway Analysis (IPA)® Canonical Pathways

Ingenuity Canonical Pathways	**-log (p-value)**	**Molecules**
Protein Ubiquitination Pathway	4.27	CDC20,CRYAB,CUL1,DNAJA1,DNAJB9,DNAJC15,Dnajc19,DNAJC2,DNAJC21,DNAJC27,DNAJC28,DNAJC9,ELOC,HLA-A,HSCB,HSPB3,HSPB6,HSPB7,HSPD1,PSMA4,PSMB5,PSMC6,SACS,UBC,UBD,UBE2E2,UBE2K,UBE2O,UBE2Q2,UBE2V2,UBE3A,UCHL1,UCHL5,USP12,USP15,USP16,USP25,USP47,USP8,USP9X,ZBTB12
EIF2 Signaling	4.15	ACTA1,ACTA2,ACTG2,BCL2,CDK11A,DDIT3,EIF1AX,EIF2AK2,EIF2S1,EIF2S2,EIF2S3,EIF3A,EIF3E,EIF3J,EIF3M,EIF4A2,EIF5B,KRAS,PPP1CB,RAP1A,RPL12,RPL21,RPL23,RPL30,RPL4,RPL5,RPL7,RPL9,RPS10,RPS24,RPS25,RPS6,RPS8,RRAS,VEGFA
Hepatic Fibrosis / Hepatic Stellate Cell Activation	3.93	ACTA2,BCL2,CCR5,CD14,CERT1,COL18A1,COL3A1,COL4A1,COL4A2,COL4A3,COL5A1,COL5A2,COL5A3,COL6A1,COL6A2,COL7A1,COL8A1,EGFR,FGF1,FLT4,FN1,IGFBP3,LEP,MMP2,MYH9,NGFR,PDGFRA,PDGFRB,RELB,TGFBR1,VEGFA
ATM Signaling	3.77	ATR,CBX3,CBX5,CREB5,GADD45A,GADD45G,H2AX,NBN,PPM1L,PPP2R5A,RAD17,RAD50,RBBP8,RNF168,SMC1A,SMC2,SMC3,TLK2,TP53
GP6 Signaling Pathway	3.46	APBB1IP,CERT1,COL18A1,COL3A1,COL4A1,COL4A2,COL4A3,COL5A1,COL5A2,COL5A3,COL6A1,COL6A2,COL7A1,COL8A1,GSK3A,LAMA2,LAMA4,LAMA5,LAMB1,LAMC1,NCK1,TLN1
Estrogen Receptor Signaling	3.03	ATP5MC1,BCL2,CACNA1A,CACNA1S,CACNA2D3,CACNG1,CARM1,CREB5,DDX5,EGFR,FOS,FOXO4,FOXO6,GNB4,GSK3A,HNRNPD,JAK2,KRAS,LEP,LIMK1,MED21,MMP14,MMP15,MMP2,NCOR1,NDUFA4,NDUFA5,NDUFB3,NDUFS4,NDUFS8,NOTCH1,NR0B2,NR3C1,PLCL2,PPP1CB,Ppp1r12a,PRKAB2,PRKAR2B,RAP1A,RELB,ROCK1,ROCK2,RPS6KB1,RRAS,RUNX2,SDHD,SRC,TP53,VEGFA,ZDHHC21

Death Receptor Signaling	2.91	ACTA1,ACTA2,ACTG2,BCL2,CYCS,DFFB,HSPB3,HSPB7,LIMK1,LMNA,MAP3K5,NFKBIB,PARP2,RELB,ROCK1,TANK,TNFRSF25
D-myo-inositol (1,4,5,6)-Tetrakisphosphate Biosynthesis	2.88	ALPL,ATP1A2,CA3,CILP,DOT1L,DUSP1,DUSP14,DUSP4,G6PC3,NUDT2,PPM1L,PPP1CB,PPP1R14C,PPP1R3A,PPP2R5A,PTPN2,PTPN23,PTPRC,PTPRO,RASA1,RNGTT,SACM1L,SET,SOCS3,SSH1,UBLCP1
D-myo-inositol (3,4,5,6)-tetrakisphosphate Biosynthesis	2.88	ALPL,ATP1A2,CA3,CILP,DOT1L,DUSP1,DUSP14,DUSP4,G6PC3,NUDT2,PPM1L,PPP1CB,PPP1R14C,PPP1R3A,PPP2R5A,PTPN2,PTPN23,PTPRC,PTPRO,RASA1,RNGTT,SACM1L,SET,SOCS3,SSH1,UBLCP1
Hereditary Breast Cancer Signaling	2.79	ATR,BRCA2,FAAP100,GADD45A,GADD45G,H2AX,HDAC9,KRAS,NBN,NPM1,PBRM1,POLR2A,POLR2K,RAD50,RAP1A,RFC1,RRAS,SLC19A1,TP53,UBC,UBD,WEE1
Caveolar-mediated Endocytosis Signaling	2.72	ACTA1,ACTA2,ACTG2,CD55,EGFR,FLNA,FLNC,HLA-A,ITGA11,ITGA8,ITGAE,RAB5A,SRC,ZBTB12
STAT3 Pathway	2.71	BCL2,EGFR,FLT4,GHR,IL17RD,JAK2,KRAS,MAP3K10,MAP3K20,NGFR,NTRK3,PDGFRA,PDGFRB,PTPN2,RAP1A,RRAS,SOCS3,SOCS6,SRC,TGFBR1,VEGFA
Hepatic Fibrosis Signaling Pathway	2.69	ACTA2,ACVR1C,ACVR2B,APC,APC2,BCL2,CACNA1A,CACNA1S,CACNA2D3,CACNG1,CCDC88A,COL18A1,COL3A1,COL5A3,CREB5,CSNK1G3,ELK1,EZH2,FLT4,FOS,FOXO4,FTL,FZD2,ITGA11,ITGA8,ITGAE,JAK2,KRAS,LEP,LRP1,MYLK3,NFKBIB,NGFR,PDGFRA,PDGFRB,PPARG,PRKAR2B,RAP1A,RELB,Rhou,ROCK1,ROCK2,RPS6KB1,RRAS,SDHD,TGFBR1,TRPM7,VEGFA,WNT16,WNT4
Oleate Biosynthesis II (Animals)	2.65	ALDH6A1,FADS1,FADS2,SCD,UFSP2
NER (Nucleotide Excision Repair, Enhanced Pathway)	2.57	CETN2,Cops2,GTF2H1,GTF2H2,H4C1,H4C14,H4C4,H4C6,H4C8,MNAT1,NEDD8,POLR2A,POLR2K,RFC1,SLC19A1,TCEA1,XPA
3-phosphoinositide Degradation	2.47	ALPL,ATP1A2,CA3,CILP,DOT1L,DUSP1,DUSP14,DUSP4,G6PC3,NUDT2,PPM1L,PPP1CB,PPP1R14C,PPP1R3A,PPP2R5A,PTPN2,PTPN23,PTPRC,PTPRO,RASA1,RNGTT,SACM1L,SET,SOCS3,SSH1,UBLCP1
Role of BRCA1 in DNA Damage Response	2.45	ABRAXAS1,ATR,BRCA2,BRCC3,E2F5,FAAP100,GADD45A,NBN,PBRM1,RAD50,RBBP8,RFC1,SLC19A1,TP53
Unfolded protein response	2.37	BCL2,CEBPG,CEBPZ,DDIT3,DNAJA1,DNAJA2,DNAJB9,DNAJC15,DNAJC21,DNAJC9,ERO1B,MAP3K5,PPARG,SCAP,SREBF2
Role of CHK Proteins in Cell Cycle Checkpoint Control	2.36	ATR,E2F5,NBN,PPM1L,PPP2R5A,RAD17,RAD50,RFC1,SLC19A1,TLK2,TP53
VEGF Signaling	2.36	ACTA1,ACTA2,ACTG2,BCL2,EIF1AX,EIF2S1,EIF2S2,EIF2S3,FLT4,KRAS,RAP1A,ROCK1,ROCK2,RRAS,SRC,VEGFA
D-myo-inositol-5-phosphate Metabolism	2.35	ALPL,ATP1A2,CA3,CILP,DOT1L,DUSP1,DUSP14,DUSP4,G6PC3,NUDT2,PPM1L,PPP1CB,PPP1R14C,PPP1R3A,PPP2R5A,PTPN2,PTPN23,PTPRC,PTPRO,RASA1,RNGTT,SACM1L,SET,SOCS3,SSH1,UBLCP1
Sirtuin Signaling Pathway	2.32	ATG10,ATG12,ATG3,ATP5MC1,CLOCK,DOT1L,FOXO4,GABPA,GADD45A,GADD45G,GLS,H1f4,NBN,NDUFA4,NDUFA5,NDUFB3,NDUFS4,NDUFS8,PCK1,PDHA1,POLR

		1C,PPARG,PPID,RBBP8,RELB,SDHD,SMARCA5,TIMM44,TOMM20,Tomm5,TOMM7,TOMM70,TP53,TUBA4A,VDAC3,XPA
Necroptosis Signaling Pathway	2.24	AXL,CAPN5,CAPN6,CAPN7,CASP1,CYLD,DNM1L,EIF2AK2,IRF3,NGFR,PLA2G4B,PPID,RNF31,TIMM44,TOMM20,Tomm5,TOMM7,TOMM70,TP53,TRPM7,UBC,VDAC3
PTEN Signaling	2.16	BCAR1,BCL2,EGFR,FLT4,FOXO4,FOXO6,GHR,GSK3A,ITGA11,ITGA8,ITGAE,KRAS,NGFR,NTRK3,PDGFRA,PDGFRB,RAP1A,RELB,RPS6KB1,RRAS,TGFBR1
Regulation of eIF4 and p70S6K Signaling	2.16	EIF1AX,EIF2S1,EIF2S2,EIF2S3,EIF3A,EIF3E,EIF3J,EIF3M,EIF4A2,ITGA11,ITGA8,ITGAE,KRAS,PAIP2,PPM1L,PPP2R5A,RAP1A,RPS10,RPS24,RPS25,RPS6,RPS6KB1,RPS8,RRAS
Virus Entry via Endocytic Pathways	2.15	ACTA1,ACTA2,ACTG2,AP1S2,AP2A1,AP3S1,CD55,CXADR,FLNA,FLNC,HLA-A,KRAS,RAP1A,RRAS,SRC,ZBTB12
Apoptosis Signaling	2.15	BAK1,BCL2,CAPN5,CAPN6,CAPN7,CYCS,DFFB,KRAS,LMNA,MAP3K5,NFKBIB,RAP1A,RELB,ROCK1,RRAS,TP53
Stearate Biosynthesis I (Animals)	2.12	ACOT7,DBT,DHCR24,LPGAT1,PTGR1,PTGR2,SLC27A3,SLC27A6,TECR,THEM4
Agrin Interactions at Neuromuscular Junction	2.1	ACTA1,ACTA2,ACTG2,EGFR,GABPA,KRAS,LAMA2,LAMB1,LAMC1,RAP1A,RRAS,SRC
RHOA Signaling	2.09	ACTA1,ACTA2,ACTG2,ARHGAP5,ARPC5L,LIMK1,LPAR6,MYLK3,PLXNA1,PPP1CB,Ppp1r12a,RAPGEF6,RDX,ROCK1,ROCK2,SEPTIN5,SEPTIN7,SEPTIN9
3-phosphoinositide Biosynthesis	2.06	ALPL,ATP1A2,CA3,CILP,DOT1L,DUSP1,DUSP14,DUSP4,G6PC3,NUDT2,PPM1L,PPP1CB,PPP1R14C,PPP1R3A,PPP2R5A,PTPN2,PTPN23,PTPRC,PTPRO,RASA1,RNGTT,SACM1L,SET,SOCS3,SSH1,UBLCP1
WNT/β-catenin Signaling	2.05	ACVR1C,ACVR2B,APC,APC2,APPL1,AXIN2,CSNK1G3,FZD2,GSK3A,LRP1,PPARD,PPM1L,PPP2R5A,RARA,SOX17,SOX8,SRC,TGFBR1,TP53,UBC,UBD,WNT16,WNT4
Actin Cytoskeleton Signaling	1.99	ACTA1,ACTA2,ACTG2,APC,APC2,ARPC5L,BCAR1,CD14,FGF1,FGF18,FGF7,FLNA,FN1,GIT1,ITGA11,ITGA8,ITGAE,KRAS,LIMK1,MYH9,MYLK3,PPP1CB,Ppp1r12a,RAP1A,RDX,ROCK1,ROCK2,RRAS,SSH1,TLN1
Senescence Pathway	1.98	ACVR1C,ACVR2B,ANAPC13,ATR,CACNA1A,CACNA1S,CACNA2D3,CACNG1,CAPN5,CAPN6,CAPN7,CCNE2,CDC27,CDKN2B,DHCR24,DLD,E2F5,EZH2,FOXO4,GADD45A,GADD45G,IRF3,ITSN2,KRAS,MAPKAPK3,NBN,NFATC2,PDHA1,PPM1L,PPP2R5A,RAD50,RAP1A,RRAS,TGFBR1,TP53
Epithelial Adherens Junction Signaling	1.94	ACVR1C,ACVR2B,ARPC5L,EGFR,FARP2,FGF1,KRAS,LIMK1,NECTIN1,NOTCH1,NOTCH2,NOTCH3,PPM1L,PPP2R5A,PRKAB2,RAP1A,ROCK1,ROCK2,RRAS,SRC,TGFBR1
Mitotic Roles of Polo-Like Kinase	1.88	ANAPC13,CDC20,CDC27,ESPL1,PPM1L,PPP2R5A,SLK,SMC1A,SMC3,STAG2,WEE1
Acetyl-CoA Biosynthesis I (Pyruvate Dehydrogenase Complex)	1.88	DBT,DLD,PDHA1
Ceramide Degradation	1.88	ACER2,ACER3,ASAH2

Tumor Microenvironment Pathway	1.88	BCL2,CD274,COL3A1,CSPG4,FGF1,FGF18,FGF7,FN1,FOS,FOXO4,FOXO6,HLA-A,JAK2,KRAS,LEP,MMP14,MMP15,MMP2,PLAU,RAP1A,RELB,RRAS,VEGFA
Apelin Liver Signaling Pathway	1.87	APLNR,COL18A1,COL3A1,COL5A3,GSK3A,PDGFRB
Coronavirus Pathogenesis Pathway	1.78	ADAM17,BCL2,CASP1,CCNE2,DDIT3,E2F5,EEF1A2,ELK1,FOS,FURIN,HDAC9,IRF3,IRF7,NFKBIB,NPM1,RELB,RPS10,RPS24,RPS25,RPS6,RPS8,TGFBR1,TOMM70,TP53,TRIM25
GADD45 Signaling	1.77	ATR,CCNE2,GADD45A,GADD45G,TP53
Valine Degradation I	1.77	ACADSB,ALDH6A1,DBT,DLD,HIBCH
ERK/MAPK Signaling	1.76	BCAR1,CREB5,DUSP1,DUSP4,ELK1,FOS,HSPB3,HSPB7,ITGA11,ITGA8,ITGAE,KRAS,MKNK2,PLA2G4B,PPARG,PPM1L,PPP1CB,PPP1R14C,PPP1R3A,PPP2R5A,PRKAR2B,RAP1A,RRAS,SRC,TLN1,VRK2
Amyotrophic Lateral Sclerosis Signaling	1.75	BCL2,CACNA1A,CACNA1S,CACNA2D3,CACNG1,CAPN5,CAPN6,CAPN7,CASP1,CYCS,GRIA4,NOS1,RAB5A,SSR4,TP53,VEGFA
DNA Double-Strand Break Repair by Homologous Recombination	1.7	ATRX,BRCA2,NBN,RAD50
Interferon Signaling	1.69	BAK1,BCL2,IFI35,IFIT3,ISG15,JAK2,PTPN2
FAK Signaling	1.68	ACTA1,ACTA2,ACTG2,BCAR1,CAPN5,CAPN6,CAPN7,EGFR,ITGA11,ITGA8,ITGAE,KRAS,RAP1A,RRAS,SRC,TLN1
Regulation of Cellular Mechanics by Calpain Protease	1.67	CAPN5,CAPN6,CAPN7,CCNE2,EGFR,ITGA11,ITGA8,ITGAE,KRAS,RAP1A,RRAS,SRC,TLN1
NGF Signaling	1.65	CREB5,ELK1,KRAS,MAP3K10,MAP3K5,MAP3K6,NGFR,RAP1A,RELB,ROCK1,ROCK2,RPS6KA3,RPS6KB1,RRAS,TP53,TRAF4
Transcriptional Regulatory Network in Embryonic Stem Cells	1.63	CDYL,H4C1,H4C14,H4C4,H4C6,H4C8,RIF1,SET,SMARCAD1
Superpathway of Inositol Phosphate Compounds	1.59	ALPL,ATP1A2,CA3,CILP,DOT1L,DUSP1,DUSP14,DUSP4,G6PC3,NUDT2,Ppip5k2,PPM1L,PPP1CB,PPP1R14C,PPP1R3A,PPP2R5A,PTPN2,PTPN23,PTPRC,PTPRO,RASA1,RNGTT,SACM1L,SET,SOCS3,SSH1,UBLCP1
Sphingosine and Sphingosine-1-phosphate Metabolism	1.55	ACER2,ACER3,ASAH2
CDK5 Signaling	1.54	CACNA1A,KRAS,LAMA2,LAMA5,LAMB1,LAMC1,NGFR,PPM1L,PPP1CB,PPP1R14C,PPP1R3A,PPP2R5A,PRKAR2B,RAP1A,RRAS
IL-15 Production	1.5	AXL,CLK1,Clk4,DDR2,EGFR,FLT4,IRF3,JAK2,NTRK3,PDGFRA,PDGFRB,RELB,RET,RYK,SRC,TEC
nNOS Signaling in Skeletal Muscle Cells	1.49	CACNA1A,CACNA1G,CACNA1S,CACNA2D3,CACNG1,NOS1,SNTB1,SNTB2
Branched-chain α-keto acid Dehydrogenase Complex	1.48	DBT,DLD
Sertoli Cell-Sertoli Cell Junction Signaling	1.47	ACTA1,ACTA2,ACTG2,BCAR1,CLDN19,ELK1,GSK3A,ITGA11,ITGA8,ITGAE,KRAS,MAP3K10,MAP3K20,MAP3K5,MAP3K6,NECTIN1,NOS1,PALS2,PRKAR2B,RAP1A,RRAS,SRC,SYMPK,TUBA4A

Kinetochore Metaphase Signaling Pathway	1.45	ANAPC13,CDC20,CDC27,CENPC,ESPL1,H2AC18/H2AC19,H2AX,PPP1CB,PPP1R14C,PPP1R3A,PPP2R5A,SMC1A,SMC3,STAG2
Bladder Cancer Signaling	1.42	E2F5,EGFR,FGF1,FGF18,FGF7,HDAC9,KRAS,MMP14,MMP15,MMP2,RAP1A,RASSF1,RRAS,TP53,VEGFA
Pancreatic Adenocarcinoma Signaling	1.42	BCL2,BRCA2,CCNE2,CDKN2B,E2F5,EGFR,ELK1,HDAC9,JAK2,KRAS,NOTCH1,PLD4,RELB,TGFBR1,TP53,VEGFA
FAT10 Cancer Signaling Pathway	1.4	ACVR1C,ACVR2B,NFKBIB,NGFR,RELB,TGFBR1,TP53,UBD
Paxillin Signaling	1.36	ACTA1,ACTA2,ACTG2,ARFIP2,BCAR1,ITGA11,ITGA8,ITGAE,KRAS,NCK1,RAP1A,RRAS,SRC,TLN1
p38 MAPK Signaling	1.36	CREB5,DDIT3,DUSP1,ELK1,HSPB3,HSPB7,MAP3K5,MAPKAPK3,MEF2C,MKNK2,PLA2G4B,RPS6KA3,RPS6KB1,TGFBR1,TP53
UVC-Induced MAPK Signaling	1.36	ATR,EGFR,FOS,KRAS,RAP1A,RRAS,SRC,TP53
Integrin Signaling	1.33	ACTA1,ACTA2,ACTG2,ARHGAP5,ARPC5L,BCAR1,CAPN5,CAPN6,CAPN7,GIT1,ITGA11,ITGA8,ITGAE,KRAS,MYLK3,NCK1,PPP1CB,Ppp1r12a,RAP1A,Rhou,ROCK1,RRAS,SRC,TLN1
γ-linolenate Biosynthesis II (Animals)	1.32	FADS1,FADS2,SLC27A3,SLC27A6
Oxidative Phosphorylation	1.31	ATP5MC1,ATP5MF,ATPAF1,COX4I2,Cox6c,COX7B,CYCS,DMAC2L,NDUFA4,NDUFA5,NDUFB3,NDUFS4,NDUFS8,SDHD
Insulin Secretion Signaling Pathway	1.31	CACNA1A,CACNA1G,CACNA1S,CACNA2D3,CACNG1,CREB5,DLD,EIF2S1,EIF2S2,EIF2S3,EIF4A2,FURIN,GHR,GPAA1,JAK2,PDHA1,PLCL2,PRKAR2B,RAP1A,RPS6KB1,SEC11C,SPCS3,SRC,SRP14,SRP19,SRP54,SRP9,SSR4,STX16

Table 2-3. Transcripts involved in the *EIF2 Signaling Pathway* – Translational Regulation.

Gene	Gene Description	TUMOR vs HEALTHY		TUMOR+FOLFIRI HEALTHY	
		P-value	Fold change	P-value	Fold change
TRIB3	tribbles pseudokinase 3	4.74E-02	**2.10**		
PIK3CB	phosphatidylinositol-4,5-bisphosphate 3-kinase, catalytic subunit beta	4.48E-03	**1.76**		
RPL15	ribosomal protein L15	2.74E-04	-1.51		
RPS15	ribosomal protein S15	6.57E-04	-1.54		
SREBF1	sterol regulatory element binding transcription factor 1	2.37E-02	-1.96		
MYC	MYC proto-oncogene, bHLH transcription factor	6.28E-03	-2.24		
EIF2AK2	eukaryotic translation initiation factor 2-alpha kinase 2	2.70E-03	**1.96**	1.17E-04	**2.34**
RPL5	ribosomal protein L5	1.28E-03	**1.83**	1.27E-07	**2.59**
RPL21	ribosomal protein L21	4.52E-04	**1.73**	8.53E-09	**2.28**
EIF2S2	eukaryotic translation initiation factor 2 subunit beta	1.62E-02	**1.72**	9.19E-05	**2.28**
RPL30	ribosomal protein L30	9.28E-04	**1.71**	4.18E-06	**2.01**
EIF3J	eukaryotic translation initiation factor 3, subunit J	3.80E-02	**1.62**	3.35E-04	**2.18**
EIF5B	eukaryotic translation initiation factor 5B	4.39E-02	**1.61**	3.76E-02	**1.60**
EIF2S1	eukaryotic translation initiation factor 2 subunit alpha	1.82E-03	**1.58**	2.58E-05	**1.83**
RPS24	ribosomal protein S24	9.57E-03	**1.54**	3.24E-06	**2.14**
EIF2S3	eukaryotic translation initiation factor 2 subunit gamma	4.10E-03	**1.53**	2.11E-04	**1.67**
RPL4	ribosomal protein L4	8.26E-03	**1.51**	1.78E-06	**1.97**
DDIT3	DNA-damage inducible transcript 3	4.92E-02	**1.50**	6.32E-03	**1.68**
RRAS	RAS related	2.25E-04	-1.72	2.63E-03	-1.51
ACTA1	actin, alpha 1, skeletal muscle	1.12E-03	-1.73	9.95E-04	-1.70
CDK11A		NS		NS	
EIF1AX	eukaryotic translation initiation factor 1A, X-linked	NS		NS	
RPS10	ribosomal protein S10	NS		NS	
EIF4A2	eukaryotic translation initiation factor 4A2			6.87E-03	**1.66**
KRAS	KRAS proto-oncogene, GTPase			1.24E-02	**1.65**
PPP1CB	protein phosphatase 1 catalytic subunit beta			1.19E-03	**1.65**
RPS8	ribosomal protein S8			4.77E-06	**1.59**
RPS25	ribosomal protein s25			2.68E-05	**1.57**
EIF3M	eukaryotic translation initiation factor 3, subunit M			1.45E-03	**1.54**
EIF3A	eukaryotic translation initiation factor 3, subunit A			1.94E-02	**1.53**
RPL7	ribosomal protein L7			4.40E-07	**1.52**
VEGFA	vascular endothelial growth factor A			1.06E-02	**1.52**
RPL23	ribosomal protein L23			3.70E-04	**1.52**
RAP1A	RAP1A, member of RAS oncogene family			1.34E-02	**1.51**
ACTA2	actin alpha 2, smooth muscle			1.35E-04	-2.10
ACTG2	actin gamma 2, smooth muscle			2.30E-02	-2.72
EIF3E				NS	
RPL12	ribosomal protein L12			NS	
RPL9	ribosomal protein L9			NS	
RPS6	ribosomal protein S6			NS	

Table 2-4. Transcripts involved in the *Protein Ubiquitination Pathway*.

Gene	Gene Description	TUMOR vs HEALTHY		TUMOR+FOLFIRI HEALTHY	
		P-value	Fold Change	P-value	Fold Change
UBD	ubiquitin D	1.57E-03	3.44	3.73E-03	3.03
USP16	ubiquitin specific peptidase 16	1.78E-02	1.79	5.37E-04	2.26
UCHL5	ubiquitin C-terminal hydrolase L5	1.72E-02	1.69	2.04E-05	2.48
PSMA4	proteasome 20S subunit alpha 4	1.07E-02	1.59	3.59E-04	1.90
USP15	ubiquitin specific peptidase 15	2.54E-02	1.59	1.51E-03	1.83
USP8	ubiquitin specific peptidase 8	3.19E-03	1.57	2.17E-03	1.54
USP47	ubiquitin specific peptidase 47	3.09E-02	1.54	4.01E-03	1.73
HSPD1	heat shock protein family D (Hsp60) member 1	1.46E-02	1.54	4.69E-05	2.00
PSMC6	proteasome 26S subunit, ATPase 6	3.39E-02	1.51	7.13E-04	1.91
DNAJC9	DnaJ heat shock protein family (Hsp40) member C9	1.82E-02	1.51	2.60E-03	1.68
CUL1	cullin 1	7.13E-03	1.50	1.50E-04	1.72
UBE2V2	ubiquitin conjugating enzyme E2 V2			9.98E-04	2.95
DNAJC21	DnaJ heat shock protein family (Hsp40) member C21			4.28E-03	2.42
DNAJC2	DnaJ heat shock protein family (Hsp40) member C2			3.29E-03	2.34
UCHL1	ubiquitin C-terminal hydrolase L1			4.22E-02	2.13
Dnajc19	DnaJ heat shock protein family (Hsp40) member C19			1.31E-05	2.11
DNAJA1	DnaJ heat shock protein family (Hsp40) member A1			1.61E-02	1.97
DNAJC28	DnaJ heat shock protein family (Hsp40) member C28			5.24E-03	1.81
ELOC	elongin C			5.31E-04	1.73
UBE2K	ubiquitin-conjugating enzyme E2K			1.56E-05	1.72
UBE2Q2	ubiquitin conjugating enzyme E2 Q2			6.74E-03	1.70
DNAJB9	DnaJ heat shock protein family (Hsp40) member B9			1.27E-02	1.62
DNAJC15	DnaJ heat shock protein family (Hsp40) member C15			2.68E-04	1.60
SACS	sacsin molecular chaperone			9.37E-03	1.60
HSCB	HscB mitochondrial iron-sulfur cluster co-chaperone			2.21E-02	1.59
HSPB3	heat shock protein family B (small) member 3			5.73E-03	1.57
USP25	ubiquitin specific peptidase 25			2.94E-03	1.57
DNAJC27	DnaJ heat shock protein family (Hsp40) member C27			1.98E-04	1.53
USP12	ubiquitin specific peptidase 12			5.25E-03	1.53
UBE3A	ubiquitin protein ligase E3A			9.46E-03	1.52
USP9X	ubiquitin specific peptidase 9, X-linked			9.10E-03	1.51
PSMB5	proteasome 20S subunit beta 5			2.61E-04	-1.50
UBC	ubiquitin C			5.79E-03	-1.52
HSPB6	heat shock protein family B (small) member 6			5.76E-03	-1.53
UBE2O	ubiquitin-conjugating enzyme E2O			3.35E-04	-1.63
CRYAB	crystallin, alpha B			6.36E-03	-1.68
HSPB7	heat shock protein family B (small) member 7			3.02E-02	-1.74
UBE2E2	ubiquitin-conjugating enzyme E2E 2			2.71E-05	-1.75
CDC20	cell division cycle 20	3.85E-02	-2.05	2.58E-02	-2.00
ZBTB12	zinc finger and BTB domain containing 12			6.27E-03	-2.31

Table 2-5. Transcripts involved in cell death-associated signaling including *Death Receptor Signaling, Necroptosis Signaling Pathway, Apoptosis Signaling* and Autophagy.

Gene	Gene Description	TUMOR vs HEALTHY		TUMOR+FOLFIRI vs HEALTHY	
		P-value	Fold change	P-value	Fold change
Atg3	autophagy related 3	3.80E-03	1.71	5.28E-05	2.02
Bclaf1	BCL2-associated transcription factor 1	3.01E-02	1.54	2.68E-03	1.77
Bcl2	BCL2, apoptosis regulator	2.28E-02	2.01	8.09E-03	2.29
Capn7	calpain 7	7.86E-04	1.55	1.72E-04	1.59
Casp1	caspase 1	4.00E-02	1.65	1.24E-03	2.23
Cyld	CYLD lysine 63 deubiquitinase	5.41E-04	1.65	2.56E-04	1.69
Cycs	cytochrome c, somatic	1.35E-02	1.59	4.30E-05	2.05
Eif2ak2	eukaryotic translation initiation factor 2-alpha kinase 2	2.70E-03	1.96	1.17E-04	2.34
Irf3	interferon regulatory factor 3	9.69E-03	1.67	5.23E-03	1.76
Pla2g4b	phospholipase A2 group IVB	1.08E-02	1.91	1.07E-02	1.87
Rock1	Rho-associated coiled-coil containing protein kinase 1	7.69E-03	1.78	7.07E-04	2.02
Trpm7	transient receptor potential cation channel, subfamily M, member 7	1.78E-02	1.55	2.08E-03	1.74
Timm44	translocase of inner mitochondrial membrane 44	1.93E-02	1.63	1.28E-03	1.86
Tomm5	translocase of outer mitochondrial membrane 5	9.42E-03	1.77	6.23E-05	2.29
Atg10	autophagy related 10			4.27E-02	1.59
Atg12	autophagy related 12			3.40E-04	1.60
Dnm1l	dynamin 1-like			1.28E-03	1.68
Hspb3	heat shock protein family B (small) member 3			5.73E-03	1.57
Kras	KRAS proto-oncogene, GTPase			1.24E-02	1.65
Ppid	peptidylprolyl isomerase D			1.82E-03	2.26
Rap1a	RAP1A, member of RAS oncogene family			1.34E-02	1.51
Tnfrsf25	TNF receptor superfamily member 25			8.30E-03	3.01
Tank	TRAF family member-associated NFKB activator			7.90E-04	1.82
Tomm20	translocase of outer mitochondrial membrane 20			1.59E-04	1.57
Tomm7	translocase of outer mitochondrial membrane 7			4.78E-07	1.93
Tomm70	translocase of outer mitochondrial membrane 70			1.57E-03	1.54
Vdac3	voltage-dependent anion channel 3			2.33E-04	1.74
Acta2	actin alpha 2, smooth muscle			1.35E-04	-2.10
Actg2	actin gamma 2, smooth muscle			2.30E-02	-2.72
Acta1	actin, alpha 1, skeletal muscle	1.12E-03	-1.73	9.95E-04	-1.70
Axl	Axl receptor tyrosine kinase			9.48E-03	-1.52
Bak1	BCL2-antagonist/killer 1			5.34E-03	-1.52
Capn5	calpain 5			1.20E-02	-1.73
Capn6	calpain 6			6.81E-03	-1.78
Dffb	DNA fragmentation factor subunit beta			1.29E-02	-1.54
Hspb7	heat shock protein family B (small) member 7			3.02E-02	-1.74
Lmna	lamin A/C			5.80E-04	-1.59
Limk1	LIM domain kinase 1	4.73E-03	-1.65	2.24E-05	-2.05
Map3k5	mitogen-activated protein kinase kinase kinase 5			1.22E-04	-1.58
Ngfr	nerve growth factor receptor			2.11E-03	-3.20
Nfkbib	NFKB inhibitor beta			5.56E-04	-1.51

Parp2	poly (ADP-ribose) polymerase 2			1.88E-03	-1.82
Rras	RAS related	2.25E-04	-1.72	2.63E-03	-1.51
Relb	RELB proto-oncogene, NF-kB subunit			3.29E-03	-1.53
Rnf31	ring finger protein 31			3.75E-05	-1.73
Tp53	tumor protein p53			2.57E-04	-1.54
Ubc	ubiquitin C			5.79E-03	-1.52

Table 2-6. Transcripts involved in the *Unfolded Protein Response pathway* and metabolism of myofibril-derived amino acids including *Valine Degradation I* and *Branched-chain α-keto acid Dehydrogenase Complex (BCKDHC)* pathways.

Gene Name	Gene Description	TUMOR vs HEALTHY		TUMOR+FOLFIRI vs HEALTHY	
		P-value	Fold change	P-value	Fold change
Aldh6a1	aldehyde dehydrogenase 6 family, member A1	1.48E-04	**1.54**	2.69E-04	**1.50**
Bcl2	BCL2, apoptosis regulator	2.28E-02	**2.01**	8.09E-03	**2.29**
Ddit3	DNA-damage inducible transcript 3	4.92E-02	**1.50**	6.32E-03	**1.68**
Dld	dihydrolipoamide dehydrogenase	3.52E-02	**1.54**	1.63E-03	**1.86**
Dnajc9	DnaJ heat shock protein family (Hsp40) member C9	1.82E-02	**1.51**	2.60E-03	**1.68**
Ero1b	endoplasmic reticulum oxidoreductase 1 beta	3.02E-04	**2.20**	9.79E-05	**2.27**
Nkap	NFKB activating protein	8.77E-03	**1.62**	1.22E-03	**1.77**
Tab3	TGF-beta activated kinase 1 (MAP3K7) binding protein 3	3.46E-03	**1.89**	1.94E-04	**2.32**
Scap	SREBF chaperone	2.66E-03	-1.53	1.45E-04	-1.69
Acvr1c	activin A receptor type 1C			2.22E-03	**7.10**
Acadsb	acyl-CoA dehydrogenase, short/branched chain			8.14E-05	**1.82**
Cebpg	CCAAT/enhancer binding protein gamma			3.18E-03	**1.65**
Cebpz	CCAAT/enhancer binding protein zeta			6.60E-03	**1.62**
Dbt	dihydrolipoamide branched chain transacylase E2			1.96E-04	**1.68**
Dnaja1	DnaJ heat shock protein family (Hsp40) member A1			1.61E-02	**1.97**
Dnaja2	DnaJ heat shock protein family (Hsp40) member A2			2.17E-04	**1.60**
Dnajb9	DnaJ heat shock protein family (Hsp40) member B9			1.27E-02	**1.62**
Dnajc15	DnaJ heat shock protein family (Hsp40) member C15			2.68E-04	**1.60**
Dnajc21	DnaJ heat shock protein family (Hsp40) member C21			4.28E-03	**2.42**
Tgfbr1	Transforming growth factor, beta receptor 1			1.64E-03	**1.57**
Hibch	3-hydroxyisobutyryl-CoA hydrolase			1.17E-03	**1.67**
Pparg	peroxisome proliferator-activated receptor gamma			3.03E-02	**1.66**
Map3k5	mitogen-activated protein kinase kinase kinase 5			1.22E-04	-1.58
Srebf2	sterol regulatory element binding transcription factor 2			7.28E-06	-1.55

Table 2-7. Transcripts involved in modification of the extracellular matrix including *Hepatic Fibrosis/ Hepatic Stellate Cell Activation, GP6 Signaling Pathway, Apelin Liver Signaling Pathway* and *Hepatic Fibrosis Signaling Pathway*.

Gene Name	Gene Description	TUMOR vs HEALTHY		TUMOR+FOLFIRI vs HEALTHY	
		P-value	Fold change	P-value	Fold change
Cacna2d3	calcium voltage-gated channel auxiliary subunit alpha2delta 3	1.19E-02	**2.86**	3.54E-03	**3.13**
Csnk1g3	casein kinase 1, gamma 3	1.66E-02	**1.52**	4.99E-03	**1.61**
Ccdc88a	coiled coil domain containing 88A	3.61E-04	**2.26**	5.95E-07	**2.91**
Ezh2	enhancer of zeste 2 polycomb repressive complex 2 subunit	6.21E-03	**2.31**	6.04E-04	**2.59**
Fgf1	fibroblast growth factor 1	4.85E-03	**1.55**	4.14E-04	**1.64**
Itgae	integrin subunit alpha E	3.77E-02	**1.64**	2.42E-03	**1.93**
Lep	leptin	1.02E-02	**13.04**	1.38E-03	**18.39**
Mylk3	myosin light chain kinase 3	3.08E-02	**2.25**	3.65E-02	**2.24**
Rhou	ras homolog family member U	1.60E-02	**1.52**	3.02E-03	**1.67**
Rock1	Rho-associated coiled-coil containing protein kinase 1	7.69E-03	**1.78**	7.07E-04	**2.02**
Trpm7	transient receptor potential cation channel, subfamily M, member 7	1.78E-02	**1.55**	2.08E-03	**1.74**
Wnt16	Wnt family member 16	7.68E-03	**2.24**	3.61E-03	**2.28**
Apbb1ip	amyloid beta precursor protein binding family B member 1 interacting protein	4.28E-03	-1.81	1.33E-02	-1.60
Cacng1	calcium voltage-gated channel auxiliary subunit gamma 1	3.86E-05	-1.64	2.27E-05	-1.62
Cacna1s	calcium voltage-gated channel subunit alpha1 S	1.22E-03	-1.67	8.48E-05	-1.80
Col3a1	collagen type III alpha 1 chain	1.88E-04	-2.12	1.58E-05	-2.30
Col4a1	collagen type IV alpha 1 chain	3.92E-05	-1.85	1.09E-08	-2.23
Col4a3	collagen type IV alpha 3 chain	3.49E-04	-1.70	3.62E-08	-2.18
Col5a1	collagen type V alpha 1 chain	7.49E-03	-1.75	5.87E-04	-2.02
Col5a3	collagen type V alpha 3 chain	6.94E-06	-2.12	3.90E-05	-1.86
Egfr	epidermal growth factor receptor	1.44E-03	-1.51	3.03E-04	-1.54
Elk1	ETS transcription factor ELK1	1.20E-04	-1.84	3.19E-05	-1.84
Lamb1	laminin subunit beta 1	6.06E-04	-1.70	1.56E-07	-2.13
Lamc1	laminin subunit gamma 1	1.39E-03	-1.51	5.80E-07	-1.83
Rras	RAS related	2.25E-04	-1.72	2.63E-03	-1.51
Wnt4	Wnt family member 4	1.12E-02	-1.77	1.29E-02	-1.68
Cacnb4	calcium voltage-gated channel auxiliary subunit beta 4	2.49E-02	**2.15**		
Cacna1d	calcium voltage-gated channel subunit alpha1 D	2.64E-02	**1.78**		
Col22a1	collagen type XXII alpha 1 chain	4.16E-03	**1.63**		
Col27a1	collagen type XXVII alpha 1 chain	1.96E-02	**1.65**		
Fgfr2	fibroblast growth factor receptor 2	4.37E-02	**1.77**		
Foxo4	forkhead box O4	3.84E-03	**1.64**		
Myh10	myosin heavy chain 10	5.38E-03	**1.55**		
Myh6	myosin heavy chain 6	3.09E-03	**1.81**		
Myh7b	myosin heavy chain 7B	2.19E-05	**1.99**		
Pik3cb	phosphatidylinositol-4,5-bisphosphate 3-kinase, catalytic subunit beta	4.48E-03	**1.76**		
Cebpb	CCAAT/enhancer binding protein beta	1.82E-02	-1.59		
Itgam	integrin subunit alpha M	3.41E-03	-1.81		

Itgb2	integrin subunit beta 2	3.54E-02	-1.62		
Itgb3	integrin subunit beta 3	2.73E-02	-1.67		
Myc	MYC proto-oncogene, bHLH transcription factor	6.28E-03	-2.24		
Mylpf	myosin light chain, phosphorylatable, fast skeletal muscle	4.23E-03	-1.51		
Tgfb1	transforming growth factor, beta 1	2.31E-02	-1.76		
Vav2	vav guanine nucleotide exchange factor 2	3.66E-03	-1.70		
Acvr1c	activin A receptor type 1C			2.22E-03	**7.10**
Apc	APC regulator of WNT signaling pathway			1.28E-02	**1.50**
Ccr5	C-C motif chemokine receptor 5			7.87E-03	**2.21**
Cert1	ceramide transporter 1			7.58E-04	**1.68**
Foxo4	forkhead box O4			4.03E-04	**1.74**
Igfbp3	insulin-like growth factor binding protein 3			2.85E-03	**1.64**
Jak2	Janus kinase 2			7.48E-03	**1.55**
Kras	KRAS proto-oncogene, GTPase			1.24E-02	**1.65**
Nck1	NCK adaptor protein 1			6.44E-03	**1.51**
Pparg	peroxisome proliferator-activated receptor gamma			3.03E-02	**1.66**
Prkar2b	protein kinase cAMP-dependent type II regulatory subunit beta			1.55E-02	**2.62**
Rap1a	RAP1A, member of RAS oncogene family			1.34E-02	**1.51**
Rock2	Rho-associated coiled-coil containing protein kinase 2			2.08E-03	**2.21**
Rps6kb1	ribosomal protein S6 kinase B1			1.70E-03	**1.96**
Sdhd	succinate dehydrogenase complex subunit D			2.02E-04	**1.68**
Tgfbr1	transforming growth factor, beta receptor 1			1.64E-03	**1.57**
Vegfa	vascular endothelial growth factor A			1.06E-02	**1.52**
Acta2	actin alpha 2, smooth muscle			1.35E-04	-2.10
Acvr2b	activin A receptor type 2B			4.20E-02	-1.51
Apc2	APC regulator of WNT signaling pathway 2			3.46E-05	-1.94
Aplnr	apelin receptor			1.03E-03	-1.64
Cacna1a	calcium voltage-gated channel subunit alpha1 A			1.03E-02	-1.58
Creb5	cAMP responsive element binding protein 5			2.65E-02	-1.54
Cd14	CD14 molecule			1.16E-02	-1.66
Col4a2	collagen type IV alpha 2 chain			3.39E-07	-2.01
Col5a2	collagen type V alpha 2 chain			1.15E-05	-1.72
Col6a1	collagen type VI alpha 1 chain			6.96E-04	-1.74
Col6a2	collagen type VI alpha 2 chain			8.97E-04	-1.81
Col7a1	collagen type VII alpha 1 chain			1.90E-04	-2.65
Col8a1	collagen type VIII alpha 1 chain			3.56E-02	-1.64
Col18a1	collagen type XVIII alpha 1 chain			5.67E-03	-1.61
Fn1	fibronectin 1			7.13E-03	-1.70
Flt4	fms-related tyrosine kinase 4			3.08E-02	-1.50
Fos	Fos proto-oncogene, AP-1 transcription factor subunit			1.61E-02	-1.58
Fzd2	frizzled class receptor 2			3.62E-02	-1.74
Gsk3a	glycogen synthase kinase 3 alpha			6.08E-06	-1.52
Itga11	integrin subunit alpha 11			1.30E-03	-1.69
Itga8	integrin subunit alpha 8			5.79E-03	-1.62
Lama2	laminin subunit alpha 2			2.17E-06	-1.71
Lama4	laminin subunit alpha 4			1.50E-04	-1.55
Lama5	laminin subunit alpha 5			1.94E-05	-1.67
Lrp1	LDL receptor related protein 1			7.99E-03	-1.66
Mmp2	matrix metallopeptidase 2			3.48E-03	-1.55
Ngfr	nerve growth factor receptor			2.11E-03	-3.20

Nfkbib	NFKB inhibitor beta	5.56E-04	-1.51
Pdgfra	platelet derived growth factor receptor alpha	1.11E-03	-1.53
Pdgfrb	platelet derived growth factor receptor beta	2.13E-04	-1.58
Relb	RELB proto-oncogene, NF-kB subunit	3.29E-03	-1.53
Tln1	talin 1	4.06E-04	-1.61

Table 2-8. Transcriptional regulators affected by tumor and FOLFIRI.

TUMOR vs HEALTHY	**Description**	**Fold Change**	**p-value**
PURA	purine rich element binding protein A	**1.99**	4.39E-02
FOXO4	forkhead box O4	**1.64**	5.34E-03
EIF2S1	eukaryotic translation initiation factor 2 subunit alpha	**1.58**	1.83E-02
SKIL	SKI-like proto-oncogene	**1.57**	2.24E-02
ZBTB17	zinc finger and BTB domain containing 17	**-1.54**	2.23E-02
CEBPB	CCAAT/enhancer binding protein beta	**-1.59**	1.34E-07
MYOD1	myogenic differentiation 1	**-1.75**	1.11E-05
SREBF1	sterol regulatory element binding transcription factor 1	**-1.96**	1.27E-02
MYC	MYC proto-oncogene, bHLH transcription factor	**-2.24**	1.61E-02
TUMOR+FOLFIRI vs HEALTHY	**Description**	**Fold Change**	**p-value**
SUB1	SUB1 regulator of transcription	**1.91**	2.92E-02
NFYB	nuclear transcription factor Y subunit beta	**1.81**	1.68E-02
MEF2C	myocyte enhancer factor 2C	**1.78**	7.29E-03
SUPT16H	SPT16 homolog, facilitates chromatin remodeling subunit	**1.73**	4.30E-03
MBD2	methyl-CpG binding domain protein 2	**1.53**	3.06E-01
TP53	tumor protein p53	**-1.54**	5.92E-05
NOTCH1	notch receptor 1	**-1.7**	2.48E-02
NAB2	Ngfi-A binding protein 2	**-1.8**	4.53E-03
NOTCH3	notch receptor 3	**-1.98**	3.38E-03
RUNX2	RUNX family transcription factor 2	**-2.05**	3.62E-03
PAX7	paired box 7	**-2.34**	3.75E-02

LITERATURE CITED

Ahn, K. H., Kim, S., Yang, M., & Lee, D. W. (2021). A Pillar-Based High-Throughput Myogenic Differentiation Assay to Assess Drug Safety. *Molecules*, *26*(19), 5805. https://doi.org/10.3390/molecules26195805

Almasud, A. A., Giles, K. H., Miklavcic, J. J., Martins, K. J. B., Baracos, V. E., Putman, C. T., Guan, L. L., & Mazurak, V. C. (2017). Fish oil mitigates myosteatosis and improves chemotherapy efficacy in a preclinical model of colon cancer. *PLoS ONE*, *12*(8), 1–17. https://doi.org/10.1371/journal.pone.0183576

Anoveros-barrera, A., Bhullar, A. S., Stretch, C., Esfandiari, N., Dunichand-hoedl, A. R., Karen, J. B., Bigam, D., Khadaroo, R. G., Mcmullen, T., Bathe, O. F., Damaraju, S., Richard, J., Putman, C. T., Baracos, V. E., & Mazurak, V. C. (2019). *Clinical and biological characterization of skeletal muscle tissue biopsies of surgical cancer patients*. *December 2018*, 1356–1377. https://doi.org/10.1002/jcsm.12466

Argilés, J. M., & López-Soriano, F. J. (1991). The energy state of tumor-bearing rats. *Journal of Biological Chemistry*, *266*(5), 2978–2982. https://doi.org/10.1016/S0021-9258(18)49943-7

Attaix, D., Aurousseau, E., Combaret, L., Kee, A., Larbaud, D., Rallière, C., Souweine, B., Taillandier, D., & Tilignac, T. (1998). *Ubiquitin-proteasome-dependent proteolysis in skeletal muscle*.

Baracos, V. E., Martin, L., Korc, M., Guttridge, D. C., & Fearon, K. C. H. (2018). Cancer-associated cachexia. *Nature Reviews Disease Primers*, *4*(1), 1–18. https://doi.org/10.1038/nrdp.2017.105

Barreto, R., Mandili, G., Witzmann, F. A., Novelli, F., Zimmers, T. A., & Bonetto, A. (2016). Cancer and chemotherapy contribute to muscle loss by activating common signaling pathways. *Frontiers in Physiology*, *7*(OCT), 1–13. https://doi.org/10.3389/fphys.2016.00472

Barreto, R., Waning, D. L., Gao, H., Liu, Y., Zimmers, T. A., & Bonetto, A. (2016). Chemotherapy-related cachexia is associated with mitochondrial depletion and the activation of ERK1/2 and p38 MAPKs. *Oncotarget*, *7*(28), 43442–43460. https://doi.org/10.18632/oncotarget.9779

Belizário, J. E., Lorite, M. J., & Tisdale, M. J. (2001). *Proteases in skeletal muscles from mice undergoing cancer cachexia*. *84*, 1135–1140.

Blackwell, T. A., Cervenka, I., Khatri, B., Brown, J. L., Rosa-Caldwell, M. E., Lee, D. E., Perry, R. A., Brown, L. A., Haynie, W. S., Wiggs, M. P., Bottje, W. G., Washington, T. A., Kong, B. C., Ruas, J. L., & Greene, N. P. (2018). Transcriptomic analysis of the development of skeletal muscle atrophy in cancer-cachexia in tumor-bearing mice. *Physiological Genomics*, *50*(12), 1071–1082. https://doi.org/10.1152/physiolgenomics.00061.2018

Blauwhoff-Buskermolen, S., Versteeg, K. S., De Van Der Schueren, M. A. E., Den Braver, N. R., Berkhof, J., Langius, J. A. E., & Verheul, H. M. W. (2016). Loss of muscle mass during chemotherapy is predictive for poor survival of patients with metastatic colorectal cancer. *Journal of Clinical Oncology*, *34*(12), 1339–1344. https://doi.org/10.1200/JCO.2015.63.6043

Bohnert, K. R., Gallot, Y. S., Sato, S., Xiong, G., Hindi, S. M., & Kumar, A. (2016). *Inhibition of ER stress and unfolding protein response pathways causes skeletal muscle wasting during cancer cachexia*. *9*, 3053–3068. https://doi.org/10.1096/fj.201600250RR

Campelj, D. G., Timpani, C. A., Petersen, A. C., Hayes, A., Goodman, C. A., & Rybalka, E. (2020). The Paradoxical Effect of PARP Inhibitor BGP-15 on Irinotecan-Induced Cachexia and Skeletal Muscle Dysfunction. *Cancers*, *12*(12), 3810. https://doi.org/10.3390/cancers12123810

Cao, S., & Rustum, Y. M. (2000). Synergistic antitumor activity of irinotecan in combination with 5-fluorouracil rats bearing advanced colorectal cancer: Role of drug sequence and dose. *Cancer Research*, *60*(14), 3717–3721.

Chen, J. L., Walton, K. L., Qian, H., Colgan, T. D., Hagg, A., Watt, M. J., Harrison, C. A., & Gregorevic, P. (2016). *Differential Effects of IL6 and Activin A in the Development of Cancer-Associated Cachexia*. *76*(18), 5372–5382. https://doi.org/10.1158/0008-5472.CAN-15-3152

Chen, R., Dai, R. Y., Duan, C. Y., Liu, Y. P., Chen, S. K., Yan, D. M., Chen, C. N., Wei, M., & Li, H. (2011). *Unfolded Protein Response Suppresses Cisplatin-Induced Apoptosis via Autophagy Regulation in Human Hepatocellular Carcinoma Cells*. *57*, 9.

Daly, L. E., Ní Bhuachalla, É. B., Power, D. G., Cushen, S. J., James, K., & Ryan, A. M. (2018). Loss of skeletal muscle during systemic chemotherapy is prognostic of poor survival in patients with foregut cancer. *Journal of Cachexia, Sarcopenia and Muscle*, *9*(2), 315–325. https://doi.org/10.1002/jcsm.12267

Damaraju, V. L., Kuzma, M., Cass, C. E., Putman, C. T., & Sawyer, M. B. (2018). Multitargeted kinase inhibitors imatinib, sorafenib and sunitinib perturb energy metabolism and cause

cytotoxicity to cultured C2C12 skeletal muscle derived myotubes. *Biochemical Pharmacology*, *155*, 162–171. https://doi.org/10.1016/j.bcp.2018.07.001

Eley, H. L., Russell, S. T., & Tisdale, M. J. (2007). Effect of branched-chain amino acids on muscle atrophy in cancer cachexia. *Biochemical Journal*, *407*(1), 113–120. https://doi.org/10.1042/BJ20070651

Fabian, G., Farago, N., Feher, L. Z., Nagy, L. I., Kulin, S., Kitajka, K., Bito, T., Tubak, V., Katona, R. L., Tiszlavicz, L., & Puskas, L. G. (2011). High-Density Real-Time PCR-Based in Vivo Toxicogenomic Screen to Predict Organ-Specific Toxicity. *International Journal of Molecular Sciences*, *12*(9), 6116–6134. https://doi.org/10.3390/ijms12096116

Gallot, Y. S., & Bohnert, K. R. (2021). Confounding Roles of ER Stress and the Unfolded Protein Response in Skeletal Muscle Atrophy. *International Journal of Molecular Sciences*, *22*(5), 2567. https://doi.org/10.3390/ijms22052567

Halle, J. L., Counts, B. R., Zhang, Q., & Carson, J. A. (2022). Short duration treadmill exercise improves physical function and skeletal muscle mitochondria protein expression after recovery from FOLFOX chemotherapy in male mice. *The FASEB Journal*, *36*(8). https://doi.org/10.1096/fj.202200460R

He, W. A., Berardi, E., Cardillo, V. M., Acharyya, S., Aulino, P., Thomas-ahner, J., Wang, J., Bloomston, M., Muscarella, P., Nau, P., Shah, N., Butchbach, M. E. R., Ladner, K., Adamo, S., Rudnicki, M. A., Keller, C., Coletti, D., Montanaro, F., & Guttridge, D. C. (2013). *NF- κ B – mediated Pax7 dysregulation in the muscle microenvironment promotes cancer cachexia*. *123*(11), 4821–4835. https://doi.org/10.1172/JCI68523DS1

Ingenuity Pathway Analysis. (n.d.). *QIAGEN Digital Insights*. Retrieved November 30, 2022, from https://digitalinsights.qiagen.com/products-overview/discovery-insights-portfolio/analysis-and-visualization/qiagen-ipa/

Jang, M. K., Park, C., Hong, S., Li, H., Rhee, E., & Doorenbos, A. Z. (2020). Skeletal Muscle Mass Change During Chemotherapy: A Systematic Review and Meta-analysis. *Anticancer Research*, *40*(5), 2409–2418. https://doi.org/10.21873/anticanres.14210

Järvinen, T., Ilonen, I., Kauppi, J., Salo, J., & Räsänen, J. (2018). Loss of skeletal muscle mass during neoadjuvant treatments correlates with worse prognosis in esophageal cancer: A retrospective cohort study. *World Journal of Surgical Oncology*, *16*(1), 17–19. https://doi.org/10.1186/s12957-018-1327-4

Jennings, P., Limonciel, A., Felice, L., & Leonard, M. O. (2013). An overview of transcriptional regulation in response to toxicological insult. *Archives of Toxicology*, *87*(1), 49–72. https://doi.org/10.1007/s00204-012-0919-y

Jung, H.-W., Kim, J. W., Kim, J.-Y., Kim, S.-W., Yang, H. K., Lee, J. W., Lee, K.-W., Kim, D.-W., Kang, S.-B., Kim, K., Kim, C.-H., & Kim, J. H. (2015). Effect of muscle mass on toxicity and survival in patients with colon cancer undergoing adjuvant chemotherapy. *Supportive Care in Cancer*, *23*(3), 687–694. https://doi.org/10.1007/s00520-014-2418-6

Krzystek-korpacka, M., Matusiewicz, M., & Diakowska, D. (2007). *Impact of weight loss on circulating IL-1 , IL-6 , IL-8 , TNF- α , VEGF-A , VEGF – C and midkine in gastroesophageal cancer patients*. *40*, 1353–1360. https://doi.org/10.1016/j.clinbiochem.2007.07.013

Lecker, S. H., Jagoe, R. T., Gilbert, A., Gomes, M., Baracos, V., Bailey, J., Price, S. R., Mitch, W. E., & Goldberg, A. L. (2004). *Multiple types of skeletal muscle atrophy involve a*

common program of changes in gene expression. 39–51. https://doi.org/10.1096/fj.03-0610com

Ma, J. F., Sanchez, B. J., Hall, D. T., Tremblay, A. K., & Marco, S. D. (2017). *STAT 3 promotes IFN c / TNF a -induced muscle wasting in an NF- j B-dependent and IL- 6 -independent manner*. *9*(5), 622–637. https://doi.org/10.15252/emmm.201607052

Martin, A., & Freyssenet, D. (2021). Phenotypic features of cancer cachexia-related loss of skeletal muscle mass and function: Lessons from human and animal studies. *Journal of Cachexia, Sarcopenia and Muscle*, *12*(2), 252–273. https://doi.org/10.1002/jcsm.12678

Martin, L., Birdsell, L., MacDonald, N., Reiman, T., Clandinin, M. T., McCargar, L. J., Murphy, R., Ghosh, S., Sawyer, M. B., & Baracos, V. E. (2013). Cancer cachexia in the age of obesity: Skeletal muscle depletion is a powerful prognostic factor, independent of body mass index. *Journal of Clinical Oncology*, *31*(12), 1539–1547. https://doi.org/10.1200/JCO.2012.45.2722

Merrick, B. A., & Bruno, M. E. (2004). *Genomic and proteomic profiling for biomarkers and signature profiles of toxicity*. *6*(6), 8.

Mihaly, S. R., & Morioka, S. (2014). TAK1 control of cell death. *Cell Death and Differentiation*, *21*(11), 1667–1676. https://doi.org/10.1038/cdd.2014.123

Parzych, K. R., & Klionsky, D. J. (2014). *An Overview of Autophagy : 20*(3), 460–473. https://doi.org/10.1089/ars.2013.5371

Peris-Moreno, D., Cussonneau, L., Combaret, L., Polge, C., & Taillandier, D. (2021). Ubiquitin Ligases at the Heart of Skeletal Muscle Atrophy Control. *Molecules*, *26*(2), 407. https://doi.org/10.3390/molecules26020407

Peris-Moreno, D., Taillandier, D., & Polge, C. (2020). MuRF1/TRIM63, Master Regulator of Muscle Mass. *International Journal of Molecular Sciences*, *21*(18), 6663. https://doi.org/10.3390/ijms21186663

Pin, F., Barreto, R., Couch, M. E., Bonetto, A., & O'Connell, T. M. (2019). Cachexia induced by cancer and chemotherapy yield distinct perturbations to energy metabolism. *Journal of Cachexia, Sarcopenia and Muscle*, *10*(1), 140–154. https://doi.org/10.1002/jcsm.12360

Riedl, S. J., & Shi, Y. (2004). *MOLECULAR MECHANISMS OF CASPASE REGULATION DURING APOPTOSIS*. *5*(November). https://doi.org/10.1038/nrm1496

Schiessel, D. L., & Baracos, V. E. (2018). Barriers to cancer nutrition therapy: Excess catabolism of muscle and adipose tissues induced by tumour products and chemotherapy. *Proceedings of the Nutrition Society*, *77*(4), 394–402. https://doi.org/10.1017/S0029665118000186

Sun, R., Zhang, S., Lu, X., Hu, W., Lou, N., Zhao, Y., Zhou, J., Zhang, X., & Yang, H. (2016). Comparative molecular analysis of early and late cancer cachexia-induced muscle wasting in mouse models. *Oncology Reports*, *36*(6), 3291–3302. https://doi.org/10.3892/or.2016.5165

Taillandier, D., & Polge, C. (2019). Skeletal muscle atrogenes: From rodent models to human pathologies. *Biochimie*, *166*, 251–269. https://doi.org/10.1016/j.biochi.2019.07.014

Tseng, Y. C., Kulp, S. K., Lai, I. L., Hsu, E. C., He, W. A., Frankhouser, D. E., Yan, P. S., Mo, X., Bloomston, M., Lesinski, G. B., Marcucci, G., Guttridge, D. C., Bekaii-Saab, T., & Chen, C. S. (2015). Preclinical Investigation of the Novel Histone Deacetylase Inhibitor AR-42 in the Treatment of Cancer-Induced Cachexia. *Journal of the National Cancer Institute*, *107*(12), djv274. https://doi.org/10.1093/jnci/djv274

VanderVeen, B. N., Cardaci, T. D., Madero, S. S., McDonald, S. J., Bullard, B. M., Price, R. L., Carson, J. A., Fan, D., & Murphy, E. A. (2022). 5-Fluorouracil disrupts skeletal muscle immune cells and impairs skeletal muscle repair and remodeling. *Journal of Applied Physiology*, *133*(4), 834–849. https://doi.org/10.1152/japplphysiol.00325.2022

van Vugt JLA, van Putten Y, van der Kall IM, Buettner S, D'Ancona FCH, Dekker HM, Kimenai HJAN, de Bruin RWF, Warlé MC, IJzermans JNM. Estimated skeletal muscle mass and density values measured on computed tomography examinations in over 1000 living kidney donors. Eur J Clin Nutr. 2019;73(6):879-886.

Xue, H., Le Roy, S., Sawyer, M. B., Field, C. J., Dieleman, L. A., & Baracos, V. E. (2009). Single and combined supplementation of glutamine and n-3 polyunsaturated fatty acids on host tolerance and tumour response to 7-ethyl-10-[4-(1- piperidino)-1-piperidino]carbonyloxy-camptothecin (CPT-11)/5-fluorouracil chemotherapy in rats bearing Ward col. *British Journal of Nutrition*, *102*(3), 434–442. https://doi.org/10.1017/S0007114508199482

Yang, W. E. I., Huang, J., Wu, H. U. I., Wang, Y., Du, Z., Ling, Y., Wang, W., Wu, Q., & Gao, W. (2020). *Molecular mechanisms of cancer cachexia - induced muscle atrophy (Review)*. 4967–4980. https://doi.org/10.3892/mmr.2020.11608

Yu, Z., Zhu, J. I. E., Wang, H., Li, H., & Jin, X. (2022). *Function of BCLAF1 in human disease (Review)*. https://doi.org/10.3892/ol.2021.13176

CHAPTER 3: TUMOR RESPONSE TO FOLFIRI CHEMOTHERAPY IS MODIFIED BY TARGETING THE COMPLEMENT SYSTEM IN RATS BEARING THE WARD COLON TUMOR

3.1 Introduction

The complement system is a highly complex component of the immune system consisting of several small proteins which circulate in the blood as inactive precursors. When stimulated by one of several triggers, proteases cleave and activate these proteins resulting in a cascade of cytokine released alongside stimulation of phagocytes to clear foreign and damaged material, inflammation to attract additional phagocytes, and activation of the cell-killing membrane attack complex (MAC). Normally, the complement system recognizes targets and opsonizes them for phagocytosis. It can attack and destroy bacteria and viruses by assembling the membrane attack complex (Figure 3-1). However, dysregulation of the entire complement cascade within tissues (e.g. brain, kidney) may lead to damage and functional disturbances. There has been a growing interest in the role that this cascading pathway plays in the pathology of a diverse array of disorders, including cancer.

Role of the complement system in cancer. Recent evidence suggests that complement responses in the tumor microenvironment (TME) may play a critical role in tumor evasion from host immune responses to facilitate tumor growth (Afshar-Kharghan, 2017; Kolev et al., 2022). Specifically, the complement system has been described to promote colon tumorigenesis (Ding et al., 2022; Nabizadeh et al., 2016) and metastasis formation (Piao et al., 2018). Colon tumor expression of complement elements is associated with a poor prognosis (Bao et al., 2021; Deng et al., 2022), and genetic loss or pharmacological blockade of the complement system impedes

colorectal tumorigenesis (Downs-Canner et al., 2016). We further speculated that pharmacological modifiers of the complement system may enhance the anti-tumor effect of cytotoxic chemotherapy. This hypothesis has not yet been tested.

Aberrant complement system activation may result in injury to normal tissue. The complement system may mistakenly attack host tissue in a process described as bystander lysis. Such attack is known to contribute to the pathology of a spectrum of human inflammatory diseases, of an acute or chronic nature (McGeer et al., 2017). The toxicity profile of FOLFIRI chemotherapy is principally in the gastrointestinal tract and includes inflammation and immune reaction locally in the large bowel (JR Hecht, 1998; Rothenberg, 2001). It remains unknown as to whether the complement cascade is in any way involved. Our research group also has unpublished results documenting inflammatory reactions (Farhangfar, 2012), including activation of the canonical pathway for the complement system at the transcriptional level in skeletal muscle after FOLFIRI treatment in our animal model (Chapter 2). It thus remains unclear as to whether introduction of an inhibitor of the complement cascade would reduce, worsen, or not change FOLFIRI side effects.

Modification of the complement system. Finding agents that can prevent or compensate for abnormal complement activity is a research priority. Complement inhibitors have been established as a well-recognized class of anti-inflammatory therapeutics (Markiewski et al., 2008; Ricklin & Lambris, 2008), with a variety of indications in conditions with aberrant inflammatory processes, including malignancy. AUR1402 is a derivative of aurin tricarboxylic acid (ATA), which is a molecule that blocks the complement cascade by inhibiting activity of the alternative C3 convertase as well as assembly of the membrane attack complex (MAC; C5b-9). Given that

complement responses may be significant contributors to treatment response of anti-cancer treatment as well as toxicities associated with the therapeutic index of FOLFIRI chemotherapy in peripheral tissues (gastrointestinal and skeletal muscle), we sought to investigate effects of a novel orally active small molecular weight inhibitor of the complement system, AUR1402, on improving these outcomes. This agent is under investigation for potential use as a medical countermeasure for multiple acute and chronic conditions and has previously shown gastrointestinal protective effects in a lethal rodent model of systemic inflammatory response syndrome (SIRS) (Aurin Biotech, unpublished data). This is the first time this agent is being tested in an animal model of colon cancer with concurrent chemotherapy, as we planned to assess body weight and food intake, clinically relevant outcomes adversely affected by the FOLFIRI chemotherapy regimen.

3.2 Materials and Methods

Experimental procedures were reviewed and approved by the University of Alberta Institutional Animal Care Committee and conducted in accordance with the Guidelines of the Canadian Council on Animal Care.

3.2.1 Animal Model and Study Design

Laboratory rat use, diet design, tumor implantation and FOLFIRI formulation (CPT-11 and 5-FU) are detailed previously (Chapter 2). A schematic of the study design is presented in Figure 3-2. Our pre-clinical model of (Ward colon adenocarcinoma in the Fisher 344 rat) incorporates FOLFIRI chemotherapy regimen (CPT-11 and 5-FU). The regimen is adjusted in dose and schedule to recapitulate the efficacy and toxicity of colon cancer therapy seen clinically in the

advanced disease setting (Cao & Rustum, 2000). This published model forms a solid, clinically relevant base for our studies (Almasud et al., 2017; Xue et al., 2007).

Briefly, the Ward colorectal carcinoma (0.05g) was subcutaneously implanted in the hind flank of female Fischer 344 rats aged 11-12 weeks (n=46). When tumor volume reached ~2 cm^3 (~14 days following implantation), rats were randomly assigned to one of 3 experimental groups: one group which continued to receive the control diet (control; n=19), a second which received a diet with AUR1402 incorporated to deliver 90 mg/kg body weight (Control diet + Low Dose AUR1402; n=10) and a third group which received a diet with AUR1402 incorporated to deliver 156 mg/kg body weight (Control diet + High Dose AUR1402; n=17). AUR1402 was tested at two dose levels: 90 mg/kg and 156 mg/kg. These dose levels have previously shown efficacy in rodent inflammatory disease models and were within the dose range demonstrated to be safe for rats and mice in chronic administration studies.

On the morning following randomization to AUR1402 and control treatment, all animals began their first cycle of FOLFIRI treatment which included CPT-11 [50 mg/kg body weight, intraperitoneal] and 5-FU [50 mg/kg body weight, intraperitoneal], administered 24 hours apart. Atropine (1 mg/kg s.c.) was administered immediately before each CPT-11 injection to alleviate early-onset cholinergic symptoms. The second cycle of FOLFIRI consisted of the same drug regimen repeated one week after cycle 1. Body weight, food intake and tumor volume were assessed daily. Animals from Control and High-Dose groups were euthanized on Day 1 (n=4), Day 2 (n=6) and Day 4 (n=6). Animals from all groups were euthanized on Day 14 (n=30). Carbon dioxide (CO^2) asphyxiation was used for euthanization of rats.

3.2.2 Tumor Response

The primary outcome, treatment response, was assessed via daily tumor volume measurements with subsequent histological assessment of tumor samples following completion of the two-week FOLFIRI chemotherapy regimen. Subcutaneous tumor length (L), width (W) and height (H) were measured daily using calipers, and tumor volume was calculated using the following equation: tumor volume (cm3) = 0.5 × L(cm) × W(cm) × H(cm) (Almasud et al., 2017; Xue et al., 2007). Tumor volume was recorded before FOLFIRI treatment, and the following days; relative tumor volume for each tumor was calculated relative to its volume prior to FOLFIRI treatment. Formalin-fixed tumor tissue was embedded in paraffin wax, sectioned, and stained with haematoxylin and eosin (H&E) for histopathological examination. All images were acquired under 200× magnification with an Axio scan Z1 whole slide scanner (Zeiss).

3.2.3 Safety/Toxicity Assessment: Body Weight and Food Intake

The most prominent toxicity associated with the FOLFIRI chemotherapy regimen is gastrointestinal toxicity with associated reduction in food intake and concordant loss in body weight; this has been well characterized in our model from our previous investigations (Almasud et al., 2017; Xue et al., 2007).

Food Intake. Rodent diet for all experiments carried out in this study has been previously described (Almasud et al., 2017). Rats were allowed feed and water *ad libitum* and food intake was assessed daily after chemotherapy exposure. **Body weight** was assessed every day for all groups, and at the same time as tumor volume assessment (Almasud et al., 2017). Relative food

intake and relative body weight was determined by comparing to food intake and body weight prior to the chemotherapy injections, respectively.

3.2.4 Statistical Analysis

Data are expressed as mean ± SEM. Statistical analysis was performed using GraphPad Prism (GraphPad Inc., San Diego, CA). Differences among groups were tested using one-way repeated measures analysis of variance (ANOVA) on the effect of AUR1402 followed by post-hoc Tuckey's test. A probability $p<0.05$ was accepted as being statistically significant.

3.3 Results

3.3.1 AUR1402 treatment is safe and does not modify gastrointestinal toxicity induced by FOLFIRI chemotherapy

Following each cycle of FOLFIRI chemotherapy, relative food intake initially decreased in all groups, but returned to baseline by the end of the cycle (Figure 3-3A). Following the first cycle of FOLFIRI, the maximum reduction in food intake of control animals was 59.61 ± 0.05% (Day 17) which corresponded to a 5.38 ± 0.01% reduction in body weight relative to baseline. This was expected and consistent with previous studies (Almasud et al., 2017; Xue et al., 2007). Animals treated with AUR1402 at 90 mg/kg experienced a 65.81 ± 0.07% maximum reduction in food intake (Day 16) and animals treated with AUR1402 at 156mg/kg experienced a 66.09 ± 0.05% maximum reduction in food intake (Day 15). This corresponded to a 6.69 ± 0.01% and 6.43 ± 0.01% body weight loss for low and high dose AUR1402-treated animals, respectively (Figure 3-3B).

Relative food intake also decreased after the second FOLFIRI cycle and was lowest for all groups on the day following CPT-11 injection. Control animals experienced a maximum of 58.76 ± 0.10% reduction in food intake corresponding to a 6.95 ± 0.01% decrease in body weight. Similar to cycle 1 FOLFIRI chemotherapy, low dose AUR1402-treated animals experienced a 65.52 ± 0.09% decrease in food intake corresponding to 10.93% reduction in body weight. Food intake of animals treated with high dose AUR1402 decreased by 62.38 ± 0.07%, corresponding to a 7.73 ± 0.01% reduction in body weight. There were no significant differences to changes in body weight or food intake between control and AUR1402-treated groups during either cycle of FOLFIRI treatment.

3.3.2 Treatment with AUR1402 confers an augmented tumor response to FOLFIRI chemotherapy

The average daily dose of AUR1402 during the chemotherapy period in the low dose group was 89.86 ± 8.78 mg/kg whereas animals in the high dose group received 155.71 ± 14.46 mg/kg. The difference in cumulative dose over the first 3 days after the first cycle of FOLFIRI chemotherapy is depicted in Figure 3-4A. Tumors grew to 1.9 ± 0.3 cm^3 in size and were similar between all groups before starting chemotherapy treatment. Relative tumor volume was compared to the baseline volume when chemotherapy was initiated (Day 14).

Effects of AUR1402 on tumor response to chemotherapy are shown in Figure 4B. As shown in our prior studies, tumors shrank by at least 65% 2-3 days into each cycle of treatment, and then showed regrowth. AUR1402 treatment at 90 mg/kg was without effect on tumor growth and at no time point was tumor volume significantly different from that of animals that did not

receive AUR1402. By contrast, the higher dose AUR1402 treatment at 156 mg/kg enhanced the anti-tumor activity of CPT-11/5-FU chemotherapy compared with the control diet (Figure 3-4B).

By the start of the second cycle of FOLFIRI chemotherapy (Day 21), tumor volume of control animals had recovered to 63 ± 15.5% of baseline and tumor volume of low dose AUR1402-treated animals had recovered to 58.8 ± 26% of baseline. Tumor volume of high dose AUR1402-treated animals had significantly less growth than control animals ($p=0.040$) reaching only 21.1 ± 8.7% of baseline tumor volume. Control and low-dose AUR1402-treated animals presented with similar trends in tumor growth during the second cycle of FOLFIRI chemotherapy. By contrast, high dose AUR1402-treated animals did not show a pattern of tumor regrowth. Tumor volumes were not significantly different between the low dose AUR1402 and control groups during either cycle-1 or cycle-2 of FOLFIRI treatment.

3.3.3 Histological assessment confirms elimination of tumor cells following AUR1402 treatment

To better understand the underlying biological mechanisms driving the tumor response observed with AUR1402 treatment, tumor samples from control and high dose AUR1402-treated rats were assessed via histology (Figure 3-5). The size of cross section and morphological features between the two groups were drastically different.

Histological assessment by a board-certified pathologist (JD) of tumor samples from control animals confirmed the presence of actively proliferating tumor cells concordant with the morphology of an advanced colorectal adenocarcinoma (Figure 3-5(A-C); Figure 3-6). In contrast, tumor samples of high dose AUR1402-treated animals were considerably smaller and did not

reveal any evidence of tumor cells (Figure 3-5(D-F); Figure 3-7). Interestingly, the morphological pattern was concordant with that of a benign lymph node or immune nodule (Figure 3-7). Structural components contained attributes of a germinal center and included a capsule, subcapsular sinus and numerous delimited clusters composed of medium to large cells as well as tingible body macrophages (TBMs).

3.4 Discussion

For the first time, AUR1402, a novel orally active, small molecular weight inhibitor of the complement system was used in a clinically aligned animal model of colon cancer and FOLFIRI chemotherapy. An anti-tumor effect was observed wherein tumors were eliminated in rats that received AUR1402 at 156 mg/kg in combination with two cycles of FOLFIRI. This was confirmed via histological examination. We did find the minimum effective dose of AUR1402 - of the two doses tested, one (156 mg/kg) conferred an anti-tumor response whereas the other (90 mg/kg) did not. Given preliminary data suggesting gastrointestinal (GI) protective effects of AUR1402, we hypothesized that when combined with a FOLFIRI chemotherapy regimen, treatment-associated GI toxicity would be attenuated. Animals were closely monitored, and the compound was safe and did not cause any adverse effects (i.e., weight loss, reduction in food intake).

Inflammatory cells including tumor-associated macrophages (TAMs) and myeloid-derived suppressor cells (MDSCs) can infiltrate solid tumors (Afshar-Kharghan, 2017). TAMs and MDSCs alongside other stromal cells can secrete inflammatory mediators including TGF-β, IL-6 and IL-17, which function in crosstalk between inflammatory and tumor cells in the tumor microenvironment (TME). An additional inflammatory factor which functions as an independent system and has been of focus over the last several decades is the complement system, largely due to its ability to mobilize numerous inflammatory molecules that can exert significant effects in the TME.

Although the role of complement was initially described in the context of its essential role in the innate immune response against pathogens or foreign material (Walport, 2001a, 2001b),

evidence began to emerge suggesting complement receptors expressed on effector immune cells, could recognize complement fragments deposited on the surface of tumor cells leading to increased direct or antibody-dependent cytotoxic effects, as well as phagocytosis of apoptotic tumor cells (Boross & Leusen, 2012; Macor et al., 2018). This would be mediated through formation of the membrane attack complex (MAC) and subsequent lysis and removal of malignant tumor cells.

However, more recently, preclinical investigations have shown that tumor cells employ several mechanisms to evade complement-mediated lysis (Fishelson & Kirschfink, 2019), suggesting a prominent role of complement in promoting tumor survival. For example, MAC can be removed from the cell surface by tumor cells and incorporated into the cell membrane, leading to increased epithelial-to-mesenchymal transition (EMT), survival, proliferation and metastasis formation (Fishelson & Kirschfink, 2019; Piao et al., 2018; Towner et al., 2016). It is interesting to consider these findings in light of the known activity of AUR1402, which is a derivative of aurin tricarboxylic acid (ATA), a molecule which blocks the complement cascade by inhibiting assembly of the MAC (C5b-9) in the first instance. This may in turn prevent incorporation of the MAC at sub-lytic concentrations, with increased susceptibility to anti-cancer immune responses.

Complement 3 (C3) plays a critical role in each pathway of complement activation and serum C3 levels are increased in patients with colorectal cancer (Zimmermann-Nielsen et al., 2002). C3b and C5b are produced following enzymatic cleavage of C3 and will subsequently form MAC and by-products including anaphylatoxins C3a and C5a. C3a and C5a, through their receptors C3aR, C5aR1 and C5aR2, respectively, can shift immune responses to favor tumor progression (Ding et al., 2022). For example, tumor proliferation can be promoted via C3a–C3aR

signaling (Fan et al., 2019). In addition, C5a can inhibit T Helper 1 (TH1) responses and shift towards T Helper 2 (TH2); TH2-mediated responses are ineffective in potentiating antitumor CD8+ T Cell activity (Kolev et al., 2022). C5a (via C5aR1) can also recruit and activate MDSCs in the TME, leading to suppression of anti-tumor CD8+ T-cell-mediated activity, and concurrent tumor growth (Kochanek et al., 2018; Markiewski et al., 2008). Aurin tricarboxylic acid (ATA), from which AUR1402 is derived, can also block the complement cascade by inhibiting alternative complement component 3 (C3) convertase activity. Through this action, AUR1402 may prevent formation of complement anaphylatoxins and subsequently modify activity of MDSCs in the TME.

Enhanced complement-mediated opsonic and phagocytic responses in the TME are important considerations, given results of preliminary histology suggesting the presence of tingible body macrophages (TBMs) in the tumor of AUR1402-treated rats. In pathologies involving significant apoptotic responses, including malignancies, complement activation is prevalent and complement components such as C1q can enhance phagocytosis of apoptotic cells by macrophages (Galvan et al., 2012; Mevorach et al., 1998). C3a and C5a are pro-inflammatory mediators which can facilitate monocyte and macrophage activation (Bohlson et al., 2014; Piao et al., 2018). Recent findings from Chen and coworkers (2022) reveal upregulation of gene signatures associated with complement activation in tumor samples of patients with metastatic BRAF V600E mutant colorectal cancer; this signature was associated with poor clinical outcomes as well as signatures of M2 TAMs (Chen et al., 2022). The extent to which macrophage polarization and subsequent phagocytic responses may be modified in the TME by AUR1402 remain of interest and should be investigated further.

This work is preliminary and requires replication as well as confirmation of the identity of the cell types present in the apparent secondary lymphoid structure observed at Day 29. Furthermore, a full time course of the events leading to the disappearance of the colon adenocarcinoma and the sequence of steps by which the lymphoid structure was present at the end of the study requires characterization. Given that the histology of tumors treated with AUR1402 resembled that of a benign lymph node with structural components resembling germinal centers, immune phenotyping via immunohistochemistry would be of great benefit. During blinded pathological analysis of the tumor samples, it was suggested that further insight may be obtained by staining the specimens over this time course using the proliferation marker Ki67, pan cytokeratin markers that would correspond to colon tumor cells as well as cellular markers to confirm the presence of lymphocytes, T cells, B cells and macrophages.

Based on crude measurements of tumor volume achieved in living animals, it seems clear that in the high dose AUR1402, the mass showed no regrowth after Day 18. However, specific histological analysis of early and late time points is required to understand what the mass consisted of across the time course. This is the first instance wherein a complement system inhibitor has been combined with a cytotoxic chemotherapy regimen. This provides an interesting preliminary result; however, we have not ruled out the possibility that AUR1402 has an effect on colorectal carcinoma in the absence of cytotoxic chemotherapy. An important experiment would involve determining whether the action of AUR1402 is synergistic with the chemotherapy or if a direct anti-tumor action of AUR1402 may exist. These experiments are currently underway and in either case, the preliminary results suggest AUR1402 as a compound of interest. Additional limitations

include the use of a single tumor site with a single chemotherapy regimen. Assessing the effect of AUR1402 on additional colorectal cancer cell lines would be useful.

Given the complex interactions which exist in the TME and given that the source of complement proteins can be diverse (produced by cancer cells, stromal cells, non-myeloid and myeloid immune), development of complement-targeted cancer therapeutics poses numerous challenges. Although several investigations endeavored to identify complement proteins as potential biomarkers, they did not address the role of complement as part of the underlying mechanisms driving malignancy and conferring poor outcomes. Preclinical models are thus important however currently, a significant limitation of currently available literature includes findings obtained from use of animal models with constitutive complement knockouts, yielding challenges to clinical translatability (Mak et al., 2014). As such, relevant use of preclinical models which recapitulate tumor growth and treatment response alongside treatment-associated toxicity that is clinically aligned and scaled in magnitude to that experienced by patients with cancer are important considerations. Kolev and coworkers (2022) summarized current clinical trials underway targeting complement components including C3 and C5aR1 as monotherapy and/or as combination therapy with checkpoint inhibitors (ex. anti-PD-L1) (Kolev et al., 2022). Further investigation is required to elucidate the anti-tumor mechanism of action of AUR1402. Considerations of combination therapy alongside first line chemotherapy with FOLFIRI may be worthwhile pursuits.

FIGURES

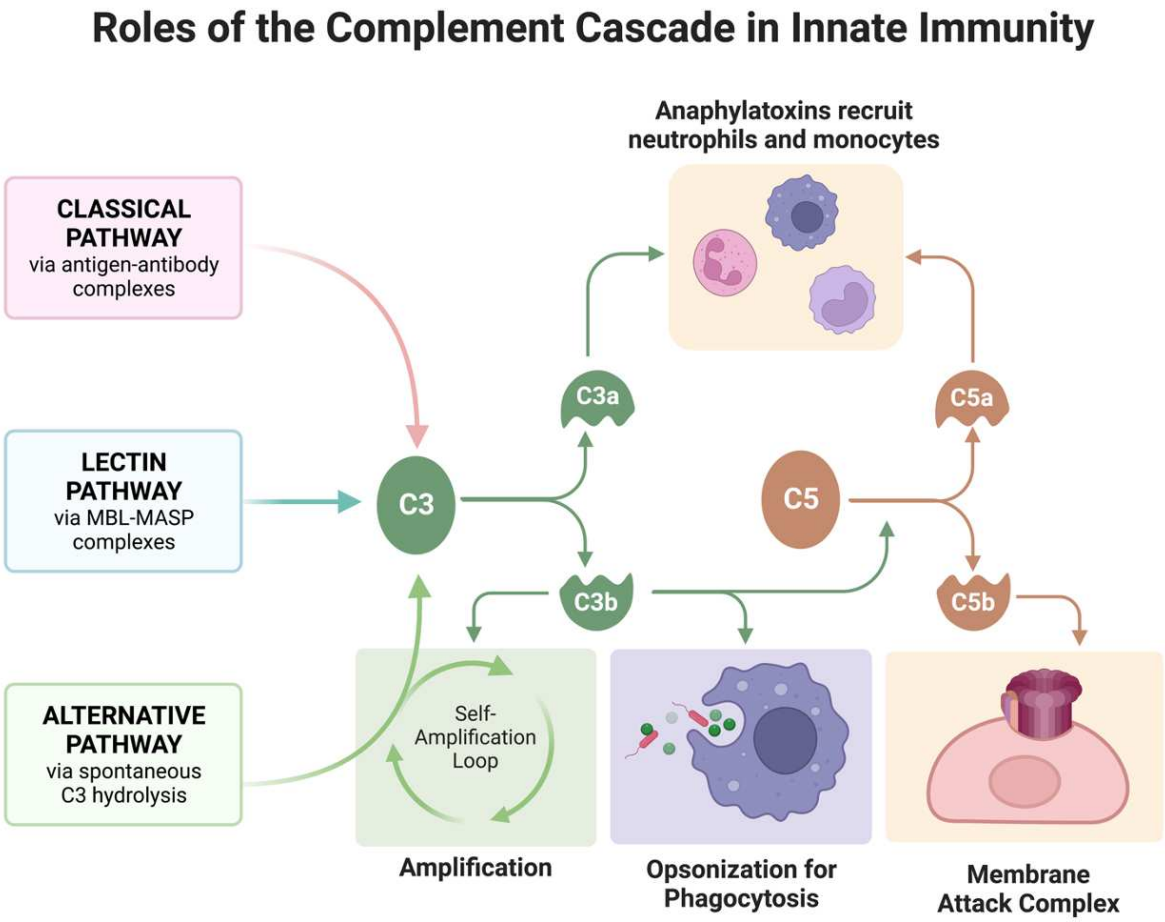

Figure 3-1. Roles of the Complement Cascade in Innate Immunity. Activation Pathways of Complement via the Classical, Lectin, and Alternative Pathways. Created using BioRender.

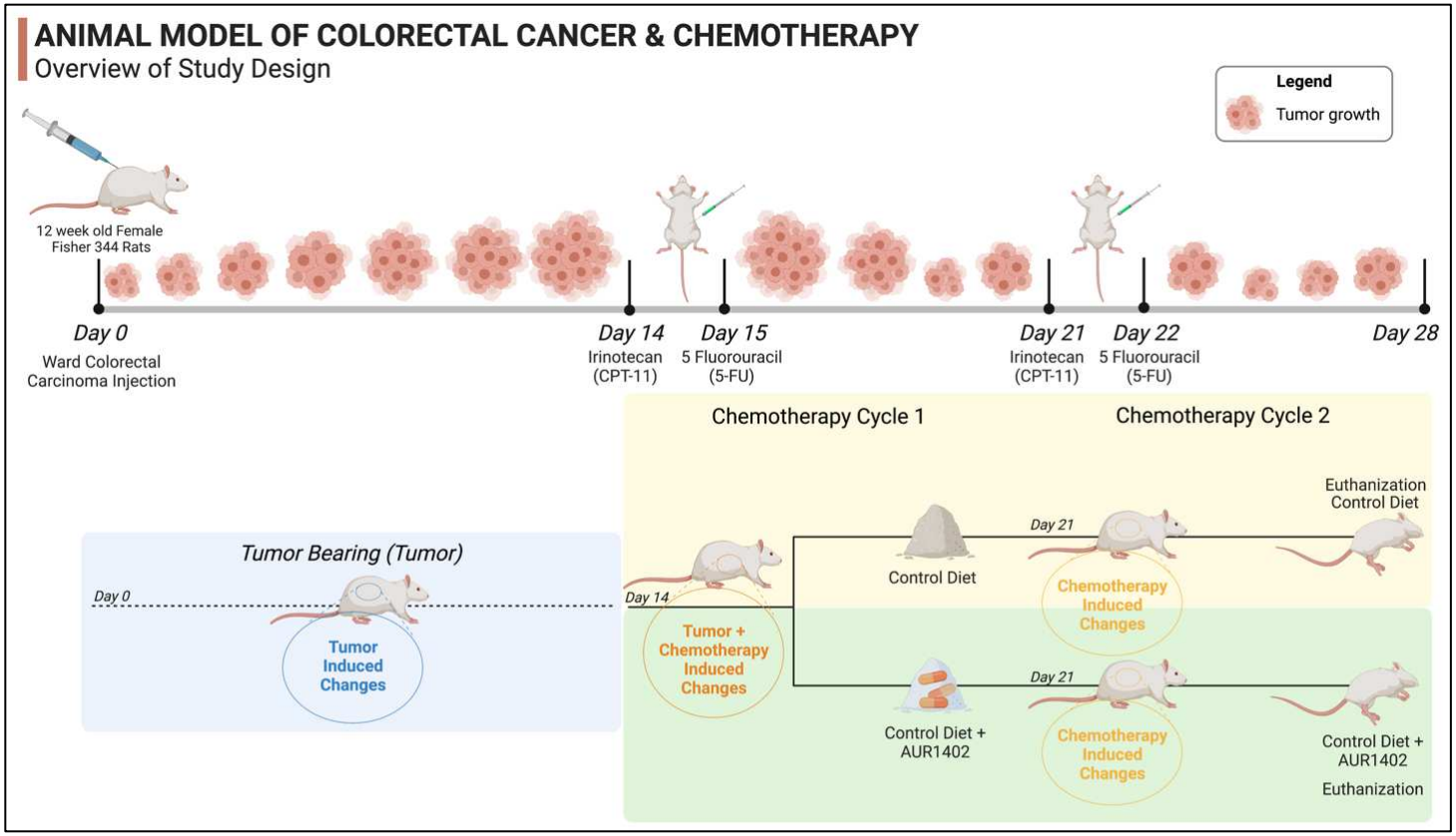

Figure 3-2. Study design to test AUR1402 in an animal model of colorectal cancer and chemotherapy treatment. Female Fisher 344 rats are subcutaneously injected with a Ward colorectal carcinoma (Day 0). After 2-weeks of tumor growth (Day 14), rats are randomly assigned to one of two experimental groups: one group will continue to receive the control diet (CONTROL) and the other will receive a diet with AUR1402 (Control diet + AUR1402). All rats will receive an intraperitoneal injection of irinotecan and 5-fluorouracil (chemotherapy) over the course of two days (one on each day). Two cycles will be administered over a 14-day period. All animals will be euthanized at Day 28. Created using BioRender.

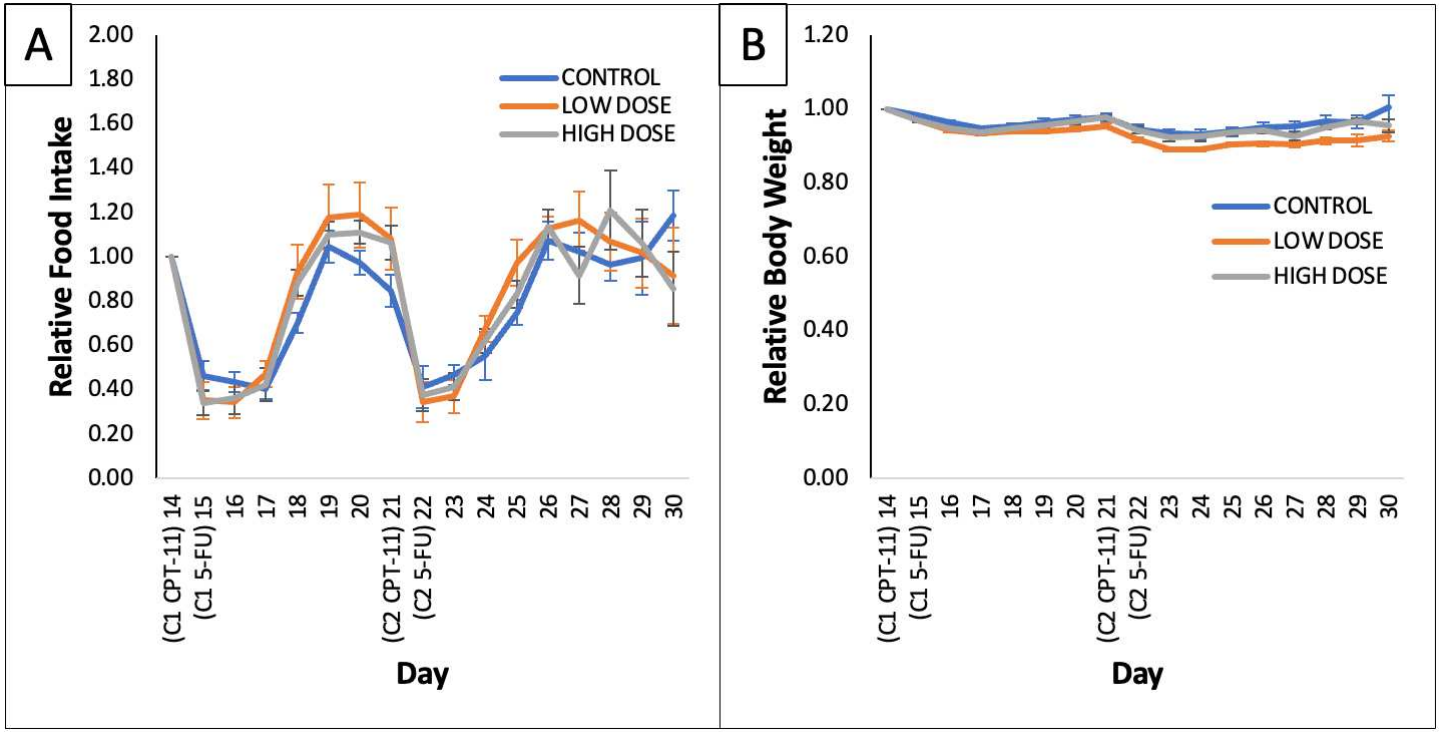

Figure 3-3. Effect of AUR1402 treatment on gastrointestinal toxicity induced by FOLFIRI chemotherapy A) Relative food intake and **B)** Relative body weight of tumor-bearing animals injected with sequential chemotherapy treatments of FOLFIRI (CPT-11 + 5-FU), relative to baseline. Values presented as mean±SE.

CONTROL: Tumor bearing animals receiving two cycles of chemotherapy on control diet; **LOW DOSE:** Tumor bearing animals receiving two cycles of chemotherapy on control diet mixed with AUR1402 90mg/kg; **HIGH DOSE:** Tumor bearing animals receiving two cycles of chemotherapy on control diet mixed with AUR1402 156mg/kg; **C1:** Chemotherapy cycle 1; **C2:** Chemotherapy cycle 2; **CPT-11**: irinotecan; **5-FU**: 5-fluorouracil

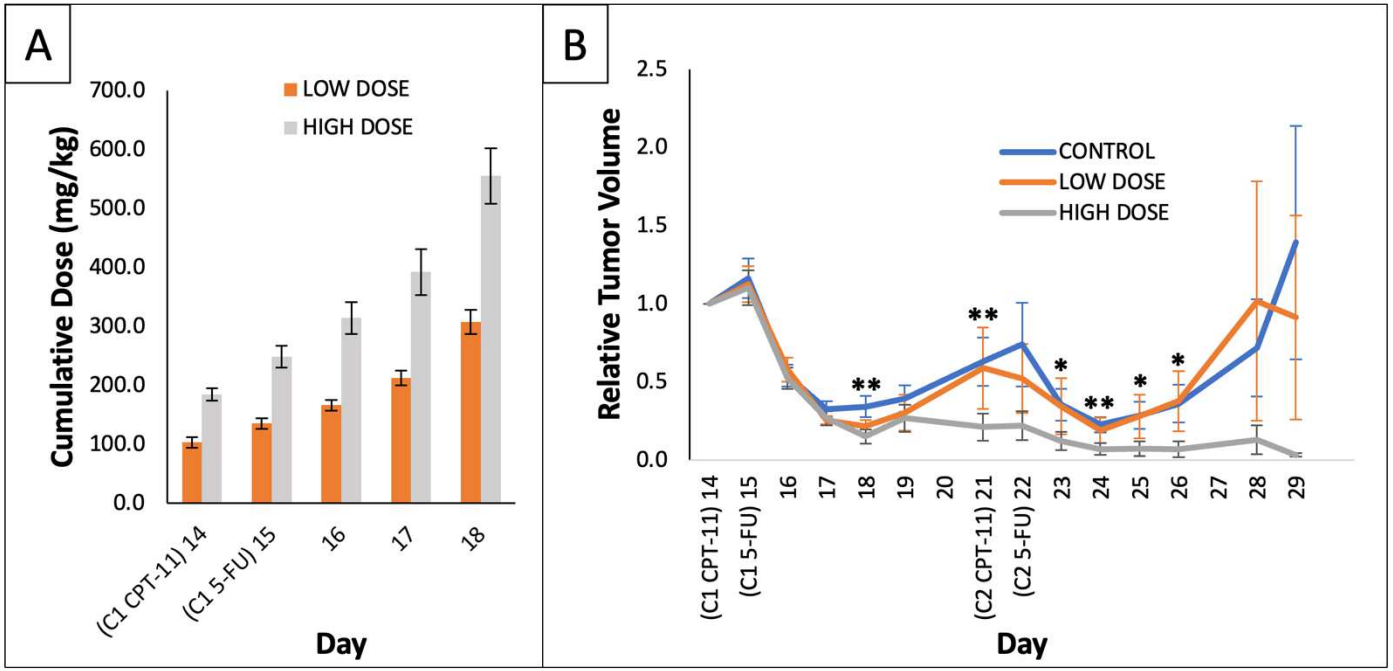

Figure 3-4. Effect of AUR1402 on tumor response to FOLFIRI chemotherapy. A) Average cumulative dose (mg/kg body weight) of AUR1402 by day following first cycle of FOLFIRI chemotherapy **B)** Tumor volume of animals injected with sequential chemotherapy treatments of FOLFIRI (CPT-11 + 5-FU), relative to baseline. Values presented as mean±SE. *$p<0.08$. **$p<0.05$ between CONTROL and HIGH DOSE groups.

CONTROL: Tumor bearing animals receiving two cycles of chemotherapy on control diet; **LOW DOSE:** Tumor bearing animals receiving two cycles of chemotherapy on control diet mixed with AUR1402 90mg/kg; **HIGH DOSE:** Tumor bearing animals receiving two cycles of chemotherapy on control diet mixed with AUR1402 156mg/kg; **C1:** Chemotherapy cycle 1; **C2:** Chemotherapy cycle 2; **CPT-11**: irinotecan; **5-FU**: 5-fluorouracil

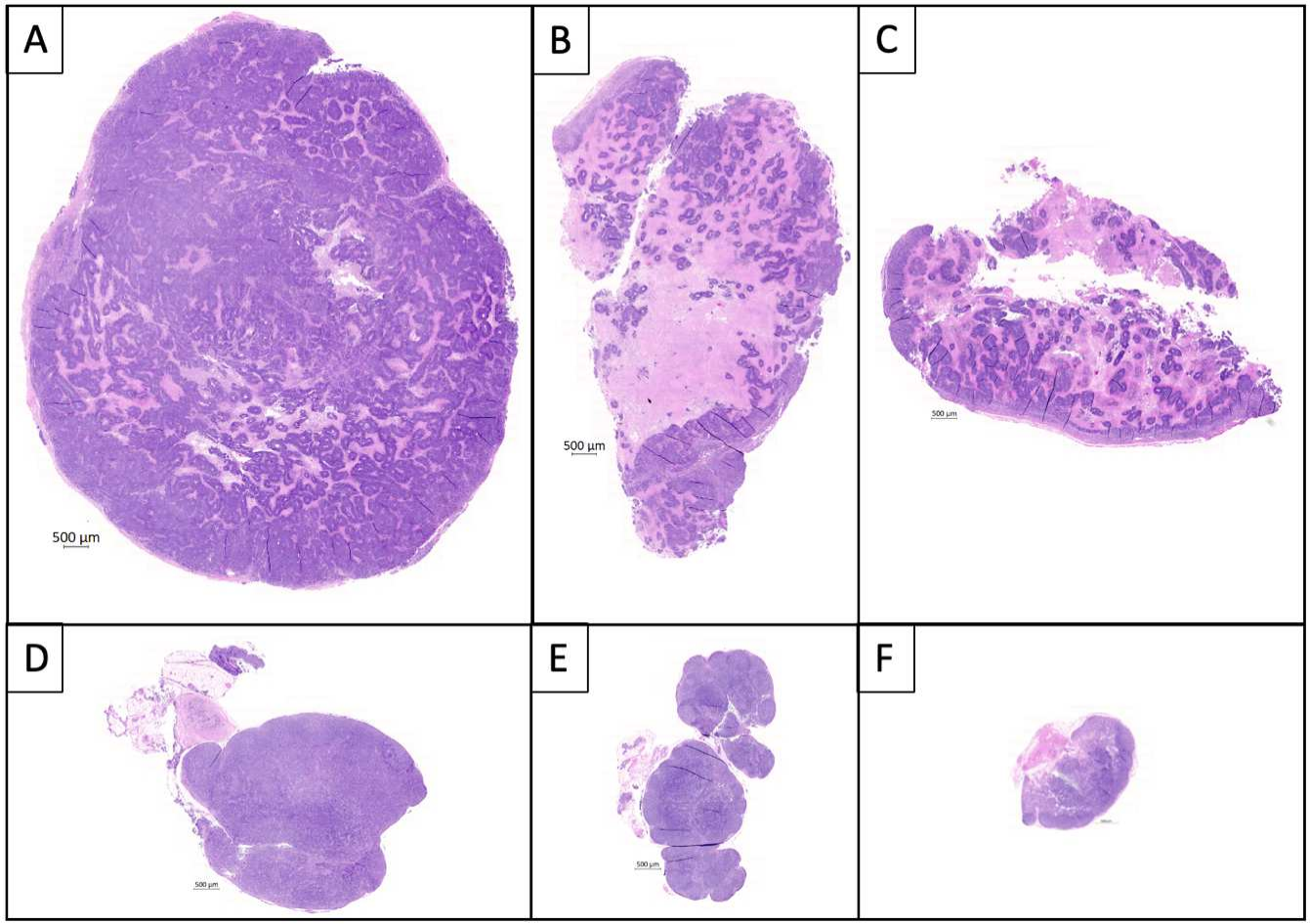

Figure 3-5. Tumor histology of FOLFIRI treated rats with or without AUR1402 A-C) Tumor bearing animals receiving two cycles of chemotherapy on control diet (Control) and **D-F)** Tumor bearing animals receiving two cycles of chemotherapy on control diet mixed with AUR1402 156mg/kg (High dose AUR1402). Tumors were stained with haematoxylin and eosin (H&E) Images acquired at under 200× magnification with Axio Scan Z1 Whole Slide Scanner (Zeiss). All panels have been scaled to the same magnitude.

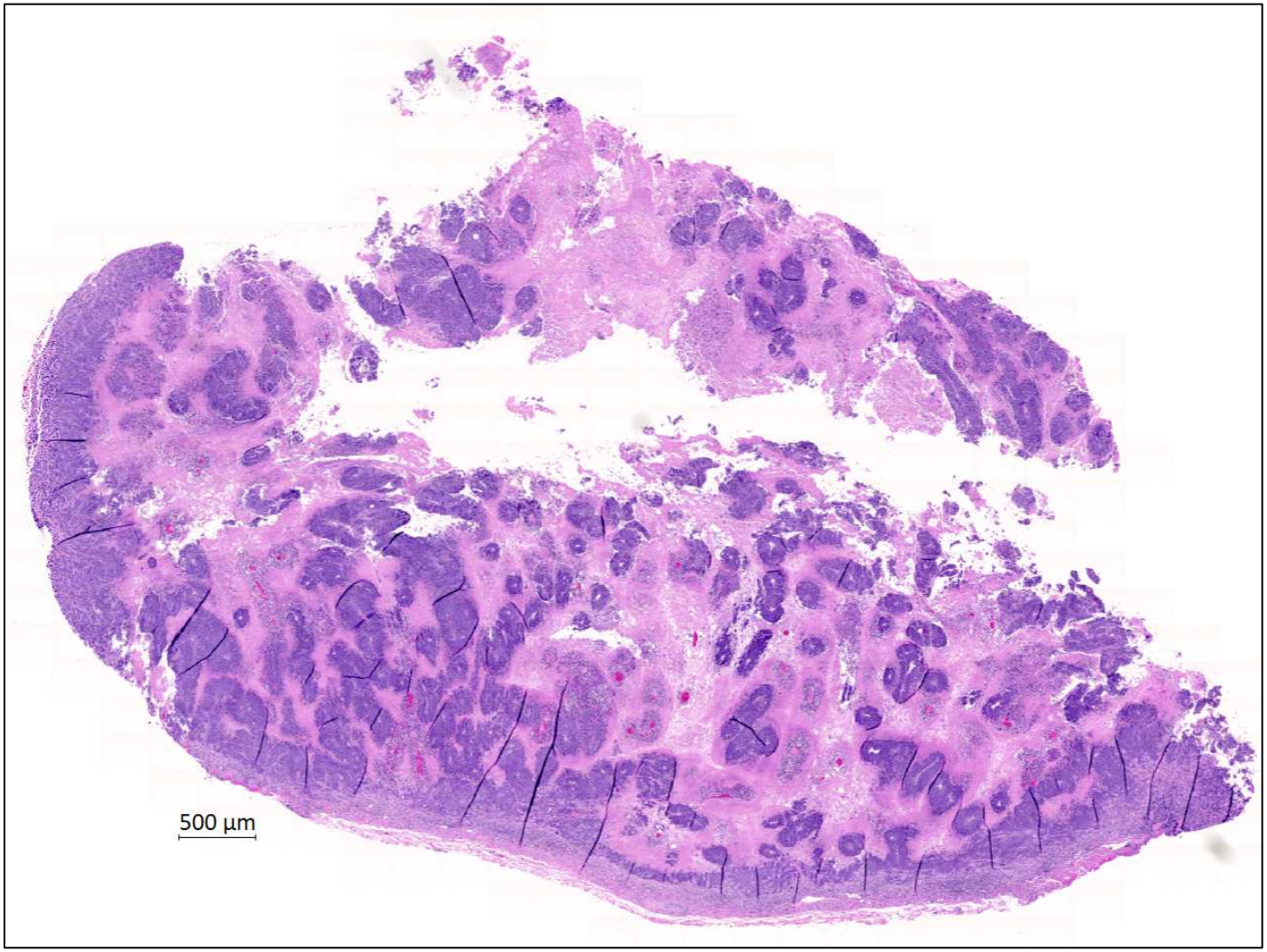

Figure 3-6. Enlarged image of Figure 3-5C to visualize morphological features of Control rats. Tumor histology of tumor bearing animals receiving two cycles of chemotherapy on control diet (Control)**.** Tumors were stained with haematoxylin and eosin (H&E) Images acquired at under 200× magnification with Axio Scan Z1 Whole Slide Scanner (Zeiss).

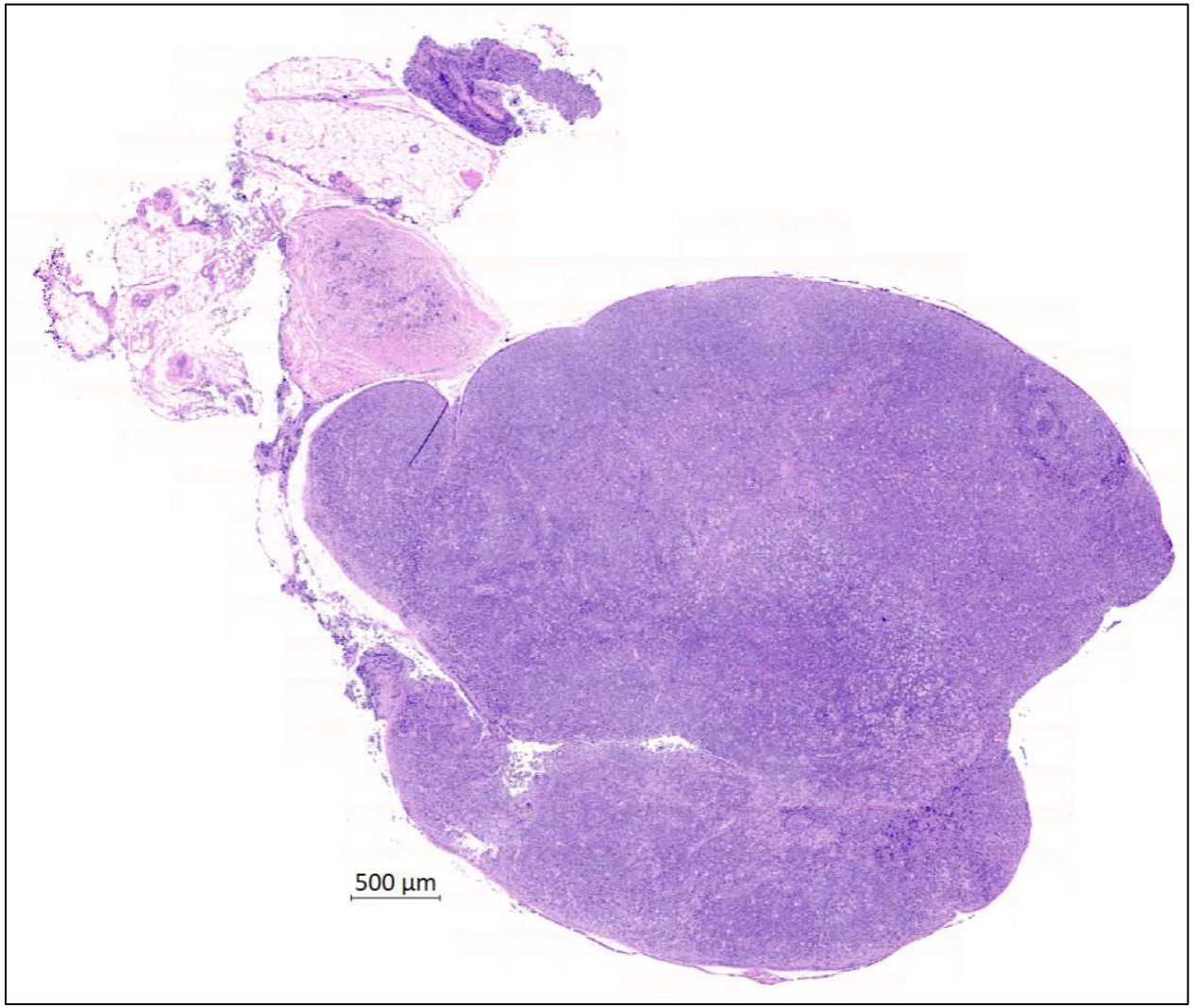

Figure 3-7. Enlarged image of Figure 3-5D to visualize morphological features of AUR1402 treated rats. Tumor bearing animals receiving two cycles of chemotherapy on control diet mixed with AUR1402 156mg/kg (High dose AUR1402). Tumors were stained with haematoxylin and eosin (H&E) Images acquired at under 200× magnification with Axio Scan Z1 Whole Slide Scanner (Zeiss).

LITERATURE CITED

Afshar-Kharghan, V. (2017). The role of the complement system in cancer. *Journal of Clinical Investigation*, *127*(3), 780–789. https://doi.org/10.1172/JCI90962

Almasud, A. A., Giles, K. H., Miklavcic, J. J., Martins, K. J. B., Baracos, V. E., Putman, C. T., Guan, L. L., & Mazurak, V. C. (2017). Fish oil mitigates myosteatosis and improves chemotherapy efficacy in a preclinical model of colon cancer. *PLoS ONE*, *12*(8), 1–17. https://doi.org/10.1371/journal.pone.0183576

Bao, D., Zhang, C., Li, L., Wang, H., Li, Q., Ni, L., Lin, Y., Huang, R., Yang, Z., Zhang, Y., & Hu, Y. (2021). Integrative Analysis of Complement System to Prognosis and Immune Infiltrating in Colon Cancer and Gastric Cancer. *Frontiers in Oncology*, *10*, 553297. https://doi.org/10.3389/fonc.2020.553297

Bohlson, S. S., O'Conner, S. D., Hulsebus, H. J., Ho, M. M., & Fraser, D. A. (2014). Complement, C1Q, and C1q-related molecules regulate macrophage polarization. *Frontiers in Immunology*, *5*(AUG). https://doi.org/10.3389/fimmu.2014.00402

Boross, P., & Leusen, J. H. W. (2012). Boosting antibody therapy with complement. *Blood*, *119*(25), 5945–5947. https://doi.org/10.1182/blood-2012-04-420760

Cao, S., & Rustum, Y. M. (2000). Synergistic antitumor activity of irinotecan in combination with 5-fluorouracil rats bearing advanced colorectal cancer: Role of drug sequence and dose. *Cancer Research*, *60*(14), 3717–3721.

Chen, K.-H., Hsu, C.-L., Su, Y.-L., Yuan, C.-T., Lin, L.-I., Tsai, J.-H., Liang, Y.-H., Cheng, A.-L., & Yeh, K.-H. (2022). Novel prognostic implications of complement activation in the tumour microenvironment for de novo metastatic BRAF V600E mutant colorectal cancer. *British Journal of Cancer*. https://doi.org/10.1038/s41416-022-02010-2

Deng, H., Chen, Y., Liu, Y., Liu, L., & Xu, R. (2022). Complement C1QC as a potential prognostic marker and therapeutic target in colon carcinoma based on single-cell RNA sequencing and immunohistochemical analysis. *Bosnian Journal of Basic Medical Sciences*, *22*(6), Article 6. https://doi.org/10.17305/bjbms.2022.7309

Ding, P., Xu, Y., Li, L., Lv, X., Li, L., Chen, J., Zhou, D., Wang, X., Wang, Q., Zhang, W., Liao, T., Ji, Q.-H., Lei, Q.-Y., & Hu, W. (2022). Intracellular complement C5a/C5aR1 stabilizes β-catenin to promote colorectal tumorigenesis. *Cell Reports*, *39*(9), 110851. https://doi.org/10.1016/j.celrep.2022.110851

Downs-Canner, S., Magge, D., Ravindranathan, R., O'Malley, M. E., Francis, L., Liu, Z., Sheng Guo, Z., Obermajer, N., & Bartlett, D. L. (2016). Complement Inhibition: A Novel Form of Immunotherapy for Colon Cancer. *Annals of Surgical Oncology*, *23*(2), 655–662. https://doi.org/10.1245/s10434-015-4778-7

Fan, Z., Qin, J., Wang, D., & Geng, S. (2019). Complement C3a promotes proliferation, migration and stemness in cutaneous squamous cell carcinoma. *Journal of Cellular and Molecular Medicine*, *23*(5), 3097–3107. https://doi.org/10.1111/jcmm.13959

Farhangfar, A. (2012). *Non digestible carbohydrates in the diet determine toxicity of irinotecan (CPT-11)/5-fluorouracil in rats independently of β- glucuronidase activity in intestinal lumen*. 94.

Fishelson, Z., & Kirschfink, M. (2019). Complement C5b-9 and Cancer: Mechanisms of Cell Damage, Cancer Counteractions, and Approaches for Intervention. *Frontiers in Immunology*, *10*, 752. https://doi.org/10.3389/fimmu.2019.00752

Galvan, M. D., Greenlee-Wacker, M. C., & Bohlson, S. S. (2012). C1q and phagocytosis: The perfect complement to a good meal. *Journal of Leukocyte Biology*, *92*(3), 489–497. https://doi.org/10.1189/jlb.0212099

JR Hecht. (1998). Gastrointestinal Toxicity of Irinotecan. *Oncology*, *12*(8), 72–78.

Kochanek, D. M., Ghouse, S. M., Karbowniczek, M. M., & Markiewski, M. M. (2018). Complementing Cancer Metastasis. *Frontiers in Immunology*, *9*, 1629. https://doi.org/10.3389/fimmu.2018.01629

Kolev, M., Das, M., Gerber, M., Baver, S., Deschatelets, P., & Markiewski, M. M. (2022). Inside-Out of Complement in Cancer. *Frontiers in Immunology*, *13*, 931273. https://doi.org/10.3389/fimmu.2022.931273

Macor, P., Capolla, S., & Tedesco, F. (2018). Complement as a Biological Tool to Control Tumor Growth. *Frontiers in Immunology*, *9*, 2203. https://doi.org/10.3389/fimmu.2018.02203

Mak, I. W., Evaniew, N., & Ghert, M. (2014). Lost in translation: Animal models and clinical trials in cancer treatment. *American Journal of Translational Research*, *6*(2), 114–118.

Markiewski, M. M., DeAngelis, R. A., Benencia, F., Ricklin-Lichtsteiner, S. K., Koutoulaki, A., Gerard, C., Coukos, G., & Lambris, J. D. (2008). Modulation of the antitumor immune response by complement. *Nature Immunology*, *9*(11), 1225–1235. https://doi.org/10.1038/ni.1655

McGeer, P. L., Lee, M., & McGeer, E. G. (2017). A review of human diseases caused or exacerbated by aberrant complement activation. *Neurobiology of Aging*, *52*, 12–22. https://doi.org/10.1016/j.neurobiolaging.2016.12.017

Mevorach, D., Mascarenhas, J. O., Gershov, D., & Elkon, K. B. (1998). Complement-dependent clearance of apoptotic cells by human macrophages. *Journal of Experimental Medicine*, *188*(12), 2313–2320. https://doi.org/10.1084/jem.188.12.2313

Nabizadeh, J. A., Manthey, H. D., Steyn, F. J., Chen, W., Widiapradja, A., Md Akhir, F. N., Boyle, G. M., Taylor, S. M., Woodruff, T. M., & Rolfe, B. E. (2016). The Complement C3a Receptor Contributes to Melanoma Tumorigenesis by Inhibiting Neutrophil and CD4 $^{+}$ T Cell Responses. *The Journal of Immunology*, *196*(11), 4783–4792. https://doi.org/10.4049/jimmunol.1600210

Piao, C., Zhang, W.-M., Li, T.-T., Zhang, C., Qiu, S., Liu, Y., Liu, S., Jin, M., Jia, L.-X., Song, W.-C., & Du, J. (2018). Complement 5a stimulates macrophage polarization and contributes to tumor metastases of colon cancer. *Experimental Cell Research*, *366*(2), 127–138. https://doi.org/10.1016/j.yexcr.2018.03.009

Ricklin, D., & Lambris, J. D. (2008). Compstatin: A complement inhibitor on its way to clinical application. *Advances in Experimental Medicine and Biology*, *632*(Davis 2006), 273–292. https://doi.org/10.1007/978-0-387-78952-1_20

Rothenberg, M. L. (2001). Irinotecan (CPT-11): Recent Developments and Future Directions–Colorectal Cancer and Beyond. *The Oncologist*, *6*(1), 66–80. https://doi.org/10.1634/theoncologist.6-1-66

Towner, L. D., Wheat, R. A., Hughes, T. R., & Morgan, B. P. (2016). Complement Membrane Attack and Tumorigenesis. *Journal of Biological Chemistry*, *291*(29), 14927–14938. https://doi.org/10.1074/jbc.M115.708446

Walport, M. J. (2001a). Complement. First of two parts. *New England Journal of Medicine*, *344*(14), 1058–1066. https://doi.org/10.1056/NEJM200104053441406

Walport, M. J. (2001b). Complement. Second of two parts. *New England Journal of Medicine*, *344*(15), 1140–1144. https://doi.org/10.1056/NEJM200104123441506

Xue, H., Sawyer, M. B., Field, C. J., Dieleman, L. A., & Baracos, V. E. (2007). Nutritional modulation of antitumor efficacy and diarrhea toxicity related to irinotecan chemotherapy in rats bearing the ward colon tumor. *Clinical Cancer Research*, *13*(23), 7146–7154. https://doi.org/10.1158/1078-0432.CCR-07-0823

Zimmermann-Nielsen, E., Iversen, L. H., Svehag, S.-E., Thorlacius-Ussing, O., & Baatrup, G. (2002). Activation capacity of the alternative and classic complement pathways in patients operated on for colorectal cancer. *Diseases of the Colon and Rectum*, *45*(4), 544–553. https://doi.org/10.1007/s10350-004-6237-6

CHAPTER 4: GENERAL DISCUSSION AND CONCLUSIONS

4.1 General Summary and Review of Objectives and Hypotheses

Therapeutic efficacy of chemotherapy is optimized based on greater efficacy against cancer cells than against healthy tissues. However, although often efficacious against several malignancies, toxicity is intrinsic to antineoplastic agents and can have detrimental effects on the quality of life of patients with cancer. Unfortunately, the focus on mechanisms of muscle–specific toxicity of cancer therapies has been a deficiency, given that the magnitude of muscle losses reported in studies of patients is considerable. Ours is the first inquiry of its type modeled on a specific chemotherapy regimen aligned with a specific tumor histologic type. This is also the first study wherein a novel orally active, small molecular weight inhibitor of the complement system was used in a preclinical model of colon cancer and FOLFIRI chemotherapy treatment.

Objective 1: Investigate the sequential effect of colorectal adenocarcinoma and subsequent cycles of FOLFIRI chemotherapy treatment on atrophy and evolution of gene expression in skeletal muscle in an experimental model.

We hypothesized that tumor and chemotherapy could each elicit unique and quantitatively important effects in the development and progression of muscle wasting. The tumor in addition to treatment with sequential cycles of FOLFIRI resulted in a succession of changes in skeletal muscle, which were each unique and brought into the understanding that at each point along this trajectory, the muscle biology is responding dynamically; this means that a multitude of responses are turned on or off and this is not a steady-state where a standardized set of biological functions are invoked

and maintained. Effective tumor control did not mitigate muscle atrophy and instead substantially worsened it. Our findings support and confirm the suspicion that there are skeletal-muscle specific side effects of antineoplastic therapy, which in addition to tumor-induced atrophy erode the muscle mass. Both the effect of the tumor and of the chemotherapy are unique and quantitatively important in the development and progression of muscle wasting.

Objective 2: Explore whether certain immunological reactions, namely inhibitors of the complement system, could potentially affect treatment response to FOLFIRI chemotherapy in a favorable manner with enhanced anti-cancer efficacy and/or reduced FOLFIRI-associated gastrointestinal toxicity

Given preliminary data suggesting gastrointestinal (GI) protective effects of the complement inhibitor (AUR1402), we hypothesized that when combined with a FOLFIRI chemotherapy regimen, treatment-associated GI toxicity would be attenuated. Although the FOLFIRI-induced changes to body weight and food intake were not affected by AUR1402, FOLFIRI-induced GI toxicity was not increased by AUR1402. Importantly, an anti-tumor effect was observed with AUR1402 treatment and resulted in tumor elimination.

While the vast majority of research focused on elucidating the mechanisms of action of cancer- and cancer treatment-associated muscle wasting has focused either on single agent treatments in healthy animals (Barreto et al., 2016; Seo et al., 2021; Sorensen et al., 2017) or excessive tumor burden compared to that observed clinically (for example (Barreto et al., 2016; Sun et al., 2016; Tseng et al., 2015), these investigations have failed to account for the possibility

that both the tumor and chemotherapy as sources of toxicity, may synergize with each other. The successive treatment of tumor is part of the clinical reality and requires consideration of the degree of tumor related progression alongside dose and total amount of chemotherapy administered. To understand the response of muscle to tumor and chemotherapy, it is important to determine at what stage of tumor growth and at what dose and duration of chemotherapy this will be assessed. As skeletal muscle is tissue predominantly under transcriptional control, we endeavored to better understand this signature using a transcriptomic approach wherein Ingenuity Pathway Analysis (IPA) was used to identify cellular pathways associated with tumor- and FOLFIRI-induced muscle wasting. We find activation of the ubiquitin proteasome proteolytic pathway by FOLFIRI treatment, a gene signature suggestive of cellular death via apoptosis and necroptosis and negative regulation of several structural components. This is suggestive of adverse effects to cellular morphology and structure associated with activation of transcriptional programs contributing to muscle protein degradation and atrophy gene response induced by FOLFIRI-associated toxicity; these pathways appeared to have been primed by tumor growth.

It is interesting to note that although there are several toxicities associated with chemotherapy regimens, (ex. severe diarrhea associated with irinotecan), the notion of chemotherapy-specific adverse reactions in skeletal muscle has not been within the lens of medical oncology. As a consequence, treatment of chemotherapy-associated muscle loss or mitigation through multimodal interventions (ex. diet, physiotherapy) has been seldom the focus of clinicians in primary cancer care settings. Although the field of toxicogenomics is relatively silent with respect to effects of cytotoxic antineoplastic therapies on skeletal muscle, transcriptomics, as a strategy to predict and better understand perturbed mechanistic and cellular responses to toxicity as well as identify bio-signatures attributable to antineoplastic agents may be a useful tool, for not

only skeletal muscle but also toxic effects elsewhere in the body in adipose tissue, liver, and cardiac tissues.

The complement inhibitor (AUR1402) had no effect on the clinical manifestations of FOLFIRI-associated gastrointestinal toxicity (body weight and food intake). We present evidence of FOLFIRI-induced muscle toxicity (despite tumor control), and it is thus interesting to consider the potential role of complement responses in contributing to and/or modifying tumor- and FOLFIRI-associated muscle toxicity. This is of particular interest as evidence suggests involvement of complement in sensing muscle injury (Frenette et al., 2000). Additionally, some studies of the complement response in injured muscle suggest the activation of the complement system to result in increased neutrophil and macrophage recruitment (Zhang et al., 2017) alongside skeletal muscle regeneration (Galvan et al., 2012; Mevorach et al., 1998). Additionally, unpublished results have reported complement 3 (C3) and membrane attack complex (MAC; C5b-9) deposition and activation in *rectus abdominis* muscle biopsies of pancreatic ductal adenocarcinoma (PDAC) patients experiencing muscle wasting (D'Lugos, 2020). This group has also shown using the KPC C57Bl6/J mouse model of pancreatic cancer-associated muscle wasting, that knockout of complement component C3 attenuates KPC-induced limb muscle atrophy and diaphragm muscle dysfunction while preserving diaphragm morphology.

4.2 Considerations for Future Studies

It should be noted that our findings are limited to a single animal model and 2 cycles of a single chemotherapy regimen. Many important facets remain to be uncovered and further combinations, cancer types and therapy require testing. It would be of great benefit to expand the

scope of future studies to assess transcriptomic profiles of skeletal muscle of different experimental models, perhaps with different colorectal cancer subtypes and chemotherapy regimens. The extent to which our findings may apply to additional tumor sites remains to be determined. In addition, female animals were used in this study as the original dose intensity was worked out in female animals, and we did not have the means to conduct dose intensity studies in male animals. Due to the fact that sexual dimorphism exists between males and females, the results described in the present study which describe FOLFIRI-induced muscle atrophy may not be (completely) transferable to male animals. The potential prevention or reversibility of the changes that we documented in muscle are untested, however encouraging results have been obtained by Almasud et al. with dietary intervention with n-3 polyunsaturated fatty acids (Almasud et al., 2017). Follow-up study designs to test treatment-induced muscle toxicity as well as anti-tumor efficacy of the AUR1402 would be insightful.

The most interesting finding with combined administration of AUR1402 with sequential cycles of FOLFIRI was the anti-tumor effect and complete disappearance of the tumor. Several questions pertaining to the mechanism of action of AUR1402 remain and include: At what point along the FOLFIRI treatment trajectory does AUR1402 exert its potent effect? Does AUR1402 have a direct cytolytic effect on cancer cells, independent of FOLFIRI toxicity? Are the anti-tumor effects of AUR1402 mediated through augmentation of innate immune responses in the tumor microenvironment? Does AUR1402 alter opsonic responses and/or modify macrophage polarization and subsequent phagocytic responses in the tumor microenvironment? As complement responses can be extensive in affecting tumorigenesis (Ding et al., 2022; Nabizadeh et al., 2016), further investigation of the mechanism(s) of action of the complement inhibitor are necessary.

To gain insight into the aforementioned questions, carefully designed follow-up experiments and biochemical analyses are required. A study design with a time course that enables sampling of tumors from animals from multiple timepoints during the course of FOLFIRI treatment may provide valuable insight related to the onset of complement inhibitor effects. Although we have been able to identify the minimum effective dose of AUR1402 required to confer an anti-tumor response when administered with FOLFIRI, the maximum tolerated dose has not yet been determined in this model. Additionally, direct, and antibody-dependent cytotoxic assays of AUR1402 with and without FOLFIRI on additional colorectal cancer cell lines and cell lines of other tumor sites could be pursued; this should be complemented with in vivo studies which are executed in immunocompetent animals.

Follow-up tumor analysis should include immunohistochemistry to identify and quantify proliferating tumor cells as well as immune cell subtypes at multiple timepoints; this is of particular interest given that the histology of tumors treated with AUR1402 resembled features otherwise found in a benign lymph node and germinal centers. Assays to assess the extent of membrane attack complex (MAC) formation and deposition alongside complement component 3 (C3) (and cleaved subunit) and complement anaphylatoxin deposition in the tumor microenvironment would be insightful given that the derivative of AUR1402, Aurin tricarboxylic acid (ATA), inhibits alternative complement component 3 (C3) convertase activity. Given the emergence of complement inhibitors in clinical trials administered as both monotherapy and/or as combination therapy with checkpoint inhibitors (Kolev et al., 2022), investigating the use of AUR1402 in a similar manner may allow for identification of additional therapeutic targets.

4.3 Conclusion

We endeavored to model the treatment setting of locally advanced colon cancer, respecting tumor mass, regimen and schedule, treatment response and toxicity. Untreated tumor bearing animals and FOLFIRI-treated, tumor bearing animals resulted in progressive atrophy and synergistic changes in skeletal muscle transcriptome. FOLFIRI specifically exacerbates a catabolic transcriptional program, despite robust tumor response. Combination with a complement inhibitor, AUR1402, potentiated tumor response to FOLFIRI without increasing treatment-associated toxicity. Further investigation is required to elucidate the mechanism of action of this agent. Considerations of combination therapy alongside first line chemotherapy with FOLFIRI may be worthwhile pursuits.

LITERATURE CITED

Almasud, A. A., Giles, K. H., Miklavcic, J. J., Martins, K. J. B., Baracos, V. E., Putman, C. T., Guan, L. L., & Mazurak, V. C. (2017). Fish oil mitigates myosteatosis and improves chemotherapy efficacy in a preclinical model of colon cancer. *PLoS ONE*, *12*(8), 1–17. https://doi.org/10.1371/journal.pone.0183576

Barreto, R., Mandili, G., Witzmann, F. A., Novelli, F., Zimmers, T. A., & Bonetto, A. (2016). Cancer and chemotherapy contribute to muscle loss by activating common signaling pathways. *Frontiers in Physiology*, *7*(OCT), 1–13. https://doi.org/10.3389/fphys.2016.00472

Ding, P., Xu, Y., Li, L., Lv, X., Li, L., Chen, J., Zhou, D., Wang, X., Wang, Q., Zhang, W., Liao, T., Ji, Q.-H., Lei, Q.-Y., & Hu, W. (2022). Intracellular complement C5a/C5aR1 stabilizes β-catenin to promote colorectal tumorigenesis. *Cell Reports*, *39*(9), 110851. https://doi.org/10.1016/j.celrep.2022.110851

D'Lugos, A. C. (2020). *The Role of Complement in Pancreatic Cancer Cachexia*. 1.

Frenette, J., Cai, B., & Tidball, J. G. (2000). Complement activation promotes muscle inflammation during modified muscle use. *American Journal of Pathology*, *156*(6), 2103–2110. https://doi.org/10.1016/S0002-9440(10)65081-X

Galvan, M. D., Greenlee-Wacker, M. C., & Bohlson, S. S. (2012). C1q and phagocytosis: The perfect complement to a good meal. *Journal of Leukocyte Biology*, *92*(3), 489–497. https://doi.org/10.1189/jlb.0212099

Kolev, M., Das, M., Gerber, M., Baver, S., Deschatelets, P., & Markiewski, M. M. (2022). Inside-Out of Complement in Cancer. *Frontiers in Immunology*, *13*, 931273. https://doi.org/10.3389/fimmu.2022.931273

Mevorach, D., Mascarenhas, J. O., Gershov, D., & Elkon, K. B. (1998). Complement-dependent clearance of apoptotic cells by human macrophages. *Journal of Experimental Medicine*, *188*(12), 2313–2320. https://doi.org/10.1084/jem.188.12.2313

Nabizadeh, J. A., Manthey, H. D., Steyn, F. J., Chen, W., Widiapradja, A., Md Akhir, F. N., Boyle, G. M., Taylor, S. M., Woodruff, T. M., & Rolfe, B. E. (2016). The Complement C3a Receptor Contributes to Melanoma Tumorigenesis by Inhibiting Neutrophil and CD4 $^{+}$ T Cell Responses. *The Journal of Immunology*, *196*(11), 4783–4792. https://doi.org/10.4049/jimmunol.1600210

Seo, D. Y., Bae, J. H., Zhang, D., Song, W., Kwak, H., Heo, J., & Jung, S. (2021). *Effects of cisplatin on mitochondrial function and autophagy-related proteins in skeletal muscle of rats*. *54*(October), 575–580.

Sorensen, J. C., Petersen, A. C., Timpani, C. A., Campelj, D. G., Cook, J., Trewin, A. J., Stojanovska, V., Stewart, M., Hayes, A., & Rybalka, E. (2017). BGP-15 protects against oxaliplatin-induced skeletal myopathy and mitochondrial reactive oxygen species production in mice. *Frontiers in Pharmacology*, *8*(APR), 1–19. https://doi.org/10.3389/fphar.2017.00137

Sun, R., Zhang, S., Lu, X., Hu, W., Lou, N., Zhao, Y., Zhou, J., Zhang, X., & Yang, H. (2016). Comparative molecular analysis of early and late cancer cachexia-induced muscle wasting in mouse models. *Oncology Reports*, *36*(6), 3291–3302. https://doi.org/10.3892/or.2016.5165

Tseng, Y. C., Kulp, S. K., Lai, I. L., Hsu, E. C., He, W. A., Frankhouser, D. E., Yan, P. S., Mo, X., Bloomston, M., Lesinski, G. B., Marcucci, G., Guttridge, D. C., Bekaii-Saab, T., & Chen, C. S. (2015). Preclinical Investigation of the Novel Histone Deacetylase Inhibitor AR-42

in the Treatment of Cancer-Induced Cachexia. *Journal of the National Cancer Institute*, *107*(12), djv274. https://doi.org/10.1093/jnci/djv274

Zhang, C., Wang, C., Li, Y., Miwa, T., Liu, C., Cui, W., Song, W. C., & Du, J. (2017). Complement C3a signaling facilitates skeletal muscle regeneration by regulating monocyte function and trafficking. *Nature Communications*, *8*(1). https://doi.org/10.1038/s41467-017-01526-z

Bibliography

1. Afshar-Kharghan, V. The role of the complement system in cancer. *Journal of Clinical Investigation* **127**, 780–789 (2017).

2. Ahn, K. H., Kim, S., Yang, M. & Lee, D. W. A Pillar-Based High-Throughput Myogenic Differentiation Assay to Assess Drug Safety. *Molecules* **26**, 5805 (2021).

3. Almasud, A. A. *et al.* Fish oil mitigates myosteatosis and improves chemotherapy efficacy in a preclinical model of colon cancer. *PLoS ONE* **12**, 1–17 (2017).

4. Anoveros-barrera, A. *et al.* Clinical and biological characterization of skeletal muscle tissue biopsies of surgical cancer patients. 1356–1377 (2019) doi:10.1002/jcsm.12466.

5. Argilés, J. M. & López-Soriano, F. J. The energy state of tumor-bearing rats. *Journal of Biological Chemistry* **266**, 2978–2982 (1991).

6. Armand, J. P. *et al.* CPT-11 (Irinotecan) in the treatment of colorectal cancer. *European Journal of Cancer* **31**, 1283–1287 (1995).

7. Attaix, D. *et al.* Ubiquitin-proteasome-dependent proteolysis in skeletal muscle. (1998).

8. Aversa, Z., Costelli, P. & Muscaritoli, M. Cancer-induced muscle wasting: Latest findings in prevention and treatment. *Therapeutic Advances in Medical Oncology* **9**, 369–382 (2017).

9. Bao, D. *et al.* Integrative Analysis of Complement System to Prognosis and Immune Infiltrating in Colon Cancer and Gastric Cancer. *Front. Oncol.* **10**, 553297 (2021).

10. Baracos, V. E., Martin, L., Korc, M., Guttridge, D. C. & Fearon, K. C. H. Cancer-associated cachexia. *Nature Reviews Disease Primers* **4**, 1–18 (2018).

11. Barreto, R. *et al.* Cancer and chemotherapy contribute to muscle loss by activating common signaling pathways. *Frontiers in Physiology* **7**, 1–13 (2016).

12. Barreto, R. *et al.* Chemotherapy-related cachexia is associated with mitochondrial depletion and the activation of ERK1/2 and p38 MAPKs. *Oncotarget* **7**, 43442–43460 (2016).

13. Belizário, J. E., Lorite, M. J. & Tisdale, M. J. proteases in skeletal muscles from mice undergoing cancer cachexia. **84**, 1135–1140 (2001).

14. Benson, A. B. *et al.* Colon Cancer, Version 1.2017. *J Natl Compr Canc Netw* **15**, 1028–1059 (2017).

15. Black, D. *et al.* Prognostic Value of Computed Tomography: Measured Parameters of Body Composition in Primary Operable Gastrointestinal Cancers. *Annals of Surgical Oncology* **24**, 2241–2251 (2017).

16. Blackwell, T. A. *et al.* Transcriptomic analysis of the development of skeletal muscle atrophy in cancer-cachexia in tumor-bearing mice. *Physiological Genomics* **50**, 1071–1082 (2018).

17. Blajchman, M. A. & Ozge-Anwar, A. H. The role of the complement system in hemostasis. *Progress in hematology* **14**, 149–182 (1986).

18. Blauwhoff-Buskermolen, S. *et al.* Loss of muscle mass during chemotherapy is predictive for poor survival of patients with metastatic colorectal cancer. *Journal of Clinical Oncology* **34**, 1339–1344 (2016).

19. Boer, B. C. *et al.* Skeletal muscle mass and quality as risk factors for postoperative outcome after open colon resection for cancer. *Int J Colorectal Dis* **31**, 1117–1124 (2016).

20. Bohlson, S. S., O'Conner, S. D., Hulsebus, H. J., Ho, M. M. & Fraser, D. A. Complement, C1Q, and C1q-related molecules regulate macrophage polarization. *Frontiers in Immunology* **5**, (2014).

21. Bohnert, K. R. *et al.* Inhibition of ER stress and unfolding protein response pathways causes skeletal muscle wasting during cancer cachexia. 3053–3068 (2016) doi:10.1096/fj.201600250RR.

22. Boross, P. & Leusen, J. H. W. Boosting antibody therapy with complement. *Blood* **119**, 5945–5947 (2012).

23. Bozzetti, F. & Bozzetti, F. Forcing the vicious circle: sarcopenia increases toxicity, decreases response to chemotherapy and worsens with chemotherapy. (2017) doi:10.1093/annonc/mdx271.

24. Campelj, D. G. *et al.* The Paradoxical Effect of PARP Inhibitor BGP-15 on Irinotecan-Induced Cachexia and Skeletal Muscle Dysfunction. *Cancers* **12**, 3810 (2020).

25. Cao, S. & Rustum, Y. M. Synergistic antitumor activity of irinotecan in combination with 5-fluorouracil rats bearing advanced colorectal cancer: Role of drug sequence and dose. *Cancer Research* **60**, 3717–3721 (2000).

26. Cespedes Feliciano, E. M. *et al.* Muscle mass at the time of diagnosis of nonmetastatic colon cancer and early discontinuation of chemotherapy, delays, and dose reductions on adjuvant FOLFOX: The C-SCANS study. *Cancer* **123**, 4868–4877 (2017).

27. Chen, J. L. *et al.* Differential Effects of IL6 and Activin A in the Development of Cancer-Associated Cachexia. **76**, 5372–5382 (2016).

28. Chen, K.-H. *et al.* Novel prognostic implications of complement activation in the tumour microenvironment for de novo metastatic BRAF V600E mutant colorectal cancer. *Br J Cancer* (2022) doi:10.1038/s41416-022-02010-2.

29. Chen, R. *et al.* Unfolded Protein Response Suppresses Cisplatin-Induced Apoptosis via Autophagy Regulation in Human Hepatocellular Carcinoma Cells. **57**, 9 (2011).

30. D'Lugos, A. C. The Role of Complement in Pancreatic Cancer Cachexia. 1 (2020).

31. Daly, L. E. *et al.* Loss of skeletal muscle during systemic chemotherapy is prognostic of poor survival in patients with foregut cancer. *Journal of Cachexia, Sarcopenia and Muscle* **9**, 315–325 (2018).

32. Damaraju, V. L., Kuzma, M., Cass, C. E., Putman, C. T. & Sawyer, M. B. Multitargeted kinase inhibitors imatinib, sorafenib and sunitinib perturb energy metabolism and cause cytotoxicity to cultured C2C12 skeletal muscle derived myotubes. *Biochemical Pharmacology* **155**, 162–171 (2018).

33. Deng, H., Chen, Y., Liu, Y., Liu, L. & Xu, R. Complement C1QC as a potential prognostic marker and therapeutic target in colon carcinoma based on single-cell RNA sequencing and immunohistochemical analysis. *Bosnian Journal of Basic Medical Sciences* **22**, 912–922 (2022).

34. Ding, P. *et al.* Intracellular complement C5a/C5aR1 stabilizes β-catenin to promote colorectal tumorigenesis. *Cell Reports* **39**, 110851 (2022).

35. Downs-Canner, S. *et al.* Complement Inhibition: A Novel Form of Immunotherapy for Colon Cancer. *Ann Surg Oncol* **23**, 655–662 (2016).

36. Eley, H. L., Russell, S. T. & Tisdale, M. J. Effect of branched-chain amino acids on muscle atrophy in cancer cachexia. *Biochemical Journal* **407**, 113–120 (2007).

37. Fabian, G. *et al.* High-Density Real-Time PCR-Based in Vivo Toxicogenomic Screen to Predict Organ-Specific Toxicity. *IJMS* **12**, 6116–6134 (2011).

38. Fan, Z., Qin, J., Wang, D. & Geng, S. Complement C3a promotes proliferation, migration and stemness in cutaneous squamous cell carcinoma. *J Cell Mol Med* **23**, 3097–3107 (2019).

39. Farhangfar, A. Non digestible carbohydrates in the diet determine toxicity of irinotecan (CPT-11)/5-fluorouracil in rats independently of β- glucuronidase activity in intestinal lumen. 94 (2012).

40. Fishelson, Z. & Kirschfink, M. Complement C5b-9 and Cancer: Mechanisms of Cell Damage, Cancer Counteractions, and Approaches for Intervention. *Front. Immunol.* **10**, 752 (2019).

41. Frenette, J., Cai, B. & Tidball, J. G. Complement activation promotes muscle inflammation during modified muscle use. *American Journal of Pathology* **156**, 2103–2110 (2000).

42. Gallot, Y. S. & Bohnert, K. R. Confounding Roles of ER Stress and the Unfolded Protein Response in Skeletal Muscle Atrophy. *IJMS* **22**, 2567 (2021).

43. Galvan, M. D., Greenlee-Wacker, M. C. & Bohlson, S. S. C1q and phagocytosis: the perfect complement to a good meal. *Journal of Leukocyte Biology* **92**, 489–497 (2012).

44. Halle, J. L., Counts, B. R., Zhang, Q. & Carson, J. A. Short duration treadmill exercise improves physical function and skeletal muscle mitochondria protein expression after recovery from FOLFOX chemotherapy in male mice. *The FASEB Journal* **36**, (2022).

45. He, W. A. *et al.* NF- κ B – mediated Pax7 dysregulation in the muscle microenvironment promotes cancer cachexia. **123**, 4821–4835 (2013).

46. Huang, D.-D. *et al.* Sarcopenia, as defined by low muscle mass, strength and physical performance, predicts complications after surgery for colorectal cancer. *Colorectal Dis* **17**, O256–O264 (2015).

47. Jang, M. K. *et al.* Skeletal Muscle Mass Change During Chemotherapy: A Systematic Review and Meta-analysis. *Anticancer Res* **40**, 2409–2418 (2020).

48. Järvinen, T., Ilonen, I., Kauppi, J., Salo, J. & Räsänen, J. Loss of skeletal muscle mass during neoadjuvant treatments correlates with worse prognosis in esophageal cancer: A retrospective cohort study. *World Journal of Surgical Oncology* **16**, 17–19 (2018).

49. Jennings, P., Limonciel, A., Felice, L. & Leonard, M. O. An overview of transcriptional regulation in response to toxicological insult. *Arch Toxicol* **87**, 49–72 (2013).

50. JR Hecht. Gastrointestinal Toxicity of Irinotecan. *Oncology* **12**, 72–8 (1998).

51. Jung, H.-W. *et al.* Effect of muscle mass on toxicity and survival in patients with colon cancer undergoing adjuvant chemotherapy. *Support Care Cancer* **23**, 687–694 (2015).

52. Kochanek, D. M., Ghouse, S. M., Karbowniczek, M. M. & Markiewski, M. M. Complementing Cancer Metastasis. *Front. Immunol.* **9**, 1629 (2018).

53. Kolev, M. *et al.* Inside-Out of Complement in Cancer. *Front. Immunol.* **13**, 931273 (2022).

54. Krzystek-korpacka, M., Matusiewicz, M. & Diakowska, D. Impact of weight loss on circulating IL-1 , IL-6 , IL-8 , TNF- α , VEGF-A , VEGF – C and midkine in gastroesophageal cancer patients. **40**, 1353–1360 (2007).

55. Lecker, S. H. *et al.* Multiple types of skeletal muscle atrophy involve a common program of changes in gene expression. 39–51 (2004) doi:10.1096/fj.03-0610com.

56. Longley, D. B., Harkin, D. P. & Johnston, P. G. 5-Fluorouracil: mechanisms of action and clinical strategies. *Nat Rev Cancer* **3**, 330–338 (2003).

57. Ma, J. F., Sanchez, B. J., Hall, D. T., Tremblay, A. K. & Marco, S. D. STAT 3 promotes IFN c / TNF a -induced muscle wasting in an NF- j B-dependent and IL- 6 -independent manner. **9**, 622–637 (2017).

58. Macor, P., Capolla, S. & Tedesco, F. Complement as a Biological Tool to Control Tumor Growth. *Front. Immunol.* **9**, 2203 (2018).

59. Mak, I. W., Evaniew, N. & Ghert, M. Lost in translation: animal models and clinical trials in cancer treatment. *Am J Transl Res* **6**, 114–118 (2014).

60. Markiewski, M. M. *et al.* Modulation of the antitumor immune response by complement. *Nat Immunol* **9**, 1225–1235 (2008).

61. Martin, A. & Freyssenet, D. Phenotypic features of cancer cachexia-related loss of skeletal muscle mass and function: lessons from human and animal studies. *Journal of Cachexia, Sarcopenia and Muscle* **12**, 252–273 (2021).

62. Martin, L. *et al.* Cancer cachexia in the age of obesity: Skeletal muscle depletion is a powerful prognostic factor, independent of body mass index. *Journal of Clinical Oncology* **31**, 1539–1547 (2013).

63. Martin, L. *et al.* Assessment of Computed Tomography (CT)-Defined Muscle and Adipose Tissue Features in Relation to Short-Term Outcomes After Elective Surgery for Colorectal Cancer: A Multicenter Approach. *Ann Surg Oncol* **25**, 2669–2680 (2018).

64. McGeer, P. L., Lee, M. & McGeer, E. G. A review of human diseases caused or exacerbated by aberrant complement activation. *Neurobiology of Aging* **52**, 12–22 (2017).

65. Merrick, B. A. & Bruno, M. E. Genomic and proteomic profiling for biomarkers and signature profiles of toxicity. **6**, 8 (2004).

66. Mevorach, D., Mascarenhas, J. O., Gershov, D. & Elkon, K. B. Complement-dependent clearance of apoptotic cells by human macrophages. *Journal of Experimental Medicine* **188**, 2313–2320 (1998).

67. Mihaly, S. R. & Morioka, S. TAK1 control of cell death. *Cell Death and Differentiation* **21**, 1667–1676 (2014).

68. Murphy, R. A. *et al.* Nutritional intervention with fish oil provides a benefit over standard of care for weight and skeletal muscle mass in patients with nonsmall cell lung cancer receiving chemotherapy. *Cancer* **117**, 1775–1782 (2011).

69. Murphy, R. A. *et al.* Supplementation with fish oil increases first-line chemotherapy efficacy in patients with advanced nonsmall cell lung cancer. *Cancer* **117**, 3774–3780 (2011).

70. Nabizadeh, J. A. *et al.* The Complement C3a Receptor Contributes to Melanoma Tumorigenesis by Inhibiting Neutrophil and CD4 $^{+}$ T Cell Responses. *J.I.* **196**, 4783–4792 (2016).

71. Nakanishi, R. *et al.* Sarcopenia is an independent predictor of complications after colorectal cancer surgery. *Surg Today* **48**, 151–157 (2018).

72. Parzych, K. R. & Klionsky, D. J. An Overview of Autophagy : **20**, 460–473 (2014).

73. Peris-Moreno, D., Cussonneau, L., Combaret, L., Polge, C. & Taillandier, D. Ubiquitin Ligases at the Heart of Skeletal Muscle Atrophy Control. *Molecules* **26**, 407 (2021).

74. Peris-Moreno, D., Taillandier, D. & Polge, C. MuRF1/TRIM63, Master Regulator of Muscle Mass. *IJMS* **21**, 6663 (2020).

75. Piao, C. *et al.* Complement 5a stimulates macrophage polarization and contributes to tumor metastases of colon cancer. *Experimental Cell Research* **366**, 127–138 (2018).

76. Pin, F., Barreto, R., Couch, M. E., Bonetto, A. & O'Connell, T. M. Cachexia induced by cancer and chemotherapy yield distinct perturbations to energy metabolism. *Journal of Cachexia, Sarcopenia and Muscle* **10**, 140–154 (2019).

77. Ricklin, D. & Lambris, J. D. Compstatin: A complement inhibitor on its way to clinical application. *Advances in Experimental Medicine and Biology* **632**, 273–292 (2008).

78. Riedl, S. J. & Shi, Y. MOLECULAR MECHANISMS OF CASPASE REGULATION DURING APOPTOSIS. **5**, (2004).

79. Rier, H. N., Jager, A., Sleijfer, S., Maier, A. B. & Levin, M. The Prevalence and Prognostic Value of Low Muscle Mass in Cancer Patients: A Review of the Literature. *The Oncologist* **21**, 1396–1409 (2016).

80. Ross, G. D., Veˇtvicˇka, V., Yan, J., Xia, Y. & Veˇtvicˇkova, J. Therapeutic intervention with complement and b-glucan in cancer. 14 (1999).

81. Rothenberg, M. L. Irinotecan (CPT-11): Recent Developments and Future Directions–Colorectal Cancer and Beyond. *The Oncologist* **6**, 66–80 (2001).

82. Schiessel, D. L. & Baracos, V. E. Barriers to cancer nutrition therapy: excess catabolism of muscle and adipose tissues induced by tumour products and chemotherapy. *Proc. Nutr. Soc.* **77**, 394–402 (2018).

83. Seo, D. Y. *et al.* Effects of cisplatin on mitochondrial function and autophagy-related proteins in skeletal muscle of rats. **54**, 575–580 (2021).

84. Shachar, S. S., Williams, G. R., Muss, H. B. & Nishijima, T. F. Prognostic value of sarcopenia in adults with solid tumours: A meta-analysis and systematic review. *European Journal of Cancer* **57**, 58–67 (2016).

85. Siegel, R. L., Miller, K. D., Fuchs, H. E. & Jemal, A. Cancer statistics, 2022. *CA A Cancer J Clinicians* **72**, 7–33 (2022).

86. Sorensen, J. C. *et al.* BGP-15 protects against oxaliplatin-induced skeletal myopathy and mitochondrial reactive oxygen species production in mice. *Frontiers in Pharmacology* **8**, 1–19 (2017).

87. Sun, R. *et al.* Comparative molecular analysis of early and late cancer cachexia-induced muscle wasting in mouse models. *Oncology Reports* **36**, 3291–3302 (2016).

88. Taillandier, D. & Polge, C. Skeletal muscle atrogenes: From rodent models to human pathologies. *Biochimie* **166**, 251–269 (2019).

89. Towner, L. D., Wheat, R. A., Hughes, T. R. & Morgan, B. P. Complement Membrane Attack and Tumorigenesis. *Journal of Biological Chemistry* **291**, 14927–14938 (2016).

90. Tseng, Y. C. *et al.* Preclinical Investigation of the Novel Histone Deacetylase Inhibitor AR-42 in the Treatment of Cancer-Induced Cachexia. *Journal of the National Cancer Institute* **107**, djv274 (2015).

91. Van Cutsem, E. *et al.* ESMO consensus guidelines for the management of patients with metastatic colorectal cancer. *Annals of Oncology* **27**, 1386–1422 (2016).

92. van Vugt, J. L. A. *et al.* Estimated skeletal muscle mass and density values measured on computed tomography examinations in over 1000 living kidney donors. *Eur J Clin Nutr* **73**, 879–886 (2019).

93. VanderVeen, B. N. *et al.* 5-Fluorouracil disrupts skeletal muscle immune cells and impairs skeletal muscle repair and remodeling. *Journal of Applied Physiology* **133**, 834–849 (2022).

94. Vega, M. C. M. D., Laviano, A. & Pimentel, G. D. Sarcopenia and chemotherapy-mediated toxicity. *Einstein (Sao Paulo, Brazil)* **14**, 580–584 (2016).

95. Walport, M. J. Complement. First of two parts. *N Engl J Med* **344**, 1058–1066 (2001).

96. Walport, M. J. Complement. Second of two parts. *N Engl J Med* **344**, 1140–1144 (2001).

97. Xue, H. *et al.* Single and combined supplementation of glutamine and n-3 polyunsaturated fatty acids on host tolerance and tumour response to 7-ethyl-10-[4-(1- piperidino)-1-piperidino]carbonyloxy-camptothecin (CPT-11)/5-fluorouracil chemotherapy in rats bearing Ward col. *British Journal of Nutrition* **102**, 434–442 (2009).

98. Xue, H., Sawyer, M. B., Field, C. J., Dieleman, L. A. & Baracos, V. E. Nutritional modulation of antitumor efficacy and diarrhea toxicity related to irinotecan chemotherapy in rats bearing the ward colon tumor. *Clinical Cancer Research* **13**, 7146–7154 (2007).

99. Yang, W. E. I. *et al.* Molecular mechanisms of cancer cachexia - induced muscle atrophy (Review). 4967–4980 (2020) doi:10.3892/mmr.2020.11608.

100. Yu, Z., Zhu, J. I. E., Wang, H., Li, H. & Jin, X. Function of BCLAF1 in human disease (Review). (2022) doi:10.3892/ol.2021.13176.

101. Zhang, C. *et al.* Complement C3a signaling facilitates skeletal muscle regeneration by regulating monocyte function and trafficking. *Nature Communications* **8**, (2017).

102. Zimmermann-Nielsen, E., Iversen, L. H., Svehag, S.-E., Thorlacius-Ussing, O. & Baatrup, G. Activation capacity of the alternative and classic complement pathways in patients operated on for colorectal cancer. *Dis Colon Rectum* **45**, 544–553 (2002).

103. Ingenuity Pathway Analysis. *QIAGEN Digital Insights* https://digitalinsights.qiagen.com/products-overview/discovery-insights-portfolio/analysis-and-visualization/qiagen-ipa/.